DOE/ID/12742--1

DE91 006304

GEOLOGY AND GEOCHEMISTRY OF THE GEYSER BIGHT GEOTHERMAL AREA, UMNAK ISLAND, ALEUTIAN ISLANDS, ALASKA

by

Christopher J. Nye[1,2], Roman J. Motyka[3], Donald L. Turner[1], and Shirley A. Liss[2]

October, 1990

[1]Geophysical Institute, University of Alaska Fairbanks, Fairbanks, Alaska, 99775

[2]Alaska Division of Geological and Geophysical Surveys, 3700 Airport Way, Fairbanks, Alaska, 99709

[3]Alaska Division of Geological and Geophysical Surveys, 400 Willoughby Ave, 3rd floor, Juneau, Alaska, 99811

Final Report
submitted to the U.S. Department of Energy
in partial fulfillment of the requirements of grants

DE-FG07-88ID12742

and

DE-FG07-88ID12744

DISCLAIMER

TABLE OF CONTENTS

ABSTRACT

The Geyser Bight geothermal area is located on Umnak Island in the central Aleutian Islands. It contains one of the hottest and most extensive areas of thermal springs and fumaroles in Alaska, and is the only documented site in Alaska with geysers. The zone of hot springs and fumaroles lies at the head of Geyser Creek, 5 km up a broad, flat, alluvial valley from Geyser Bight. At present central Umnak is remote and undeveloped.

This report describes results of a combined program of geologic mapping, K-Ar dating, detailed description of hot springs, petrology and geochemistry of volcanic and plutonic rock units, and chemistry of geothermal fluids. Our mapping documents the presence of plutonic rock much closer to the area of hotsprings and fumaroles than previously known, thus increasing the probability that plutonic rock may host the geothermal system. K-Ar dating of 23 samples provides a time framework for the eruptive history of volcanic rocks as well as a plutonic cooling age.

Heat for the geothermal system is derived from the Mt. Recheshnoi volcanic system. Mt. Recheshnoi is a large calcalkaline stratocone which has been active over at least the past 500,000 years. Petrochemical studies indicate that successive passages of magma have probably heated the crust to near its minimum melting point and produced the only high-SiO_2 rhyolites in the oceanic part of the Aleutian arc. There is no indication that there is presently a large shallow magma chamber under Mt. Recheshnoi.

Surface expressions of the geothermal system include six zones of thermal springs and small geysers dispersed over an area of 4 km^2, and three zones of

fumarolic activity. Thermal spring water chemistry indicates that at least two intermediate level hydrothermal reservoirs underlie the geothermal area and have minimum temperatures of 165 and 200°C, respectively, as estimated by geothermometry. Sulfate-water isotope geothermometers suggest a deeper reservoir with a minimum temperature of 265°C underlies the shallower reservoirs. The $^{3}He/^{4}He$ ratio of 7.4 found in gases emanating from the thermal springs provides evidence for a magmatic influence on the hydrothermal system. The 7.4 value is nearly the same as the average value found for summit fumaroles in circum-Pacific volcanic arcs.

The thermal spring waters have low to moderate concentrations of Cl (650 ppm) and total dissolved solids (1760 ppm), but are rich in B (60 ppm) and As (6 ppm) compared to most other geothermal systems. The As/Cl ratios in Geyser Bight thermal spring waters are among the highest reported for geothermal areas. The source of B and As is unknown but may be in part of magmatic origin. Convective heat discharge by springflow is estimated at 17 MW for 1988. The upper reservoir system probably contains about 5.4 x 1018 J of thermal energy, sufficient to produce up to 132 MW of electrical power for 30 years. The deeper reservoir may contain up to 7.3 x 1018 J of thermal energy, sufficient to provide 225 MW for 30 years.

ACKNOWLEDGEMENTS

Funding for the Geyser Bight study came from the U.S. Department of Energy, grants DE-FG07-88ID12742 and DE-FG07-88ID12744; the State of Alaska, Department of Natural Resources; and the Geophysical Institute, University of Alaska Fairbanks.

We wish to acknowledge J. Thompson, C. Janik, and W. Evans of the U.S. Geological Survey, Menlo Park for their help and cooperation in performing some of the chemical and isotopic analyses of thermal waters and gases, and to thank M. Reed, U.S. Department of Energy, and J. Moore, University of Utah Research Institute, for their help in acquiring the analyses of the 1988 thermal water samples. We are grateful to Eugene Pavia for his major contribution to the very difficult logistical operations required by this project and for his skilled assistance with the geologic mapping. Robin Cottrell provided technical assistance with the K-Ar measurements. David Kuentz performed the X-ray fluorescence analyses at U.C. Santa Cruz. We also thank Scott Kerr for his able seamanship and Scott Kerr and Peat Galaktionoff for their warm hospitality in Nikolski.

Any opinions, findings, conclusions, or recommendations expressed herein are those of the authors and do not necessarily reflect the views of the United States Department of Energy.

1. INTRODUCTION AND BACKGROUND

1.1 Description of the Geyser Bight Geothermal Area

The Geyser Bight geothermal area, located on Umnak Island in the central Aleutian Islands (Figure 1-1), contains one of the hottest and most extensive areas of thermal springs and fumaroles in Alaska. It is the only area in Alaska where geyser activity has been documented. Geyser Bight is remote and undeveloped. However, its accessibility from the sea and its large estimated reserve of geothermal energy should make this area an economically attractive source of power in future decades. Our estimate of minimum temperatures for intermediate level reservoirs are 165°C and 200°C; and our minimum estimate for an underlying deep reservoir is 265°C. Estimates of convective heat being dissipated by spring flow alone range from about 25 megawatts in 1947 to 16.7 megawatts in 1988. Muffler (1979) estimated that 136 megawatts of electrical energy are available over 30 years at Geyser Bight, a resource comparable in size to Beowawe and Brady Hot Springs in Nevada.

The site is located at latitude 53°13′N, longitude 168°28′W, at the approximate center of the north side of Umnak Island (Figure 1-1). The thermal area consists of five zones of numerous thermal springs and small geysers dispersed over an area of about 4 km^2 in the upper reaches of a broad glacial valley which has excellent access to the Bering Sea (Figure 1-1). The hot springs occur mostly along Geyser Creek and its tributaries and emerge in the valley floor and at the base of steep valley walls. Two small fumarole fields are located at elevations of 140 and 300 m in a small tributary valley at the headwaters of Geyser Creek. A third, superheated fumarole field was

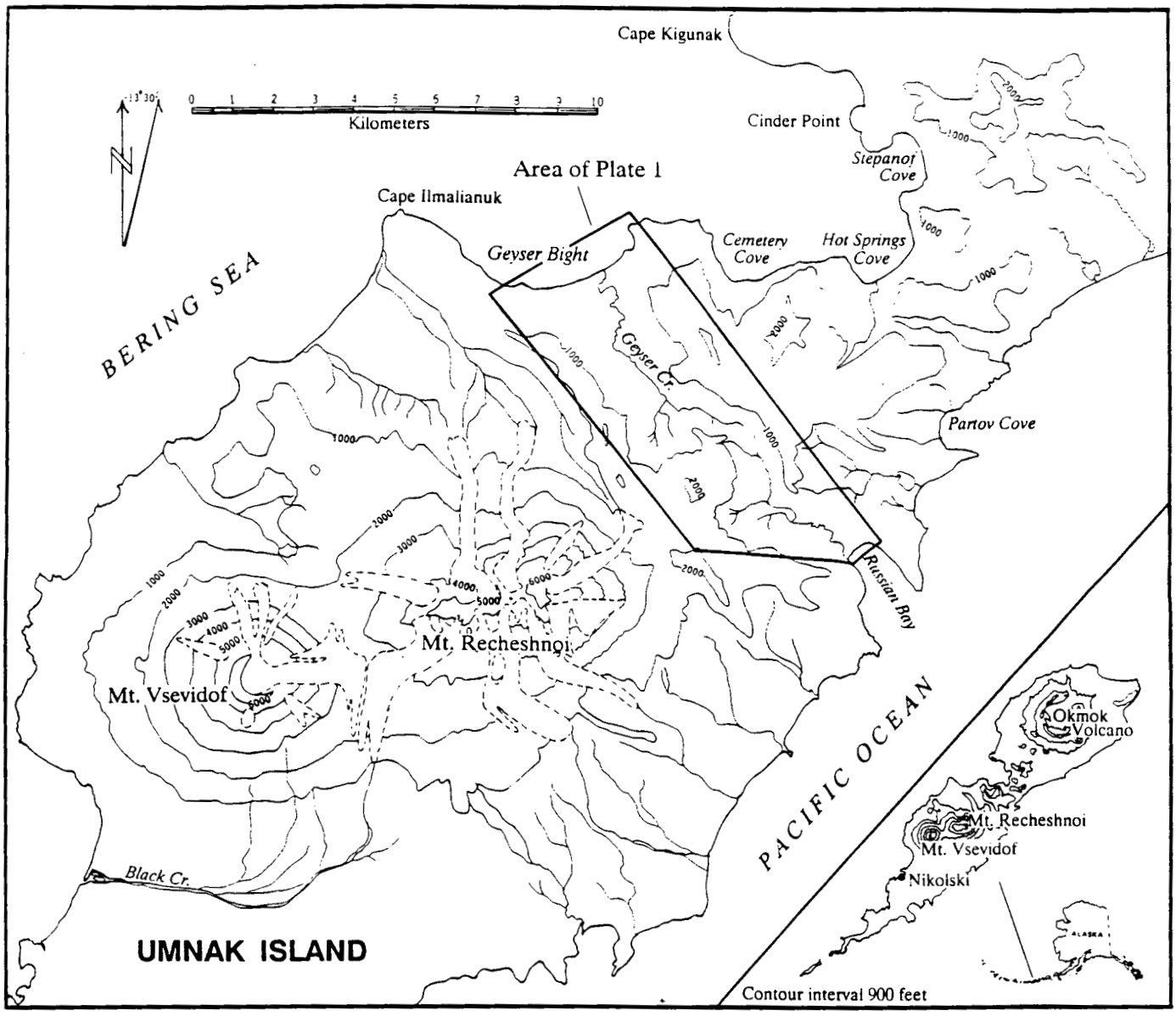

Figure 1-1. Generalized map of Umnak Island showing boundaries of geologic map (Plate 1).

discovered by our party about 2.5 km south of these previously-reported fields.

1.2 Regional Geologic Setting

Recent reviews of the geology and tectonics of the Aleutian arc region are given by Scholl and others (1987) and Stone (1988). These reviews provide a convenient entry into the extensive literature about the Aleutian arc and the Bering Sea, and are summarized here.

The part of the North American plate which underlies the Aleutian arc is oceanic west of 166°W, composed of a broad continental shelf between 166°W and about 156°W, and continental east of 156°W. The Pacific plate is oceanic throughout, except for a small sliver of continental crust at its easternmost margin. Umnak Island, and the Geyser Bight geothermal area, are just west of the oceanic-continental transition. There are no major tectonic anomalies in the arc in the vicinity of Umnak Island.

Formation of the oceanic portion of the Aleutian arc was initiated during early Tertiary time (~55 Ma), when the Kula plate buckled and began to subduct beneath itself, thus trapping a piece of oceanic crust between the arc and the edge of the Bering shelf and accreting that piece of oceanic crust to the North American plate. The trapped piece of oceanic crust is now the floor of the southwestern half of the Bering Sea. First the Kula plate and then the Pacific plate underthrust the margin of the North American plate since that time. The broad geometry of the subduction system has not changed throughout Tertiary and Quaternary time. There has been subduction under the continental portion of the arc, at least intermittently, during much of the Mesozoic, as

well as Cenozoic, although that part of the arc was not yet accreted to North America (see Panuska and Stone, 1985; Coe and others, 1985, for reviews).

The oceanic portion of the Aleutian arc formed as an igneous and sedimentary welt on abyssal oceanic crust. The arc grew to sea level by the end of the Eocene. During the Oligocene and Miocene arc growth slowed and erosive processes became relatively more important. The transition from early, rapid growth to waning activity was approximately coincident with the demise of the Kula-Pacific spreading center and the change of subduction to a more oblique angle. Starting in the Pliocene, the arc was truncated by wave action, forming a shallow platform at the summit of the ridge as wide as 100 km. The Aleutian Islands are the emergent portions of this platform. Quaternary volcanism is confined to a narrow belt in the northern part of the summit platform.

Rocks which were deposited during the early phase of rapid growth are referred to as the lower series (Scholl and others, 1987). Lower series rocks consist of volcanics, hypabyssal intrusives, stocks and plutons, and locally derived sedimentary rocks. They are pervasively altered and lightly metamorphosed, but generally at less than greenschist facies. Lower series rocks are often broadly folded and regionally tilted. The rocks of southwestern Umnak belong to the lower series, and appear to have accumulated in summit basins adjacent to active volcanic centers (McLean and Hein, 1984). In the Geyser Bight area the lower series is represented by the Tertiary sedimentary and volcanic rocks (Tvs, see Geology section). Although exposures are limited, the unit in Geyser Creek valley appears to have a higher proportion of volcanic rocks than that described by McLean and Hein (1984) to the southwest.

Rocks deposited as volcanic activity waned during the Oligocene and Miocene are termed the middle series (Scholl and others, 1987). They consist mostly of a blanket of slightly deformed, diagenetically altered, marine sedimentary rocks which drape the outer flanks of the arc. These rocks are not exposed on Umnak Island. The plutonic rocks in the Geyser Bight area also belong to the middle series. Plutonic masses comprise much of the middle series along the crest of the arc (see Scholl and others, 1987 for a summary of occurrences).

Large-scale structural features of the arc are described by Geist and others (1988). These features consist of tear-away canyons and summit basins which formed by the rotation of at least 5 discreet blocks, each 150 to 400 km long and 125 km wide. Block rotation is presumably in response to oblique subduction in the western part of the arc. Within these blocks deformation is restricted to broad folding and minor faulting (Scholl and others, 1987). Volcanoes are, in general, located at or continentward of the continentward limit of the blocks. The Geist and others (1988) analysis does not extend as far east as Umnak Island.

Chapter 2 of this report discusses the geology of the Geyser Bight region in detail.

1.3 Previous Work

Reports of the Geyser Bight hot springs appear in Grewingk (1850), Dall (1870), and in Waring (1917) and their existence was probably known to Aleut villagers at Nikolski since ancient times. Byers and Brannock (1949) conducted an extensive survey of the thermal spring areas during their reconnaissance geologic mapping of Umnak Island in 1946-48 and reported

analyses on water samples from two of the springs. Samples from four thermal springs were also collected and analyzed by I. Barnes (pers. comm., U.S. Geological Survey, 1981) in 1975 as part of a USGS reconnaissance investigation of hot spring sites in the Aleutian arc. In 1980 a party from the Alaska Division of Geological and Geophysical Surveys sampled and analyzed seven Geyser Bight thermal springs and measured spring discharges during a regional assessment of geothermal resources in the Aleutian Islands for the state of Alaska (Motyka and others, 1981). Their preliminary studies suggested that these hot springs are fed from multiple reservoirs, ranging in temperature from 160° to 190°C, which in turn are related to a deeper parent reservoir having a temperature as high as 265°C.

Prior to this study, the most detailed geologic map which included the Geyser Bight geothermal area was a 1:96,000 scale map of southwestern Umnak produced during a 6 week reconnaissance during the summer of 1947 (Byers, 1959). This map shows the major rock units which we mapped in more detail during 1988. McLean and Hein (1984) provide additional detail on Tertiary rocks southwest of Umnak's volcanoes. Byers (1959) provides petrographic descriptions and some chemical analyses of many of the rock units found in the Geyser Bight area. Byers (1961) provides detailed petrogenetic interpretations of the chemistry and mineralogy of central Umnak volcanic rocks. These interpretations focus on petrogenetic processes, rather than temporal and stratigraphic evolution of volcanic systems -- our goal in this study.

1.4 Purpose and Scope of this Study

The purpose of our resource assessment study was to obtain new geologic and geochemical data for one of Alaska's most promising geothermal resource

areas and to produce an integrated analysis of the resource with improved estimates of reservoir temperatures and of the magnitude of energy available for future development.

As fossil fuels become scarce, industry may be forced to locate in regions with readily-available energy. Thus the Geyser Bight area may become attractive for uses such as processing ore, producing hydrogen by electrolysis of water (for later use in fuel cells at other locations), seafood irradiation, or other energy-intensive industries.

The central Aleutians are sparsely populated and remote. However, rapid growth of the American bottom-fish industry in the Bering Sea and northern Pacific Ocean, as well as increased oil and gas exploration in the Bering Sea, are generating an increased need for power in the region. This industrial growth may well make development of high-quality geothermal resources attractive, even if they are not near current population centers. Economic feasibility studies at Dutch Harbor, 85 miles to the east on Unalaska Island, show that the cost of production of electricity using the Makushin geothermal resource is competitive with diesel-fired generators given sufficiently high flow rates in the geothermal wells (Spencer and others, 1982). The high cost of developing the Makushin geothermal resource is in part due to its relative inaccessibility; it is well inland on the flanks of a rugged volcano.

We believe that Geyser Bight is a particularly attractive alternative to Makushin should the Makushin field prove insufficient for industrial development in the central Aleutians or should logistical costs prevent its development.

1.5 Land Status and Accessibility

The Geyser Bight geothermal area is on federal land under the jurisdiction of the U.S. Bureau of Land Management. Its official designation is the Geyser Springs Basin Known Geothermal Area (KGRA). BLM, and under a cooperative agreement, the U.S. Fish and Wildlife Service, would be involved in any lease sale, permitting for drilling, etc., and in any further exploration or development of the resource in the near future. Under the guidelines of the 1971 Alaska Native Claims Settlement Act (ANCSA), native Alaskan groups and the State of Alaska can select federal land up to their entitlement limits . The Aleut Native Corporation, the St. George Village Association, and Tanadquisix Village Association from St. Paul Is. have each selected the entire KGRA and some surrounding areas. It is possible that some or all of the native groups have selected more than their entitlement, in which case they would have to prioritize their land claims, and receive title to only some of them. The State of Alaska has also tentatively selected land in the southern part of the KGRA, in an area including the superheated fumarole site (F3, Plate 1), but not including any of the hot spring areas. The State of Alaska has until January 2, 1994, to make additional selections. BLM is responsible for adjudicating land claims, and, by the rules of ANCSA, gives preference to native groups, once the State determines that its interests are not compromised.

There are several semi-protected bays near the Geyser Bight resource, such as Hot Springs Cove and Russian Bay. With some improvements such as breakwater construction and/or dredging, a suitable deep-water harbor could possibly be constructed at one or more of these sites. The flat floor and gentle slope of Geyser Creek valley would allow road building from the beach

to the thermal area, a distance of only 3 miles. There is a large airfield in good condition at Fort Glenn (WW II, abandoned) located at the east end of the island, about 30 miles from Geyser Creek valley. An unimproved road leads from Fort Glenn to within 10 miles of Geyser Bight.

Our field work for this project was done on foot from a tent camp in the lower Geyser Creek valley. Field gear was flown from Fairbanks to Nikolski, 35 km southwest of the field site. Nikolski is the nearest village to Geyser Bight. Gear and personnel were transported from Nikolski to the field site by two inflatable boats and one aluminum skiff. We ran through light surf into the mouth of Geyser Creek and then lined and motored halfway through the dune field to our campsite. We also used the inflatable boats to put in one spike camp at Hot Springs Cove. Surf conditions at Geyser Bight would have made small boat operations unsafe during much of our field time. Any larger field effort, or a field effort requiring heavy equipment, would probably be best facilitated by use of a landing craft from Dutch Harbor.

2. GEOLOGY OF THE GEYSER BIGHT AREA

2.1 Overview

The oldest rocks on central Umnak Island are fine-grained Tertiary volcanic and sedimentary rocks of low metamorphic grade (Tvs, Plate 1). These rocks, along with the Late Miocene dioritic pluton which intrudes them (Tdp, Plate 1) form the base of a broad wave cut platform 100 to 200 m above sea level. Plutonic rocks as young as 9.5 Ma (this report) are cut by this surface at Geyser Bight. This major unconformity was formed in the Pliocene and is regional in extent (Scholl and others, 1987). Quaternary volcanic rocks spanning at least 1.5 m.y. (this report) were erupted from several volcanoes and deposited on this platform. These volcanoes and their eroded remnants provide 600 m of relief in the immediate vicinity of Geyser Bight valley. The older of these volcanoes had vents northeast of Geyser Bight (Figure 2-1). The remnants of these volcanoes consist of central vent complexes surrounded by lava flows which dip radially outward. The volcanoes have been eroded extensively, obscuring their original constructional morphology. Mt. Recheshnoi is the closest of the Pleistocene volcanoes, and has erupted in Holocene time. It is about 2000 m tall and its summit is 8 km southwest of Geyser Bight. Mt. Recheshnoi is predominantly calc-alkaline basalt and andesite. There have been flank eruptions of quartz-andesite, andesite, and rhyolite within the last 140 ka. The youngest flank eruption was 3,000 years ago (Black, 1975). The rhyolite flank vents comprise one of only two known rhyolite occurrences west of the Valley of Ten Thousand Smokes 1000 km to the east. Mt. Vsevidof, 6 km west-southwest of Mt. Recheshnoi, is

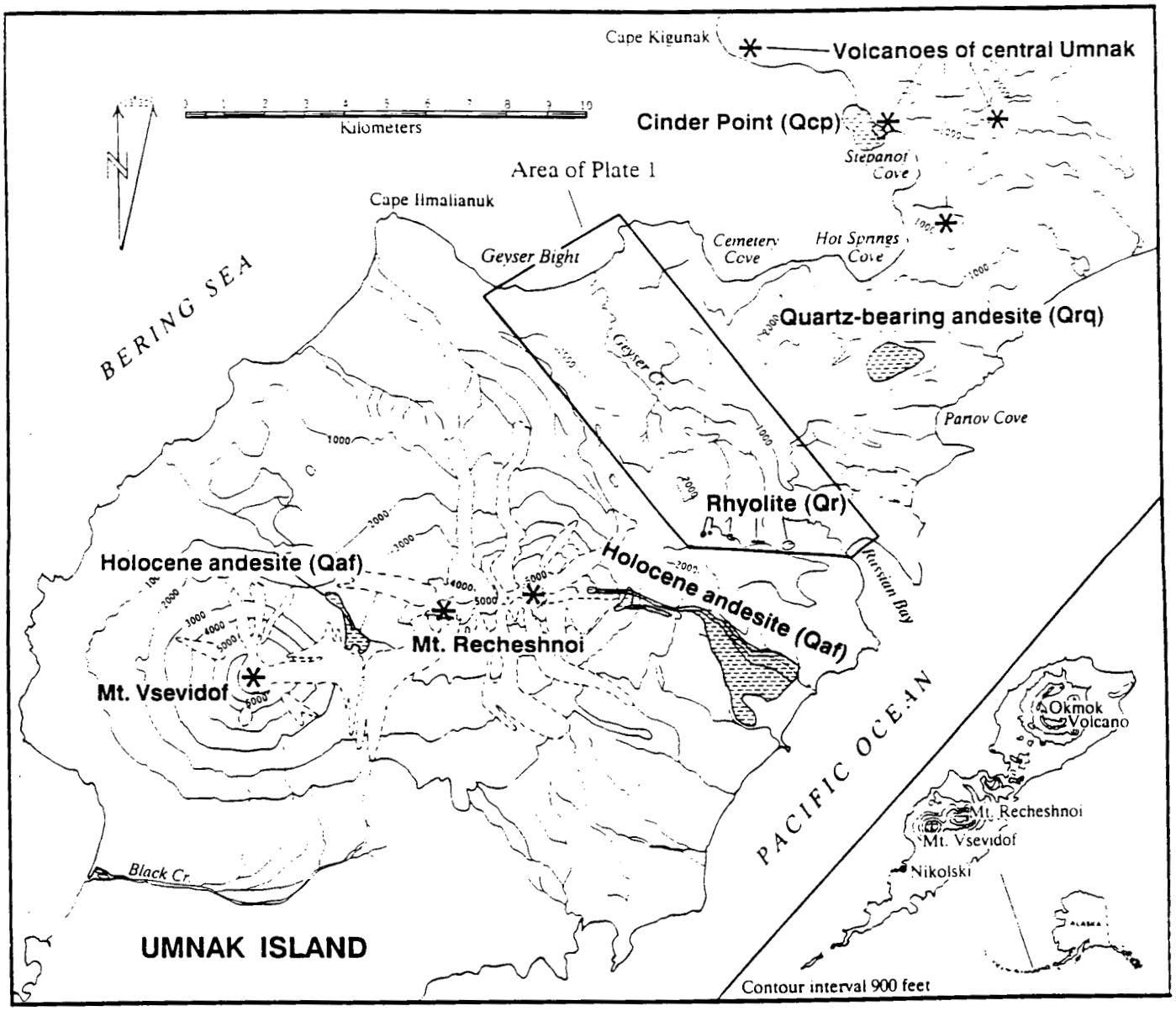

Figure 2-1. Locations of some volcanic centers on central Umnak Island.

an active volcano which appears to be dominantly Holocene in age. Flows from Mt. Vsevidof do not crop out in the Geyser Creek area.

The hot springs, fumaroles, and geysers of the Geyser Bight area are located at the head of a large Pleistocene valley cut in the bedrock units discussed above.

The remainder of this chapter describes the field geology of the Geyser Bight area in more detail. The discussion is organized by map unit (Plate 1) and arranged in chronologic order from youngest to oldest. While this section emphasizes units on the detailed geologic map (Plate 1) it also includes discussions of units which were investigated as part of this study but which are not in the map area. The rock units are, with very few exceptions, those of Byers (1959).

2.2 Description of Rock Units

2.2.1 Beach Sand (Qb)

There are active beaches at both Geyser Bight and Russian Bay. They are composed of well sorted medium- to coarse-grained sand. Beach faces are moderately steep due to frequent moderate to heavy surf.

2.2.2 Alluvium (Qal)

Alluvial silt, sand, and gravel fill the bottoms of Geyser Creek valley and Russian Bay valley. The modern streambeds contain pebbles up to a few cm in diameter but areas away from the streams can be underlain by peat and overbank mud of undetermined thickness.

These valleys presumably formed in a manner common in the Aleutians, whereby glacially carved Pleistocene valleys were drowned by post-glacial sea level rise. The deep bays thus produced were isolated by bay-mouth bars, producing lakes. These lakes were then filled by alluvium as well as overbank silt, lagunal and lacustrine deposits, and tephra. It is likely that there is glacial till below the alluvium. If this model is correct then fill in Geyser Creek valley and Russian Bay valley may be quite thick and formed of a complex intertonguing of glacial till, alluvial sand and gravel, very fine-grained overbank and lacustrine silt and peat, and tephra. Because so much deposition may have occurred at or below sea-level the average grain-size could be quite small. Alluvium in Geyser Creek valley is likely to be very thin near head of the valley.

Makushin Valley, on neighboring Unalaska Island, is a valley similar in size and, perhaps, history to Geyser Creek valley. Near its downstream end it was found to have about 7 m of sod and organic-rich silt underlain by 22 m of water-saturated silt and fine sand, in turn underlain by 20 m of glacial till(?) (Krause, 1986).

2.2.3 Dune Sand (Qd)

The beaches at Geyser Bight and Russian Bay are backed by extensive fields of inactive, vegetated dunes. The dunes are composed of well sorted medium- to coarse-grained sand similar to that forming the beaches. Older dunes (farther from the beaches) are often mantled by cm-thick red and black tephra layers with an aggregate thickness of a few meters. Dunes are typically 15-20 m high, and locally as much as 45 m high at Geyser Bight and 35 m high at Russian Bay.

2.2.4 Glacial Till (Qgt)

Irregular piles and hummocks of unstratified, locally derived boulders and cobbles lie in shallow, gently sloped basins perched above the major valleys. These deposits are of probable latest Pleistocene age. The total thicknesses of the deposits are at least several meters. These are the only late Pleistocene glacial deposits in the map area. Byers (1959) shows Pleistocene and neoglacial moraines on the flanks of Mt. Recheshnoi, southwest of the area of Plate 1. Similar hummocky drift deposits occupy similar shallow alpine valleys elsewhere on the island, usually on the flanks of Mt. Recheshnoi. An older glacial drift unit (Qgd) is described subsequently.

2.2.5 Alluvial-Colluvial Fans (Qf)

This unit comprises coarse, poorly sorted alluvial and colluvial material deposited in short, steep fans on the sides of main valleys at the mouths of minor streams and gullies.

2.2.6 Undifferentiated Colluvium (Qc)

Colluvium of undetermined origin was mapped when thick enough to prevent accurate determination of underlying bedrock. There are no associated landforms to indicate the nature of the material.

2.2.7 Holocene Tephra (Qt)

Orange, brown, and black tephra units have accumulated up to 4 m thick in some upland areas with low relief. Individual beds are typically a few cm thick, but can be a few tens of cm thick. Beds are orange to black. The tephra is mostly medium to coarse ash, although there is at least one prominent bed of lapilli-sized pumice. This unit was mapped where it was

thick enough to obscure underlying bedrock units. The unit includes some small bedrock outcrops too small to show at map scale.

2.2.8 Rhyolite (Qr)

A series of at least seven small rhyolite bodies occur along an east-west zone south of Russian Bay valley. The largest outcrop is 0.5 km in diameter, and the smallest is only about 0.1 km in diameter (Plate 1). The rhyolite forms dense, flow banded outcrops. Flow banding is typically subparallel to the trend of the outcrops and is steeply dipping. The rhyolite is glassy to devitrified and sparsely phyric. The phenocryst mineralogy is plagioclase, biotite, quartz, and minor opaque oxides. The rhyolite also contains rounded inclusions of typical Recheshnoi andesite up to several cm in diameter. These inclusions contain ~10% plag+cpx+ol set in a fine grained quenched groundmass, and appear to have been incorporated in the rhyolite while still molten. Biotite from one of the rhyolite outcrops was dated at about 135 ka (see Geochronology section).

Several observations suggest that all rhyolite outcrops may be part of a single, near-vertical, dike-like body. These include the strongly linear outcrop pattern, the dense nature of the rhyolite, and the occurrence of steeply dipping and contorted flow banding. The lack of any associated subareal deposits or subhorizontal structure indicate that the rhyolite is not the eroded remnant of an ashflow or subareal lava flow. The larger bodies may be eroded remnants of domes, and the smaller bodies may be feeders to domes which were subsequently removed by glacial erosion. Rhyolite outcrops are spatially discreet and rhyolite is not exposed in gullies between outcrops, suggesting that only fingers of the postulated dike reached the surface.

2.2.9 Holocene Andesite (Qaf)

Holocene andesite flows extend from small vents high on the eastern and western slopes of Mt. Recheshnoi (Figure 2-1). None of these flows are within the map area of Plate 1, although the easternmost two of the flows identified by Byers (1959) were sampled during this study. The older flow erupted from a vent at about 700 m and flowed about one kilometer horizontally and 350 m vertically down the flank of the volcano. The younger flow erupted from a vent at about 1260 m and flowed 6 km down the flank of the volcano. Its terminus is among Holocene beach ridges. Both flows are narrow and were apparently quite fluid.

The flows are 58% SiO_2 andesites which contain 10 to 15 volume percent phenocrysts dominated by plagioclase and including clinopyroxene, olivine, orthopyroxene and magnetite. Most of the plagioclase is normally zoned, although the older flow contains a small proportion of resorbed, reversely zoned and/or spongy plagioclase phenocrysts. The younger flow contains rounded inclusions of highly vesicular olivine + clinopyroxene + plagioclase-phyric basaltic andesite (about 55% SiO_2). The inclusions appear to have been mixed into the host andesite while still liquid. These appear very much like the quenched basaltic blobs described by Eichelberger (1975) from Glass Mountain in Oregon.

The older flow presently has small colonies of moss and some grass growing on it but most aspects of flow morphology are unaltered. The younger flow is much less vegetated and is thus substantially younger. The younger flow has well preserved lateral levees and concentric ropy flow structures in its lower part. The upper part of the flow is blocky. Black (1975) states that the

younger flow was coincident with a neoglacial advance, and is thus about 3,000 years old.

2.2.10 Quartz-bearing Andesite (Qrq)

There is a small vent on the ridge crest between Hot Springs Cove and Partov Cove (Figure 2-1) which erupted basaltic andesite scoria and stubby lava flows. The present outcrop area is about 2 km by 1 km, and elongated to the east-northeast. There is a closed depression about 250 m in diameter and 10 m deep in the west-central part of the unit which is probably the original vent. The northern part of the unit is composed of agglutinated scoria and bombs a few to several cm in diameter, which probably represent the remains of a cinder cone. Steep-fronted concentric lobes make up the eastern part of the unit. These are probably stubby flows which issued from the base of the former cone. The tops of the flows are massive andesite and have shallow eastward drainages. Rubbly flow tops and cinders were not found, although they probably formed during the initial eruption. It is most likely that cinders and loose blocks were removed when Umnak Island was buried by glacial ice. These flows erupted about 89 ka (see Geochronology section), and thus were exposed to most of the last glacial cycle. However, glacial erosion was not severe enough to radically alter the initial volcanic morphology. It may be that this unit was not heavily glaciated because of its location at the top of a high ridge.

Most of the unit is composed of basaltic andesite with about 54% SiO_2. The lavas are compositionally similar to other lavas from the area except for MgO, which is high for the SiO_2 content. This may reflect magma mixing within this unit. As noted by Byers (1959), the mineralogy of these lavas is unusual. They contain plagioclase, magnesian olivine, clinopyroxene,

orthopyroxene, magnetite, and some embayed beta-quartz. The complexity of this mineral assemblage suggests that magma mixing occurred.

The unit also contains mafic clots. These have about 65 volume percent crystals which are dominantly hornblende pseudomorphs. The clots also contain phenocrysts of plagioclase, olivine, and clinopyroxene. The groundmass consists of quenched plagioclase, pyroxene and glass, which is mostly now devitrified.

2.2.11 Lavas of Cinder Point (Qcp)

Cinder Point is a small cindercone with two lobate lava flows on the northeast edge of Inanudak Bay (Figure 2-1). The cinder cone is 178 m tall and the lava flows are nearly circular in map view and about 200 m in diameter. The summit cone has been only somewhat modified by erosion, and is therefore probably early Holocene in age. The Cinder Point cone is equally distant from both Okmok Caldera to the northeast and Mt. Recheshnoi. The cone is the westernmost of five aligned vents near Inanudak Bay (Byers 1959).

Cinder Point lavas are highly porphyritic, high-alumina basalts. The dominant phenocrysts are subhedral plagioclase crystals up to 5mm long (average 1.5mm) which have thin corroded rims, but are free of spongy zones. There are occasional multigrain aggregates of plagioclase. Cinder Point lavas contain lesser amounts of clinopyroxene and olivine crystals which are subhedral and subequant and 0.1 to 0.2 mm long.

2.2.12 Lavas of Mt. Recheshnoi (Qral, Qra, Qrd)

Mt. Recheshnoi is a large, heavily glaciated stratocone on central Umnak Island, southeast of Geyser Creek (Figure 2-1). It is of Late Quaternary age

(see Geochronology section). The central part of the cone is built on a flat erosional surface 60 m above sea level which is cut on Tertiary plutonic and sedimentary rocks. This surface is part of the regional 5.3 Ma Aleutian summit platform (Scholl and others, 1987). The east and northeast flanks of Recheshnoi overlie up to 300 meters of lava flows from older volcanoes. The central 40-50 km^2 (above 1000 m elevation) consist of pyroclastic beds and a vent complex (Byers, 1959). This area has been heavily eroded by several small valley glaciers and retains none of its original constructional volcanic form. The summit area consists of a 4 km long east-west ridge which may reflect construction from an older eastern vent and a younger western vent (Byers, 1959). Below 1,000 m the volcano consists of basalt and andesite flows with minor pyroclastic interbeds. The original constructional surface is preserved in some upland areas between glaciers, especially on the western flank. There are also some flows which fill Pleistocene glacially-carved valleys. The summit elevation is 1984 m, and deposits from the volcano cover 360 km^2.

In the Geyser Creek area this unit consists of basalt and andesite lava flows which are interbedded with minor pyroclastic units. Flows typically have a thin, brick-red, rubbly bottom which grades upward into platy lava. Thicker or more mafic flows can have massive or columnar interiors. Upper parts of the flows are again rubbly and oxidized. Intervals between flows are usually poorly exposed, but contain pyroclastic material, soil, and colluvium. Individual flows are typically 4 to 12 m thick. Some flows are substantially thicker, presumably due to local ponding. Occasional zones several tens of meters thick are brick-red throughout, and contain very thin platy flows in a rubbly matrix. These zones may have formed during single eruptive events as very rubbly aa flows continually overran their margins.

Except for the syneruptive brick-red oxidation on flow tops and bottoms lavas from this unit are unaltered. All fractures in the flows are those attributable to post eruptive cooling. We observed no tectonic fractures in the rocks. Flows dip to the north, northeast, and east, away from the summit of Mt. Recheshnoi, at gentle to moderate angles.

Most flows in the map area are truncated by the large glacial valleys which terminate at Geyser Bight and Russian Bay. These flows are shown as Qra on Plate 1. In contrast, valley-filling flows (mapped as Qral) occur near Russian Bay valley. These deposits consist of debris flows, lahars, ashflows, and minor lava flows. West of the head of Russian Bay valley these deposits are deeply incised by very steep-walled gullies as a consequence of their poorly consolidated nature. An ashflow is preserved in small benches on the northeast side of Russian Bay valley, and in thicker deposits on the southern side of the valley. These flows are of probable late Pleistocene to Early Holocene age and are, save flows from flank vents, among the most recent deposits of Mt. Recheshnoi.

There is a large, steeply dipping, northeast trending dike south of the pass between Geyser Creek and Russian Bay valley. This dike is mapped as Qrd (Plate 1). There are smaller dikes elsewhere within the Recheshnoi pile, but this dike is unusual because of its large size. It is easily distinguished on small scale radar images and photographs. It forms a barrier to stream flow and has ponded a small patch of alluvium just below the pass into Geyser Creek. It is mantled by glacial drift.

Recheshnoi lavas are usually porphyritic and contain 25 to 40 volume percent phenocrysts. Aphyric lavas are rare. Plagioclase is ubiquitous and occurs in two major textural varieties. The first variety (plagl of Table 4-

1) is characterized by euhedral, unzoned or normally zoned, twinned, inclusion free crystals. These occur both as large tabular crystals and as smaller prismatic crystals. The second variety (plag2 of Table 4-1) is characterized by tabular rounded and resorbed crystals which can be reversely zoned and often contain spongy zones or cores. Lavas with less than 56.5% SiO_2 contain prismatic euhedral to subhedral olivine crystals. Some high-Si andesites also contain olivine. Stubby prismatic clinopyroxene crystals are ubiquitous. Most andesites, but few basalts, contain elongated prisms of subhedral orthopyroxene. Orthopyroxene concentrations are usually less than clinopyroxene concentrations. Titanomagnetite is a common accessory phase. Hornblende was found in only one sample.

2.2.13 Glacial Drift (Qgd)

A section of glacial drift up to 800 m thick is exposed in the southwest wall of Geyser Creek valley, stratigraphically between lavas of Mt. Recheshnoi and the volcanics of central Umnak (see below). The drift has thick massive portions as well as thinner fine-grained portions. Massive portions are coarsely bedded and poorly sorted. They contain rounded andesitic blocks up to 1 m in diameter in a matrix dominantly composed of sand-sized material. There are thin, very fine-grained, possibly tuffaceous, laminations about 1 cm thick which are well sorted.

The lava flows in closest proximity, which yield younger and older limiting ages for the drift are given by DT88-17 and DT88-5 and are 499±14 and 1,104±37 ka, respectively (Plate 1, Geochronology section). It is likely that the drift was deposited between the periods of activity of the volcanoes of central Umnak and Mt. Recheshnoi. Available geochronologic data suggest that this time was between 500 and 800 ka.

2.2.14 Volcanics of Central Umnak (Qcuv)

The volcanics of central Umnak lie stratigraphically beneath Mt. Recheshnoi (Qcuv on Plate 1). This unit is stratigraphically equivalent to Byers' (1959) QTv. We use a different unit label on Plate 1 because the unit does not contain Tertiary rocks (see Geochronology section). Lavas and pyroclastic rocks were erupted from several small, Early Pleistocene vents located on central Umnak Island (Figure 2-1). The vent areas lie outside the map area of Plate 1, thus much of this discussion of volcano morphology relies heavily on Byers (1959). Four to six of the vents are now exposed. This unit is covered by Okmok Volcano to the northeast and Mt. Recheshnoi to the southwest, thus additional vents may be hidden. The exposed volcanoes are heavily eroded, and are 3 to 7 km in diameter and less than 800 m high. Individual vents have outwardly dipping basalt and andesite flows and a central core dominated by breccia, tuff, and feeder dikes. Byers (1959) mapped several zones of altered, silicified, or K-feldspathized rocks. We did not visit any of these areas.

In the Geyser Bight area the unit consists of south to southwest dipping basaltic and andesitic lava flows with minor pyroclastic and brecciated interbeds. Vent areas similar to those exposed east of Inanudak Bay do not occur in the area of Plate 1. The lava flows are similar in appearance and composition to those from Mt. Recheshnoi (see above), except that aphyric and sparsely phyric lavas are more common, and resorbed and corroded plagioclase is less abundant.

This unit is recognized in the field by the south to southwest dip of its lavas (into Mt. Recheshnoi and away from central Umnak) and by their lack of

both alteration and persistent tectonic fracture pattern (exhibited by the underlying Tvs unit).

2.2.15 Quartz Diorite and Quartz Monzonite Pluton (Tdp)

Dioritic and monzonitic plutonic rocks in part of Late Miocene age (see Geochronology section) crop out at low elevations on the western and eastern walls of the lower half of Geyser Creek valley (Plate 1). These rocks may be part of a larger plutonic body which crops out in a few locations at the base of Mt. Recheshnoi and Mt. Vsevidof (Byers, 1959). This larger plutonic body may be either a single large pluton or an amalgamation of several smaller bodies of Oligocene to Miocene age. Outcrop is not continuous, so field evidence of multiple plutons could not be obtained. For convenience, all plutonic rock will be referred to as a single pluton in this discussion. The pluton lies unconformably below the volcanic rocks. This unconformity represents the regional wave-cut platform at the summit of the Aleutian ridge discussed by Scholl and others, (1987). The lower contact of the pluton is not exposed. Plutonic rocks in the Geyser Bight area are, at least in part, much younger than, and therefore not related to, the Oligocene quartz diorite and diorite stocks described by McLean and Hein (1984) from southwestern Umnak (see Geochronology section).

Our mapping shows that plutonic rock occurs much farther up Geyser Creek valley than previously mapped by Byers (1959), thus increasing the probability that plutonic rock may host the geothermal system. Individual outcrops of plutonic rock are fairly homogeneous, medium-grained, and equigranular. Fractures are usually spaced a few to a few tens of cm apart. Individual outcrops often bear several fracture sets at different azimuths and dips. There is no single pervasive joint orientation on either outcrop or regional

scale. Steeply-dipping mafic and andesitic dikes a few tens of cm to a few m across are common, but have no strongly preferred orientation.

Plutonic samples in the Geyser Creek valley and on the shore of Geyser Bight are pyroxene-hornblende quartz monzonite and pyroxene-biotite-hornblende quartz diorite (Table 2-1, Figure 2-2). Samples from near Geyser Bight are quartz diorite or plagioclase-rich quartz monzonite. Samples from further up-valley are plagioclase-poor quartz monzonite. Up-valley samples have moderately higher SiO_2 and dramatically higher K_2O than samples from Geyser Bight. On the K_2O-SiO_2 plot of Figure 2-3 the trend defined by the quartz diorite and quartz monzonite steeply cuts the medium-K to high-K boundary of Gill (1981), and is much steeper than can be produced by fractional crystallization.

The more potassic samples have higher modal concentrations of K-feldspar (Table 2-1), which is presumably the major site of potassium in the rocks. The K-feldspar occurs as large discreet subhedral grains and in micrographic and myrmekitic intergrowths with quartz. These textures are igneous in origin, which indicates that the anomalous K_2O contents have an igneous, rather than a metamorphic or metasomatic origin. Much of the K-spar occurs as late stage intergrowths with quartz. This suggests that the K_2O-rich nature of the rocks is not related to accumulation of feldspar phenocrysts, but must be related to the evolution of a K_2O-rich magma. If the K_2O-rich and K_2O-poor magmas are related to each other it must be by some process other than fractional crystallization. It is more likely that they are not genetically related, and reflect independent periods of stock emplacement. High-K magmas rarely erupt in the modern Aleutian arc, but are found in some plutonic rocks elsewhere in the arc (Kay and others, 1982). McLean and Hein (1984) report

Table 2-1. Modal abundances of minerals in plutonic rock samples.

	DT88-01a	DT88-01b	DT88-02	DT88-03	DT88-04	88CNU10	88CNU11
Plagioclase	60.3	49.7	52.0	60.0	46.0	44.3	44.0
K-feldspar	3.7	6.7	14.7	6.0	19.7	19.0	22.0
Quartz	10.0	8.7	13.3	13.3	12.7	8.3	11.7
Biotite	3.7	0.3	1.3	9.0	0.0	0.0	0.0
Amphibole	15.7	29.0	12.0	0.0	16.3	9.0	9.7
Chlorite	1.7	3.7	4.3	0.3	0.7	2.3	5.7
Pyroxene	3.0	0.3	0.0	8.0	0.3	3.7	3.3
Opaque oxides	1.7	1.0	1.3	2.7	3.7	4.0	3.0
Accessories	0.3	0.7	1.0	0.7	0.7	0.0	0.7
Myrmekite	0.0	0.0	0.0	0.0	0.0	9.3	0.0

Modes are based on petrographic determination of 300 grains per sample. Myrmekite was only counted as a separate phase when intergrowths were of fine enough scale to preclude accurate counting of individual mineral species.

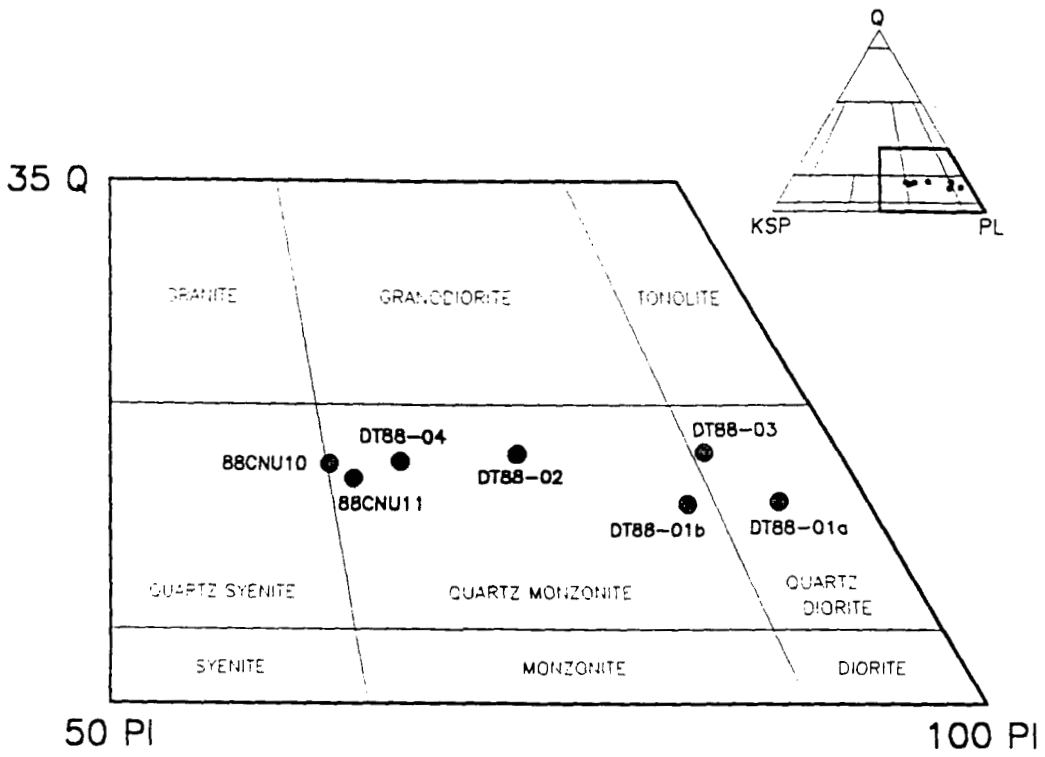

Figure 2-2. A portion of the IUGS plutonic rock classification diagram. Apices are quartz (Q), alkali feldspar (KSP), and plagioclase (PL). Samples are plotted according to modal mineralogy (Table 2-1), rather than normative mineralogy calculated from the chemical composition.

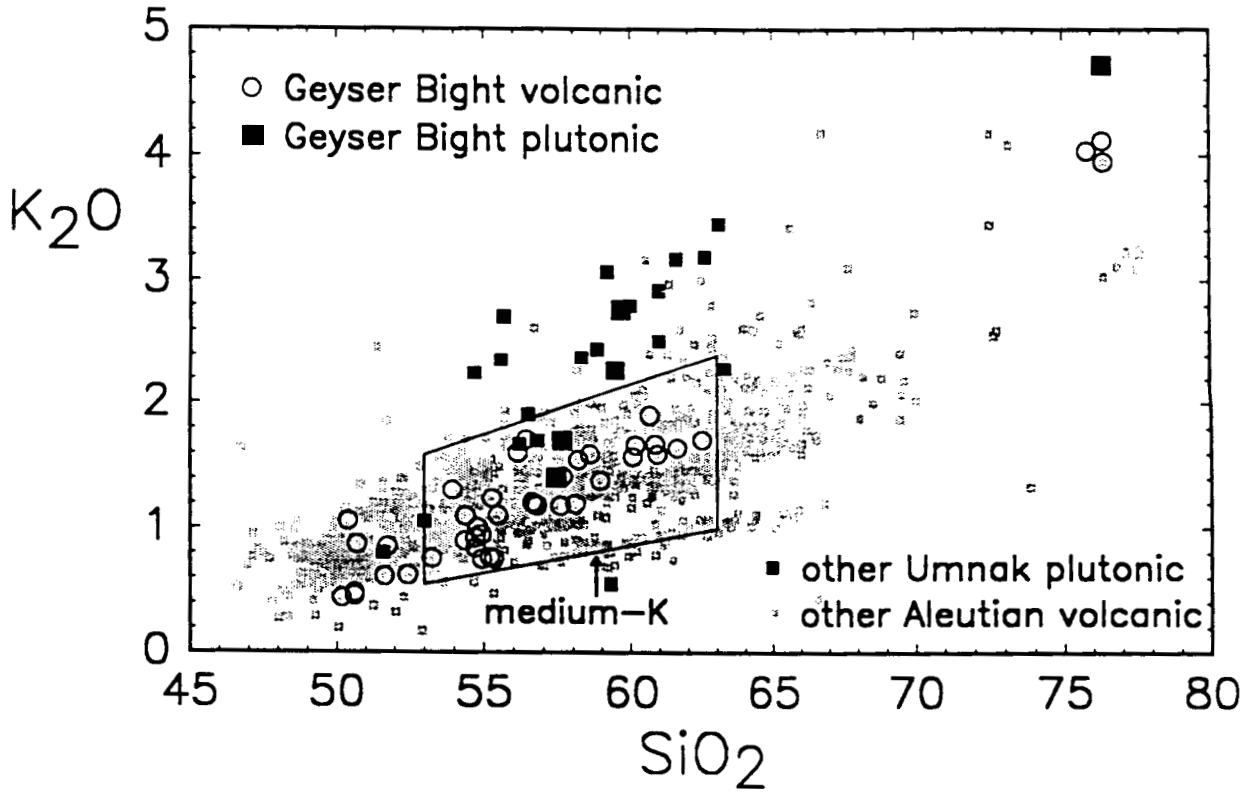

Figure 2-3. K_2O vs. SiO_2 diagram of Geyser Bight plutonic and volcanic rocks (this study; Byers, 1959). Plutonic rock compositions from southwestern Umnak (McLean and Hein, 1984) and literature values for other Quaternary Aleutian volcanic centers are shown for comparison.

31-33 Ma plutonic and hypabyssal high-K rocks of similar composition from southwestern Umnak Island (Fig. 2-3).

2.2.16 Tertiary Sedimentary and Volcanic Rocks (Tvs)

The oldest rock unit in the Geyser Bight area consists of lightly metamorphosed lava flows, dikes, sills, and sedimentary and volcanogenic clastic rocks of Tertiary age. The largest exposures on Umnak are at the southwestern end of the island where there are no overlying volcanic units. Byers (1959) reports that in this area the unit consists of gently dipping mafic lava flows with subordinate beds of argillite and tuff, all of which were intruded by gabbro and diorite which have subsequently been albitized. These rocks are gently folded and are crosscut by minor faults (Byers, 1959). Fracturing is pervasive. McLean and Hein (1984) report late Eocene to early Oligocene ages for these rocks.

In the Geyser Bight area the unit is dominantly composed of fine-grained equigranular to porphyritic hypabyssal and extrusive mafic and intermediate igneous rocks. The unit occurs as screens and blocks within the pluton, and overlies the pluton on the east and west sides of Geyser Creek valley. The exposed maximum thickness in the Geyser Bight region is about 150 m. The upper surface has gently rolling topography identical to that elsewhere on the broad, wave-cut platform which truncates this unit. The contact between the Tertiary volcanic sequence and the pluton is irregular and occasionally of moderate relief.

In the Geyser Bight area alteration of these Tertiary rocks is common. In one good exposure on the southwestern side of Geyser Creek valley hornblende quartz diorite in the lower valley wall outcrops immediately below highly

altered andesite (Tvs) which contains 70% quartz veinlets that appear to originate in the quartz diorite. Pyroxene-plagioclase andesite overlying the pluton on the east side of Geyser Creek valley is pervasively chloritized, and in some localities silicified or pyritized. Once again quartz veining is pervasive. On the east side of the Geyser Bight beach Tvs is fine-grained, but the presence of elongated plagioclase microlites suggest that the unit is volcanic, rather than sedimentary. Unequivocally sedimentary units of Tvs were not seen in the Geyser Bight area.

Tvs is distinguished from overlying volcanic rocks in the field by its pervasive tectonic fracture pattern, and lack of well preserved volcanic features. In addition, Tvs is usually highly altered.

2.2.17 Structure

Only the oldest rocks on central Umnak (Tvs) have been deformed, and these only gently. Beds usually have gentle dips, folds are open, and faults and fractures, although numerous, do not have large displacements (Byers, 1959). South of Mt. Vsevidof, folds trend northwest, and large fractures trend northeast (Byers, 1959). The amount of Tvs outcrop in Geyser Creek valley was not sufficient to allow recognition folds or faults.

Plutonic rocks are well fractured in surface outcrops. Fractures are spaced a few cm to a few tens of cm apart. Most outcrops have several joint sets, but we observed no prominent joint set, nor did we observe jointing in a preferred direction anywhere in the map area. Dikes in the pluton also have no preferred alignment.

The only fractures seen in the volcanics of central Umnak (Qcuv) and the lavas of Mt. Recheshnoi (Qra) are of volcanic cooling origin.

Motyka and others (1981) have noted that Geyser Creek Valley trends northwesterly at the same azimuth that Nakamura and others (1980) suggest is the azimuth of principal compressive stress due to the subduction of the Pacific plate. The Nakamura and others stress trajectory is based on the alignment of parasitic and flank volcanic vents of Aleutian and other Alaskan volcanoes, as well as Quaternary fault orientations. Nakamura and others (1977, 1980) suggest that dilational fractures should appear parallel to the axis of principal compression, and allow easier rise of magma to the surface. It is possible that such fractures could form local zones of weakness and localize a geothermal resource. A search for northwest-trending structures was one of our objectives in this study. As noted above there are no obvious northwest-trending fractures or faults. However, the thick and continuous cover of tephra and vegetation at low elevations may obscure some structures.

An important feature of the Nakamura and others (1977) hypothesis is that flank volcanic features are expected to be aligned parallel to the maximum compressive stress. In the Geyser Bight area this does not appear to be the case. The 3-km linear zone of rhyolite plugs above Russian Bay trends N85W, rather than N47W, which is the convergence direction between the Pacific and North American plates (Jacob and others, 1977). This E-W trend is also reflected in the attitudes of many near-vertical dikes at Geyser Bight, Cemetery Cove and Stepanof Cove. The largest dike we observed in the Geyser Creek area is the northeast-trending dike near the pass between Geyser Creek valley and Russian Bay valley. This dike is part of Mt. Recheshnoi volcano and has a trend nearly orthogonal to that predicted by Nakamura and others (1977).

Our geologic mapping and cross sections (Plate 1) indicate that valley fill is very thin at the head of the valley and that plutonic rock extends much farther up the valley than previously mapped by Byers (1959). We propose that geothermal reservoirs are most likely to occur in the highly fractured plutonic rock, although the Tvs unit may also be present, as shown on cross section B-B. Exploratory drilling at Makushin volcano on neighboring Unalaska Island has demonstrated the ability of plutonic rocks to sustain fracture permeability sufficient to host a geothermal reservoir.

2.3 Volcanic Hazards

The entire Aleutian arc is the locus of intense volcanism, and volcanic hazards are to be expected anywhere within the arc. However, at Geyser Bight and in Geyser Creek valley the volcanic hazards are surprisingly slight, despite the fact that there are two active volcanoes on the island. Mt. Vsevidof, which is unglaciated and therefore has had numerous Holocene eruptions, is 18 km southwest of Geyser Creek valley, but the bulk of Mt. Recheshnoi and the 300 m high ridge southwest of Geyser Creek protect Geyser Creek from flowage hazards. Historic activity at Mt. Vsevidof has been restricted to minor explosions and steaming, and, if this pattern of eruption continues, future activity is expected to only deposit minor amounts of ash on Geyser Creek valley.

Okmok Volcano is 30 km to the northeast and is the most active volcano on the island. Following two mid-Holocene, caldera-forming eruptions, activity has been restricted to steaming, minor ash emissions, and the emplacement of basaltic lava flows on the caldera floor. Activity in the future is expected to continue in the same pattern, with quiet, effusive, flows accompanied by minor ash eruptions. The caldera wall is about 300 m high, and breached only

to the northeast. If lava should erupt in sufficient volume to leave the caldera, it would most likely exit through the northeast breach. There is not enough information available to judge the probability of explosive eruptions, or eruptions from centers outside Okmok Caldera. Geyser Creek valley is separated from Okmok Volcano by Inanudak Bay and a ridge about 600 m tall, and is thus well protected from volcanic activity originating at Okmok (Figure 2-1).

Mt. Recheshnoi is only 10 km southwest of Geyser Creek valley, and is the closest volcano to the geothermal area. The central cone is highly eroded and is thus probably entirely Pleistocene. There have been a few Holocene flank eruptions, including andesite flows on the east and west flanks. The rhyolite bodies and quartz-andesite flows which Byers (1959) considered to be Holocene are shown in this study to be 135 ka and 89 ka old, respectively (see Geochronology section). The flank flows never entered Geyser Creek valley. There is not enough information to estimate the recurrence interval of Holocene eruptions, but the probability of volcanic flows entering Geyser Creek valley seems small. Geyser Creek valley is protected from flowage hazards by a high ridge between the valley and Mt. Recheshnoi. There are no Holocene mass-flow deposits within Geyser Creek valley or Russian Bay valley.

The most likely hazard is ash fall, which could present a temporary hazard to machinery and aircraft operation. Holocene tephra 3-4 m in cumulative thickness occurs throughout the Geyser Creek area.

3. GEOCHRONOLOGY OF VOLCANIC AND PLUTONIC EVENTS

3.1 Background

An accurate determination of the age of eruptive events is critical to the assessment of the geothermal energy resource potential of any volcanic system. We have completed ^{40}K-^{40}Ar age analyses for 23 andesite flows, one rhyolite plug and the plutonic rock which is believed to host the reservoir for the Geyser Bight geothermal system. The results provide a time framework for the mapped rock units and for the evolution of the magmatic system which drives the geothermal resource.

3.2 Analytical Methods and Reliability of Young Ages

All andesite samples were dated as whole rocks. Biotite was dated from the rhyolite plug, and both biotite and hornblende were dated from the pluton. Replicate potassium measurements were done using $LiBO_2$ flux fusion and flame photometry with a lithium internal standard. Mineral standards were used to calibrate the photometer. Argon analyses were done by isotope dilution on a computerized, 6-inch-radius mass spectrometer. Analytical data for the ^{40}K-^{40}Ar age determinations are given in Table 1 (at the end of this section). Sample localities are shown on Plate 1.

Several modifications to our analytical techniques have allowed us to obtain reproducible, stratigraphically-consistent ages on some whole-rock andesite samples as young as 60,000 years.

These are:

Reduction of air argon contamination from the extraction system by replacement of quartz-lined, air-cooled fusion bottles with water-cooled bottles without liners.

Boiling of the whole-rock samples (crushed to 16-48 mesh) for one hour in distilled water immediately before loading into the extraction system has resulted in significant lowering of atmospheric argon per unit sample weight in about 30% of the samples. The reason for this effect is not well understood. It was observed empirically by Curtis, Drake and Deino at the University of California, Berkeley and communicated to Turner, who has been able to produce similar results. One suggested explanation is that the atmospheric argon in cracks in the sample may be replaced by hydrogen during the boiling process (R. Drake, personal com.).

As a general procedure, the argon from one sample fusion is split into 2-4 aliquots and these are analyzed sequentially on the mass spectrometer. The first split is used to "flush" the spectrometer in order to reduce the well-known memory effect in static gas analysis. This effect is particularly important when analyzing young samples with small amounts of radiogenic ^{40}Ar, e.g., most of the Umnak andesites. Results from these "flushing splits" were not averaged in with the subsequent splits unless they were statistically equivalent. The results from the remaining splits were averaged to calculate the values of radiogenic ^{40}Ar, % radiogenic ^{40}Ar and age given in Table 1. With one exception

(88CNU55) the argon analyses in this study represent single fusions of each sample.

Two recent test studies of suites of young andesites from Mt. Spurr, Alaska, and the Nevados de Payachata volcanic group in the Chilean Andes, both done in our laboratory by the methods described above, have produced results which are reproducible within analytical uncertainty and which fit the volcanic stratigraphy observed in the field (Worner and others, 1989, Nye and Turner, 1990). However, dating andesites this young is definitely pushing the limits of the K-Ar method and we have encountered problems with some of the Umnak samples, as discussed in the following section.

3.3 Results

With some exceptions, ages from the 23 dated samples are in agreement with observed stratigraphic relationships and provide a well-constrained time framework for the eruptive history of this volcanic area, as well as a cooling age for the plutonic rock which is believed to host the geothermal system. Ages will be discussed from youngest to oldest, in the approximate order in which they are listed in Table 1.

The youngest, valley-filling flows (Qrf) from Mt. Recheshnoi proved too young for us to date, but three of the upper cone-building flows, (Qra) from this volcano yielded ages of 75,000, 121,000 and ≥110,000 years (minimum age based on petrographic criteria). Lower in the Qra section, we obtained an age of 258,000 years from the NE side of Geyser Creek Valley, and ages of 285,000 and 478,000 years from flows sampled above Hot springs Cove. Basal Recheshnoi flows sampled on the SW side of Geyser Creek Valley gave ages of 472,000, 489,000, 534,000 and 499,000 years. We thus have radiometric ages for Mt.

Recheshnoi flows extending from 75,000 ± 11,000 to 534,000 ± 13,000 years at the base of the section.

The 478,000 year Qra age is problematic because it is from a flow that is only one or two flows below the flow dated at 285,000 years in the same section. We observed no evidence of a paleosol or a fault separating the two dated flows. Field relations suggest that these flows should be similar in age, rather than being separated by almost 200,000 years. However, the 478,000 year age is consistent with the 472,000-534,000 year Qra ages from the SW side of Geyser Creek Valley and therefore cannot be entirely rejected on the basis of the geologic observations discussed above. The sample meets petrographic reliability criteria for whole-rock K-Ar dating. Excess argon is not normally found in significant amounts in subaerial lava flows and is unlikely to be present in the dated sample. At present, we are unable to resolve this problem. Fortunately, it does not affect the documented age span for Mt. Recheshnoi flows (Qra) discussed above.

Sample 88GPU7 is from the easternmost and largest of the seven biotite rhyolite plugs (Qr) intruding Recheshnoi flows (Qra) above Russian Bay (Plate 1). These plugs occur along an E-W-trending, linear zone two miles long and represent the only biotite rhyolite known to us in the entire Aleutian chain. Their presence could possibly suggest the occurrence of a high-level siliceous magma chamber which, if present, might provide a heat source for the geothermal system. An accurate determination of the age of the rhyolite plugs would provide an age constraint for this hypothetical magma chamber and would therefore be important to the assessment of the geothermal system. Biotite separated from the rhyolite gave an age of 135,000 ± 15,000 years. Byers (1959) considered these plugs to be post-glacial, but we observed no field

evidence to support this relationship. It therefore seems possible that the K-Ar age is valid, although it would be desirable to test the biotite for possible excess argon. We plan a future ^{40}Ar-^{39}Ar incremental heating experiment to evaluate this possibility.

Sample 88CNU55 is from the area of quartz-olivine andesite flows (Qrq) overlying Qra above Hot Springs cove. The age of about 90,000 years for this unit appears to be geologically feasible, although older than expected. The well-preserved, concentric flow fronts visible on air photos originally suggested to us that this unit had not been glaciated. However, field inspection revealed that rubbly flow tops have been removed, presumably by glacier ice. The position of this unit on a high, broad ridge uncut by canyons suggests that it was probably overlain by a broad, slow-moving icefield which may have caused relatively little erosion of underlying rocks, thus preserving the concentric flow front morphology. The uppermost Qra section which this unit overlies was dated at 285,000 ± 9,000 years and provides the only available older age constraint for the Qrq unit.

The volcanic flows of central Umnak (Qcuv) underlie the Qra unit. Their attitudes indicate source vents north of Geyser Creek Valley. Five samples from the Qcuv unit flanking Geyser Creek Valley range from 786,000 ± 21,000 years in the upper part of the section to 1,124,000 ± 48,000 years at the base of the section. An additional sample near the top of the Qcuv section above Hot Springs Cove yielded a minimum age of ≥ 426,000 years. The age span of Qcuv flows is therefore documented at ≤ 786,000 ± 21,000 to 1,124,000 ± 48,000 years.

Pyroclastic rocks (Qcup) at Stepanof Cove, presumed by Byers (1959) to be equivalent in part to the Qcuv unit, yielded a minimum age of ≥ 1,368,000 ± 54,000 years. The dated sample is from a radially-fractured andesite block believed to have cooled in place within the pyroclastic deposit. This minimum age is about 140,000 years older than the oldest age we obtained from the base of the Qcuv section on the SW side of Geyser Creek Valley and suggests that pyroclastic activity preceded the Qcuv flows.

Two samples from a single, 1.3 m-thick dike intruding the dated pyroclastic unit (Qcup) at Stepanof Cove gave ages of 1,365,000 ± 41,000 and 1,613,000 ± 56,000 years. The significantly different ages are due to variations in radiogenic ^{40}Ar content per gram of sample (potassium contents are essentially identical). We conclude that the quickly-chilled dike rock contains variable amounts of excess argon and that the younger age is therefore more likely to reflect the true cooling age for the dike. The younger age is concordant with the minimum age of ≥ 1,368,000 ± 54,000 years obtained for the pyroclastic unit that the dike intrudes. Two interpretations for the age of the pyroclastic (Qcup) unit are suggested by these data:

The pyroclastic unit may be significantly older than the minimum age of ≥ 1,368,000 ± 54,000 years we obtained.

The concordant Qcup and younger dike ages may reflect the true cooling age for these units (about 1.4 Ma) and the dike may have been a feeder for the pyroclastic eruption.

Sample DT88-1A is from the plutonic rock unit (Tdp) collected at the east side of Geyser Bight. This sample yielded concordant biotite and hornblende ages of 9.64 ± 0.29 and 9.40 ± 0.28 Ma, respectively. These concordant ages

indicate that the dated pluton has had a simple cooling history; i.e., it cooled through the argon-blocking temperatures for hornblende and biotite (from 530 ± 40 to 280 ± 40°C) at about 9.5 Ma. Cooling must have occurred in less than 300,000 years (standard deviation of ages) in order for the ages to be concordant. Our geologic mapping suggests that the Umnak geothermal reservoir system is hosted by this plutonic rock, as discussed previously.

McLean and Hein (1984) report 31-33 Ma plutonic and hypabyssal rocks from southwestern Umnak. Our much younger date for plutonic rock at Geyser Bight indicates that there have been at least two episodes of Tertiary plutonism on Umnak. The 9.5 Ma pluton is the youngest rock on Umnak truncated by the regional wave-cut surface of the Aleutian summit platform. This regional unconformity has been dated at 5.3 Ma (Scholl and others, 1987).

Table 1: Analytical Data for K-Ar Age Determinations. Samples listed in approximate stratigraphic order.

Youngest Valley-Filling Recheshnoi Flows (Qrf), E. Flank Mt. Recheshnoi

Lab No.	Field No.	Material Dated	
88115	88CNU19	WR	Insufficient radiogenic ^{40}Ar for age determination.
88115B	88CNU19	WR	Insufficient radiogenic ^{40}Ar for age determination.

Upper Cone-Building Flows (Qra), S. Flank Mt. Recheshnoi

Lab No.	Field No.	Material Dated	K_2O (wt%)	Sample Weight (g)	^{40}Ar RAD (mol/g) X 10^{-11}	$\frac{^{40}Ar\ RAD}{^{40}K}$ X 10^{-3}	% ^{40}Ar RAD	Age ± Sigma (Ma)
88101	88CNU85	WR	.601 .617 Mean = .613	12.2853	.0057	.0038	.77	.065 ± .011
88101B	88CNU85	WR	"	"	.0076	.0050	1.02	.086 ± .013 $\bar{x}_2$ = **.075 ± .011**
88084	88CNU83	WR	.877 .860 Mean = .869	11.5900	.0158	.0074	5.77	.127 ± .006
88084B	88CNU83	WR	"	"	.0146	.0068	5.34	.116 ± .006 $\bar{x}_2$ = **.121 ± .006**
88102	88CNU80	WR	.880 .870 Mean = .875	11.7469	.0141	.0065	2.70	.112 ± .010 Minimum Age
88102B	88CNU80	WR	"	"	.0136	.0063	2.59	.108 ± .008 $\bar{x}_2$ = **.110 ± .007** Minimum Age

Recheshnoi Flows (Qra), NE Side Geyser Creek Valley

Lab No.	Field No.	Material Dated	K_2O (wt%)	Sample Weight (g)	^{40}Ar RAD (mol/g) X 10^{-11}	$\frac{^{40}Ar\ RAD}{^{40}K}$ X 10^{-3}	% ^{40}Ar RAD	Age ± Sigma (Ma)
88099Q	88CNU06	WR	1.223 1.240 Mean = 1.232	10.0537	.0486	.0159	1.43	.274 ± .051
88099B	88CNU06	WR	"	"	.0420	.0138	1.24	.237 ± .041
88099C	88CNU06	WR	"	"	.0471	.0154	1.39	.265 ± .049 $\bar{x}_3$ = **.258 ± .035**

Recheshnoi Flows (Qra), Ridge Above Hot Springs Cove

Lab No.	Field No.	Material Dated	K_2O (wt%)	Sample Weight (g)	^{40}Ar RAD (mol/g) X 10^{-11}	$\frac{^{40}Ar\ RAD}{^{40}K}$ X 10^{-3}	% ^{40}Ar RAD	Age ± Sigma (Ma)
88073	88CNU56	WR	1.553 1.540 Mean = 1.547	10.2845	.0616	.0161	2.85	.277 ± .008
88073B	88CNU56	WR	"	"	.0656	.0171	3.03	.294 ± .010 $\bar{x}_2$ = **.285 ± .009**
88100	88CNU57	WR	1.440 1.460 Mean = 1.450	10.5823	.1014	.0282	6.34	.486 ± .015
88100B	88CNU57	WR	"	"	.0983	.0274	6.15	.471 ± .014 $\bar{x}_2$ = **.478 ± .012**

Basal Recheshnoi Flows (Qra), SW Side Geyser Creek Valley

Lab No.	Field No.	Material Dated	K_2O (wt%)	Sample Weight (g)	^{40}Ar RAD (mol/g) X 10^{-11}	$\frac{^{40}Ar\ RAD}{^{40}K}$ X 10^{-3}	% ^{40}Ar RAD	Age ± Sigma (Ma)
88153	DT88-10 (540' Above Base)	WR	1.550 1.570 Mean = 1.560	9.1595	.1081	.0280	12.43	.481 ± .014
88153B	DT88-10 (540' Above Base)	WR	"	"	.1040	.0269	11.97	.463 ± .014 x_2 = **.472 ± .014**
88107B	DT8814 (300' Above Base)	WR	1.653 1.680 Mean = 1.667	9.0659	.1173	.0284	7.31	.489 ± .015
88107C	DT8814	WR	"	"	.1173	.0284	7.31	.489 ± .015 $\bar{x}_2$ = **.489 ± .015**
88103	DT8816 (20' Above Base)	WR	1.200 1.223 Mean = 1.212	10.3391	.0915	.0305	5.26	.525 ± .016
88103B	DT8816	WR	"	"	.0945	.0315	5.43	.542 ± .016 $\bar{x}_2$ = **.534 ± .013**
88108	DT8817 (Base of Qra)	WR	1.190 1.187 Mean = 1.189	10.8868	.0840	.0285	3.96	.491 ± .015
88108B	DT8817	WR	"	"	.0867	.0294	4.09	.506 ± .015 $\bar{x}_2$ = **.499 ± .012**

Biotite Rhyolite Plugs (Qr) Intruding Qra, Russian Bay

Lab No.	Field No.	Material Dated	K_2O (wt%)	Sample Weight (g)	^{40}Ar RAD (mol/g) X 10^{-11}	$\frac{^{40}Ar\ RAD}{^{40}K}$ X 10^{-3}	% ^{40}Ar RAD	Age ± Sigma (Ma)
88138	88GPU07	Biotite	8.377 8.376 8.416 8.435 8.338 8.445 Mean = 8.398	.4002	.1692	.0081	1.52	.140 ± .019
88138B	88GPU07	Biotite	"	"	.1573	.0076	1.41	.130 ± .022 $\bar{x}_2$ = **.135 ± .015**

Note: This sample is presently being tested for excess Ar using 40Ar-39Ar laser step heating at the University of Toronto.

Quartz-Olivine Andesite Flows (Qrq) Overlying Qra Above Hot Springs Cove

Lab No.	Field No.	Material Dated	K_2O (wt%)	Sample Weight (g)	^{40}Ar RAD (mol/g) X 10^{-11}	$\frac{^{40}Ar\ RAD}{^{40}K}$ X 10^{-3}	% ^{40}Ar RAD	Age ± Sigma (Ma)
88105c	88CNU55	WR	1.250 1.270 Mean = 1.260	10.2996	.0167	.0054	.96	.092 ± .009
88160B	88CNU55	WR	"	9.880	.0166	.0053	.71	.092 ± .007
88160C	88CNU55	WR	"	"	.0133	.0043	.57	.073 ± .029 $\bar{x}_3$ = **.089 ± .014**

Volcanic Flows of Central Umnak (Qcuv), Above Hot Springs Cove

Lab No.	Field No.	Material Dated	K_2O (wt%)	Sample Weight (g)	^{40}Ar RAD (mol/g) X 10^{-11}	$\frac{^{40}Ar\ RAD}{^{40}K}$ X 10^{-3}	% ^{40}Ar RAD	Age ± Sigma (Ma)
88106Q	88CNU59 (Near top of Qcuv Section)	WR	1.543 1.557 Mean = 1.550	10.0698	.0950	.0247	14.04	.426 ± .013 Minimum Age
88106B	88CNU59	WR	"	"	.0951	.0248	14.04	.426 ± .013 $\bar{x}_2$ = **.426 ± .013** Minimum Age

Volcanic Flows of Central Umnak (Qcuv), NE Side Geyser Creek Valley

Lab No.	Field No.	Material Dated	K_2O (wt%)	Sample Weight (g)	^{40}Ar RAD (mol/g) X 10^{-11}	$\frac{^{40}Ar\ RAD}{^{40}K}$ X 10^{-3}	% ^{40}Ar RAD	Age ± Sigma (Ma)
88076	88CNU02	WR	.690 .700 Mean = .695	12.1284	.0805	.0468	6.74	.805 ± .024
88076B	88CNU02	WR	"	"	.0768	.0446	6.42	.767 ± .023 $\bar{x}_2$ = **.786 ± .021**
88104B	88CNU04	WR	.653 .643 Mean = .648	10.7349	.0776	.0483	19.32	.832 ± .025
88104C	88CNU04	WR	"	"	.0782	.0487	19.42	.838 ± .025 $\bar{x}_2$ = **.835 ± .025**
88077	88CNU03	WR	.770 .780 Mean = .775	12.1601	.0974	.0507	13.66	.873 ± .026
88077B	88CNU03	WR	"	"	.0933	.0486	13.12	.836 ± .025 $\bar{x}_2$ = **.854 ± .022**

Volcanic Flows of Central Unmak (Qcuv), SW Side Geyser Creek Valley

Lab No.	Field No.	Material Dated	K_2O (wt%)	Sample Weight (g)	^{40}Ar RAD (mol/g) X 10^{-11}	$\frac{^{40}Ar\ RAD}{^{40}K}$ X 10^{-3}	% ^{40}Ar RAD	Age ± Sigma (Ma)
88110	DT885	WR	.757 .760 Mean = .759	11.3441	.1234	.0657	7.33	1.130 ± .034
88110B	DT885	WR	"	"	.1166	.0620	6.92	1.068 ± .048 $\bar{x}_2$ = 1.104 ± .037
88111	DT887 (Base of Qcuv)	WR	.713 .720 Mean = .717	6.1810	.1223	.0689	5.18	1.185 ± .036
88111B	DT887	WR	"	"	.1102	.0621	4.66	1.069 ± .032 $\bar{x}_2$ = 1.124 ± .048

Pyroclastic Rocks of Central Umnak (Qcup), Stepanof Cove

Lab No.	Field No.	Material Dated	K_2O (wt%)	Sample Weight (g)	^{40}Ar RAD (mol/g) X 10^{-11}	$\frac{^{40}Ar RAD}{^{40}K}$ X 10^{-3}	% ^{40}Ar RAD	Age ± Sigma (Ma)
88117	DT8836	WR	1.090 1.083 Mean = 1.087	7.1607	.2247	.0835	8.09	1.434 ± .043 Minimum Age
88117B	DT8836	WR	"	"	.2043	.0759	7.35	1.303 ± .039 $\bar{x}_2$ = 1.368 ± .054 Minimum Age
88158,B,C	DT8837	WR	1.490 1.480 Mean = 1.485	Insufficient radiogenic ^{40} AR for age determination.				

Dikes Intruding Pyroclastic Rocks of Central Umnak, Stepanof Cove

Lab No.	Field No.	Material Dated	K_2O (wt%)	Sample Weight (g)	^{40}Ar RAD (mol/g) X 10^{-11}	$\frac{^{40}Ar\ RAD}{^{40}K}$ X 10^{-3}	% ^{40}Ar RAD	Age ± Sigma (Ma)
88114	DT8830	WR	1.070 1.073 Mean = 1.072	10.8711	.2102	.0792	10.28	1.363 ± .041
88114B	DT8830	WR	"	"	.2108	.0794	10.31	1.366 ± .041 $\bar{x}_2$ = **1.365 ± .041**
88116	DT8830P	WR	1.080 1.090 Mean = 1.085	5.7325	.2570	.0956	3.99	1.645 ± .060
88116B	DT8830P	WR	"	"	.2454	.0913	3.81	1.571 ± .077 $\bar{x}_2$ = **1.613 ± .056**

Note: Samples DT8830 and 30P were taken from the same dike. The significantly different values obtained for $^{40}ArRAD$ (mol/g) and, consequently, age suggest that the dike contains variable amounts of excess argon. The younger age is therefore likely to be closer to the true age of dike emplacement and cooling.

Plutonic Rocks (Tdp), E. Side of Geyser Bight

Lab No.	Field No.	Material Dated	K_2O (wt%)	Sample Weight (g)	^{40}Ar RAD (mol/g) X 10^{-11}	$\frac{^{40}Ar\ RAD}{^{40}K}$ X 10^{-3}	% ^{40}Ar RAD	Age ± Sigma (Ma)
88167	DT88-1A	Biotite	7.957 7.747 7.883 Mean = 7.846	0.2255	10.91	.5614	63.61	9.64 ± .29
88164	DT88-1A	Hornblende	.390 .390 .390 .397 Mean .392	1.5531	.5315	.5476	19.08	9.40 ± .28

RAD = Radiongenic, Sigma = Standard Deviation, WR = Whole Rock

Decay Constants: $\lambda_\varepsilon + \lambda_{\varepsilon'} = 0.581 \times 10^{-10}/yr.$

$\lambda_\beta = 4.962 \times 10^{-10}/yr.$

$^{40}K/K_{total} = 1.167 \times 10^{-4} mol/mol$

4. GEOCHEMISTRY OF VOLCANIC ROCKS

4.1 Introduction

The chemical compositions of magmas change in response to igneous processes. By measuring the composition of erupted magmas it is possible to recognize which of these processes have operated during the life of the volcanic system. This approach can provide direct information about the magmatic plumbing system which is the source of geothermal heat. Among the processes which can be recognized are fractional crystallization, magma mixing, and variations in partial melting. During fractional crystallization, crystals with compositions different than the host magma separate and drive the composition of the remaining liquid along a specific path. Mixing of chemically distinct magma batches also produces recognizable chemical trends. Initial melts produced in the source region have recognizable chemical features which reflect the origin and mode of melting. In addition, temporal variations in chemistry provide direct information about the evolution of the plumbing system. In some cases inferences can be made about the location and size of the dominant magma chamber.

This chapter describes the chemical composition of Geyser Bight magmas and interprets variations in chemical composition in terms of igneous processes which can constrain the geologic evolution of the geothermal system. The data discussed were obtained by X-ray fluorescence spectroscopy at the University of California at Santa Cruz. Duplicate analyses of all samples indicates that mean analytical precision is less than 1.5 relative percent for SiO_2, TiO_2, Fe_2O_3, Al_2O_3, CaO, and K_2O, less than 2% for MgO, and about 5% for Na_2O and

P_2O_5. Extreme values for Na_2O imprecision exceed 20% relative. Sample locations are in Plate 1 and Figure 4-1. All analytical data are in Table 4-2 (at the end of this secion).

4.2 Chemical Variation of Lavas

Harker diagrams of Geyser Bight lavas are shown in Figure 4-1. Most of the samples are medium-K andesite as defined by Gill (1981). There is also some basalt and rare rhyolite, but no dacite. The basalt and andesite are compositionally similar to other Aleutian lavas in most respects. FeO_t, MgO, CaO, and Al_2O_3 fall with increasing SiO_2, K_2O increases dramatically, and Na_2O and TiO_2 are scattered. Scatter in Al_2O_3, and, to a lesser extent TiO_2 is probably related to differential crystal accumulation. Scatter in Na_2O is in part due to analytical imprecision.

Most samples fall within the calc-alkaline field of Miyashiro (1974). Most of those samples which fall above or near the Th-Ca dividing line are part of a chemically anomalous high FeO_t, high TiO_2 group described below. Samples from Mt. Recheshnoi especially are strongly calcalkaline. Mt. Recheshnoi is among the most calcalkaline volcanoes in the Aleutian arc, and bears many similarities to the calcalkaline volcanoes of the eastern arc. There is a continuum of compositions between 50% and 63% SiO_2, but there are no magmas between 63% and 76% SiO_2. This constitutes a major compositional gap. Rhyolitic compositions are from the series of rhyolite domes west of Russian Bay valley and from granophyres within the pluton. Rhyolite is rare in Pleistocene Aleutian volcanoes. It is only known from about 5 centers arcwide. These are : 1) a small pod on the flank of Okmok caldera, 35 km to the northeast; 2) a few pumice samples from Shishaldin; 3) Novarupta, the site of the climactic 1912 eruption of the Valley of Ten Thousand Smokes; and 4) a

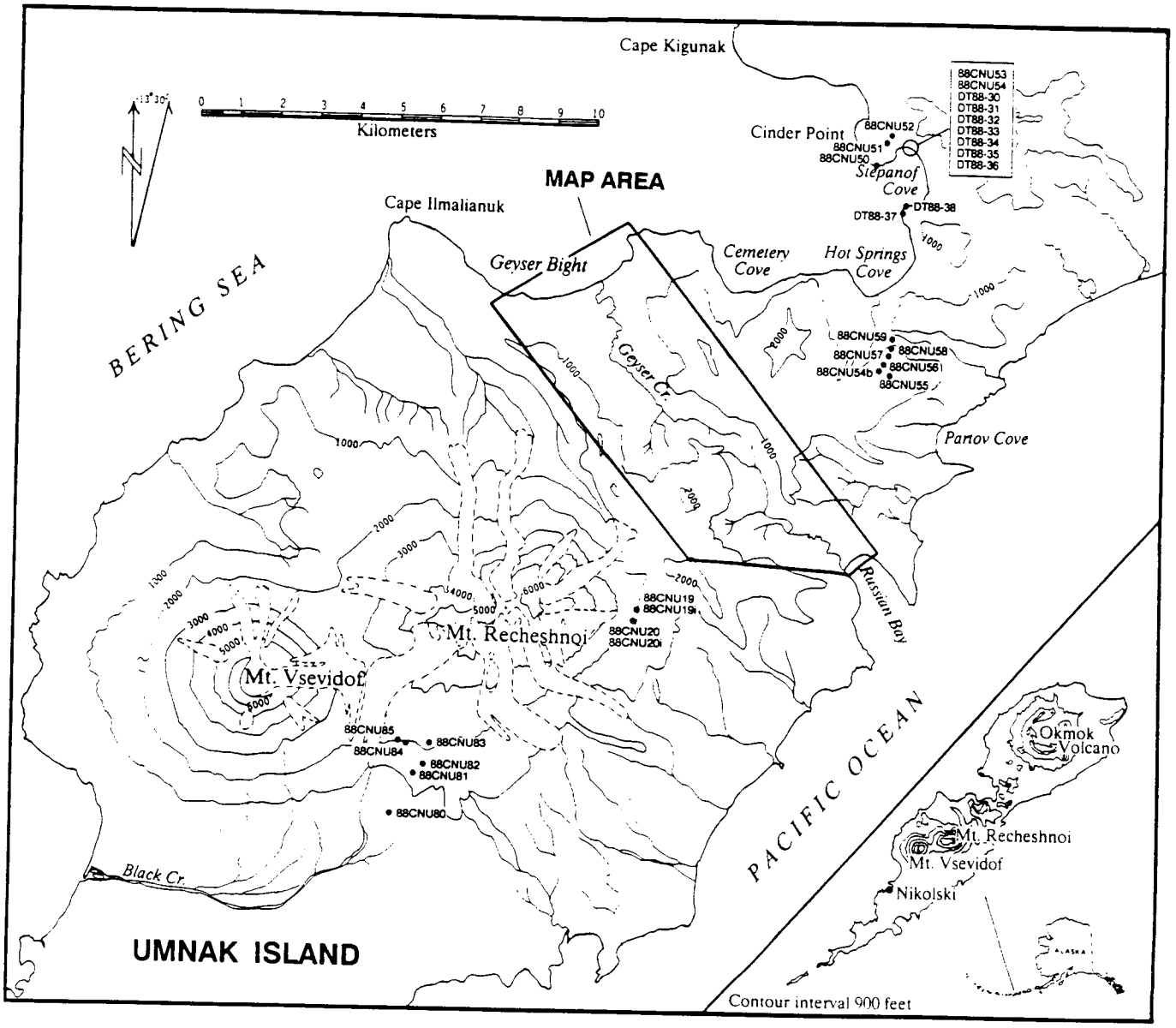

Figure 4-1. Locations of samples outside the area of Plate 1 for which there are analytical data in Table 4-1 (at the end of this section).

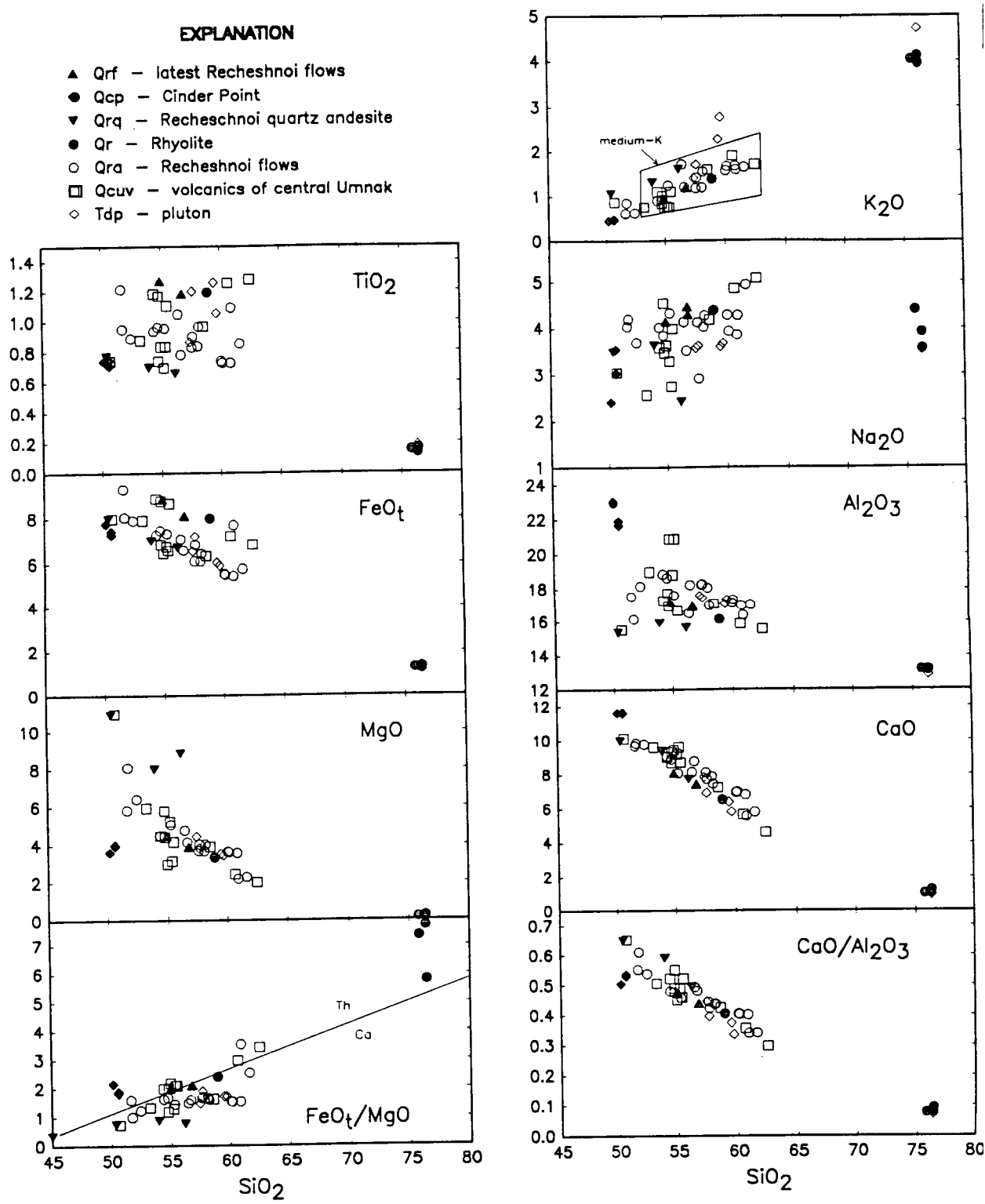

Figure 4-2. Silica variations of igneous rocks from Geyser Bight valley and the surrounding region. The Th-Ca dividing line is from Miyashiro (1974), and the medium-K region is from Gill (1981).

single pumice sample from Augustine volcano. Only Novarupta (1000 km eastward along the arc) has erupted more silicic magma.

A group of samples most noticeable in FeO_t vs SiO_2 (Fig. 4-2) defines a trend parallel to the main evolutionary trend but at higher iron contents. These samples are also characterized by high TiO_2; relatively low MgO (and therefore high FeO_t/MgO); relatively low Al_2O_3 concentrations (which form a linear trend between 52% SiO_2 and 17.5% Al_2O_3, and 63% SiO_2 and 15.5% Al_2O_3); and fewer phenocrysts than other samples. These samples will be referred to as the high FeTi group. Samples which fall in this group include lavas which erupted from the central Umnak vents at intervals throughout their lifetimes (but not all Qcuv samples); some, but not all, of the recent lavas from Mt. Recheshnoi; the Holocene Recheshnoi andesite flows (Qrf), and from quenched blobs within the rhyolite. The quartz andesite samples are not part of the high FeTi group.

The group of samples at lower FeO_t are unlikely to be related to the sparsely phyric high FeTi group by simple crystal accumulation because that accumulation should raise both FeO_t and MgO. Instead, crystal rich samples have lower Fe, yet higher Mg.

Plutonic rocks are compositionally similar to Recheshnoi and central Umnak andesites except for the high K_2O contents of quartz monzonites and granophyres, but not quartz diorites. This presumably reflects some unspecified difference in petrogenetic processes between plutonic and volcanic rocks. Because the plutonic samples are not related to the present magmatic plumbing system they are not discussed further here. Additional discussion of their composition is included with the discussion of map units.

Cinder Point is a small monogenetic cone on the flanks of Okmok Volcano. Its composition and history probably has little bearing on the Recheshnoi geothermal system. Cinder Point samples are different from most of the other samples in that they have high Al_2O_3, CaO, and normative plagioclase, and low MgO. They also have large, monomineralic, polycrystalline, plagioclase aggregates, often rounded and embayed, up to 5 mm in diameter. The composition of the Cinder Point samples probably reflects selective accumulation of these crystals.

4.3 Petrogenesis of lavas

Several processes may relate lavas to each other. These include fractional crystallization, variable P-T-PH_2O fractionation path, magma mixing, crystal sorting, crustal assimilation, crustal melting, and variations in primary magmas. Each of these processes are discussed in turn below. It is difficult to decipher which of these processes operate and to what extent without additional trace element and isotopic data. Even with abundant trace element and isotope data it is often difficult to construct exact petrogenetic models. Nevertheless, some first order qualitative observations can be made with the data at hand.

4.3.1 Crystal Fractionation

Much of the variation in composition among the basalts and andesites is probably due to fractional crystallization. Separation of some 70% of pl±ol+cpx±opx+mt crystals (by weight) can account for similar compositional variations in other Aleutian volcanoes of similar bulk composition (e.g. Kay and others, 1982; Nye and Turner, 1990). However, scatter about expected

fractionation trends in most variation diagrams requires that other secondary processes are involved.

4.3.2 Magma Mixing

Magma mixing is difficult to quantify with only major element whole-rock geochemical data and petrographic data. Quantitative tests of magma mixing require modelling of incompatible and compatible trace elements and a good knowledge of the composition of phenocrysts. There are some aspects of the composition of Geyser Bight lavas that suggest, however, that magma mixing may be common.

First, there are commonly two textural types of plagioclase within the lavas (see Table 4-1). One population is euhedral to subhedral, normally zoned, and inclusion free. The other population is rounded and resorbed (often with euhedral rims), has reversals in zoning, and usually contain discrete concentric zones of glassy inclusions. The second plagioclase morphology reflects a period of disequilibrium which may be associated with magma mixing or xenocryst entrainment. In order to positively assess whether or not the two plagioclase populations require magma mixing it would be necessary to measure either the chemical difference between the two types of plagioclase or the amount of chemical change across the boundary between the spongy zone and the euhedral rim. In andesitic systems these differences are often greater than can be caused by polybaric fractionation or by changes in the partial pressure of water (see Gill, 1981, for discussion).

Second, the covariation of K_2O with MgO is not as expected for magmas related by fractional crystallization. Figure 4-3 shows all Geyser Bight samples as well as a calculated path for about 70% fractional crystallization

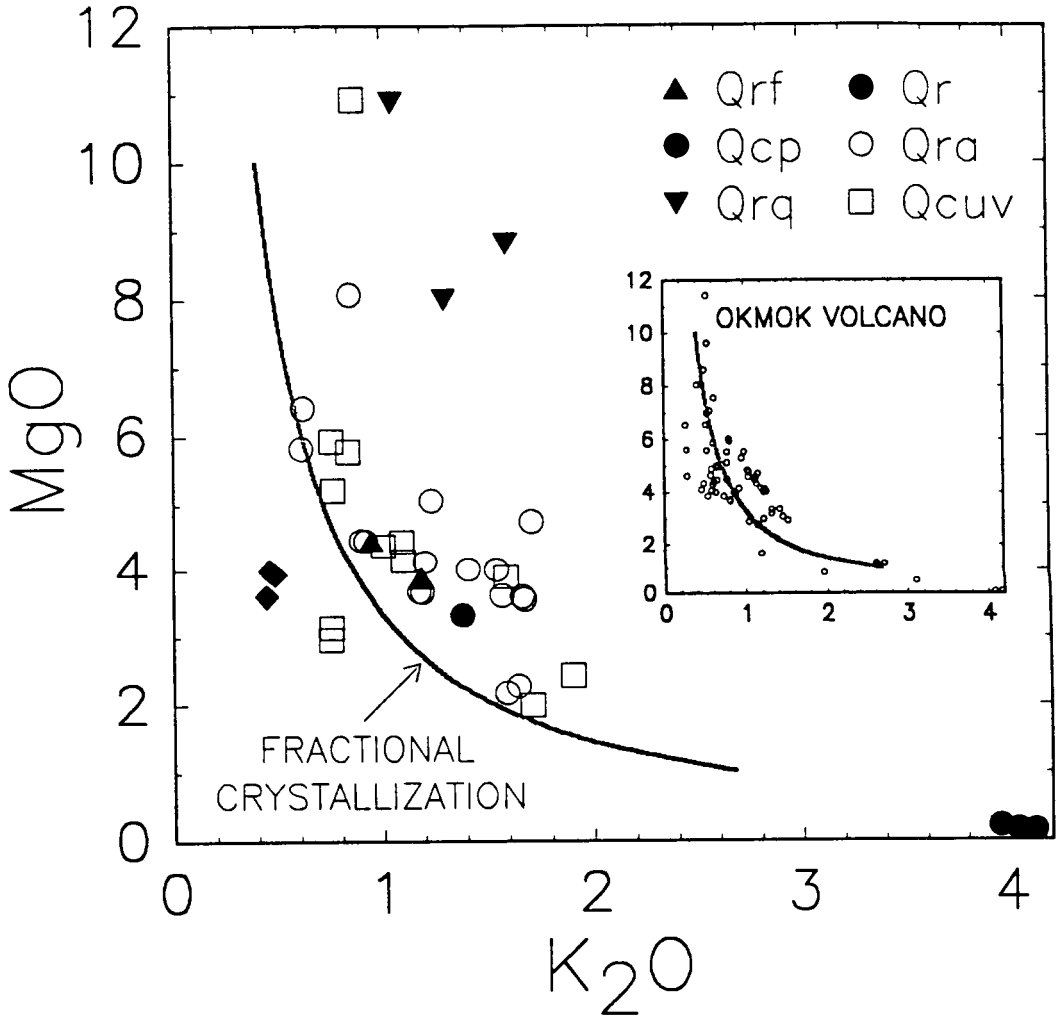

Figure 4-3. K_2O and MgO variations in Geyser Bight area magmas. Parameters of the fractional crystallization path are discussed in the text. Okmok volcano data are from the literature.

from a parent with 0.4% K_2O and 10% MgO. The path assumes that MgO behaves as if it were a compatible trace element with a solid/liquid distribution coefficient (Kd) of 2.2, and that K_2O has Kd of 0. Because K_2O is not an essential constituent of any fractionating mineral (until biotite crystallizes in the rhyolite) it can be treated as a trace element. The Geyser Bight samples all diverge from the strong curvilinear path which is predicted. Those samples that lie on chords on the concave side of the model line may be partly explained by intertrend mixing of basalt and silicic andesite. Divergence from the predicted trend may also result from variations in K_2O content of parent magmas as well as minor accumulation of mafic minerals. Those samples falling below the curve are those which have anomalously high Al_2O_3 and may have selectively accumulated plagioclase. Certainly the quartz andesite flows are so far above the model fractionation line that magma mixing must be involved. The extreme disequilibrium of the mineral assemblage in this unit provides strong evidence of this mixing.

Also shown in Figure 4-3 are data from Okmok Volcano. Okmok is highly tholeiitic and is generally considered to not be greatly affected by magma mixing (e.g. Kay and others, 1982; Kay and Kay, 1985). While the Okmok data conform more closely to the calculated fractionation line there is still considerable scatter. For most Geyser Bight samples magma mixing is therefore probably not a dominant process for units other than the quartz andesite, although it may be a common minor process.

4.3.3 Crystal Accumulation

The possibility that differential accumulation of crystals within the host magmas has modified the composition of those magmas is always a concern when describing porphyritic magmas such as most of those considered here. Indeed,

plagioclase accumulation is probably a major factor in determining the final composition of the lavas from Cinder Point (as discussed above). Most of the scatter in Al_2O_3 for samples from Mt. Recheshnoi, however, can be explained by about 10% plagioclase accumulation, an amount far less than the modal amount of plagioclase. Selective crystal accumulation should influence Al_2O_3 and normative plagioclase the most because plagioclase dominates the modal mineralogy. The lack of correlation between Al_2O_3 or normative plagioclase and the percentage of phenocrysts in the rock, however, indicates that crystal accumulation is not a major influence on magma composition.

4.3.4 Crustal Melting

While repeated transit of basaltic and andesitic magma through the arc crust might be expected to partially melt that crust, magmas clearly owing their origin to such a process are rare in the Aleutians. One possible exception is the rhyolite from Russian Bay valley (Qr, Plate 1). This rhyolite is probably not derived from the acid andesites by fractional crystallization, or else there would probably not be the prominent compositional gap between 63% and 76% SiO_2. Instead, the rhyolite was probably produced by partial melting of the arc crust with heat provided by the more mafic magmas (see Smith and Leeman, 1987, for a discussion of a similar mechanism at Mt. St. Helens). If rhyolite had been produced over much of the lifetime of the volcano then there should be back-mixed dacites or andesites. Such rocks are rare, the best example being the quartz andesite (Qrq) exposed between Hot Springs Cove and Partov Cove. This lack of back-mixed magmas suggests that the production of rhyolite was temporally restricted.

4.3.5 Other Processes

The high FeTi group of magmas cannot be simply related to other magmas by fractional crystallization, magma mixing, or crystal accumulation. These magmas have petrographic and geochemical similarities to the tholeiitic series rocks described by Kay and others (1982). These similarities included high FeO_t and TiO_2, high FeO_t/MgO, and low crystal contents. Kay and others (1982) and Kay and Kay (1985) suggest that these rocks are the result of crystallization at low pressure, low water content, and high temperature. The position of the cotectic governing the evolution of these magmas, as deduced from experimental work, does not seem to be shifted from that governing the evolution of other magmas (see following section). Thus, if the Kay and others (1982) explanation is correct, the magnitude of lowered pressure and/or water pressure is not sufficient to be reflected in normative mineralogy. The origin of the high FeTi magmas remains enigmatic.

Variations in parental magma chemistry are expected, but with the data at hand there is no way to evaluate the magnitude of their effects. Similarly, crustal assimilation may affect the final compositions of some magmas. In fact, if the presence of rhyolite signals mobilization and eruption of partial melts of the crust then crustal contamination is quite likely. Recognition of crustal contamination, however, requires more data than are at hand.

4.4 Inferences for Depth of Fractionation

Understanding the size, depth, and mean lifetime of crustal magma chambers is of obvious importance to the understanding of geothermal energy at active volcanoes. However, these aspects of magmatic evolution are among the most difficult to quantify. Some progress has been made in recent years by

observing the magnitude and direction of shifts of cotectics in multiply-saturated systems with changes in pressure and water pressure. This is done by equilibrating natural melts with their phenocryst assemblages in a laboratory at known P_{total} and P_{H2O} and then measuring the composition of the equilibrium liquid. There are abundant data for mid-ocean ridge basalts (MORB) at low pressure and with no water. Data on andesitic compositions at moderate P_{total} and P_{H2O} are much less common, in part due to the difficulty of the experiments.

The available data are summarized in Figure 4-4 on a projection onto normative diopside, silica and plagioclase from within the tetrahedron diopside, silica, plagioclase and olivine. The dry, 1 atmosphere cotectic is given by the MORB data (references in figure caption). Additional anhydrous experiments at 8 Kb and hydrous experiments at 2 and 5 Kb from are plotted. The cotectic shifts towards plagioclase with increasing pressure and water pressure, as both reduce the stability of plagioclase. The 2 to 5 Kb "damp" cotectic is shifted farther than the 8 Kb dry cotectic. All Geyser Bight data are shifted towards plagioclase and overlap the 2 and 5 Kb cotectics. This requires that most of the chemical evolution of Geyser Bight magmas, and thus most of their residence time in the crust, must have been at a minimum depth of 6 to 15 kilometers. If the magmas were anhydrous, that depth must be well over 25 kilometers. The presence of relict amphibole in a few samples suggests the magmas were hydrous. The fact that the plutonic samples plot along the same inferred cotectic as Geyser Bight lavas suggests that the magmas principal crustal residence is at a similar depth to that at which the pluton originally formed. The Cinder Point samples plot much closer to the

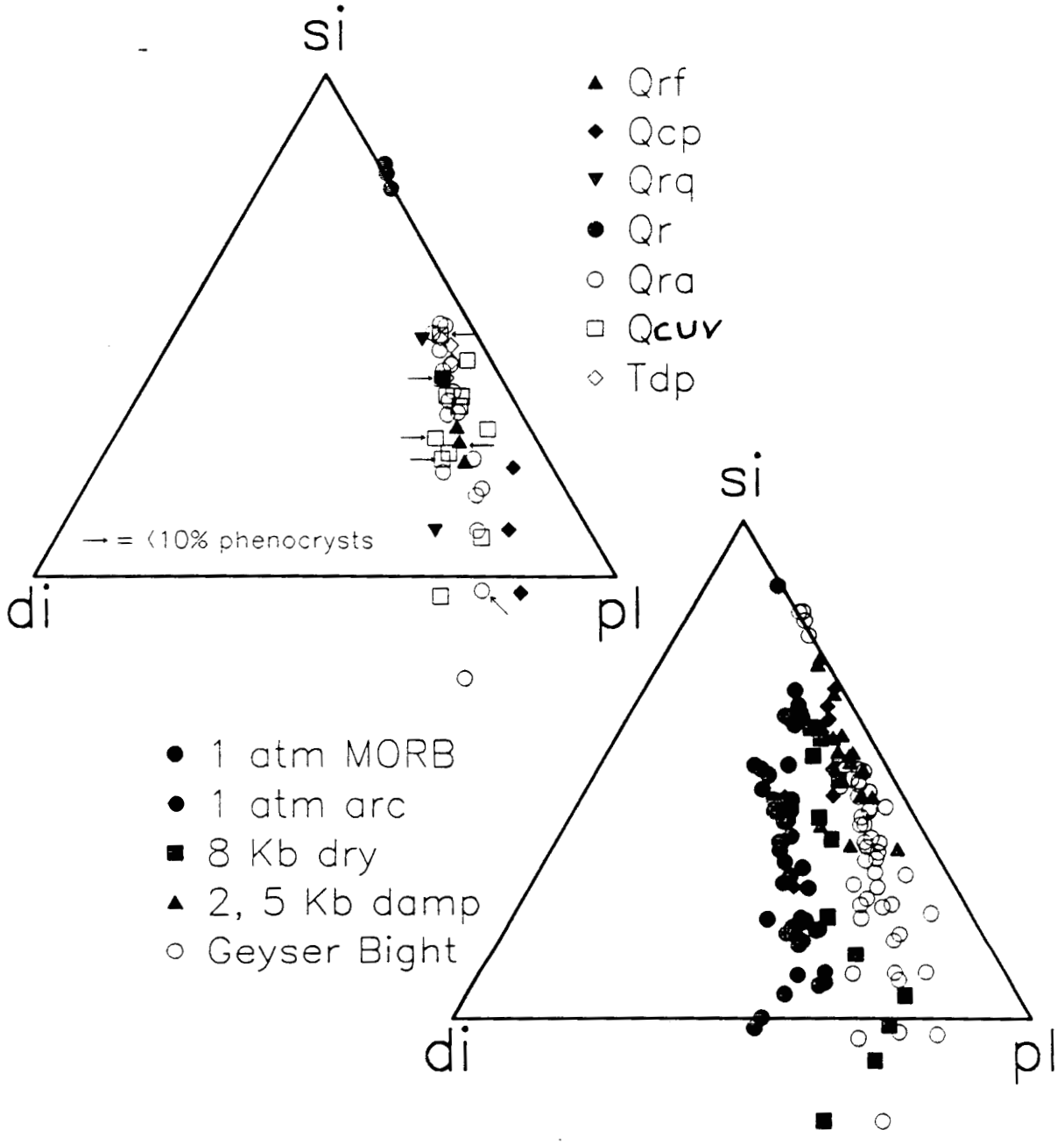

Figure 4-4. Projections from olivine onto the plane diopside-silica-plagioclase within a normative tetrahedron (Grove et al., 1982). Data other than those from Geyser Bight are from Baker and Eggler (1987), Grove et al. (1982), Grove and Bryan (1983), and Walker et al. (1979).

plagioclase apex than others. This probably reflects plagioclase accumulation in these samples rather than a deeper origin.

4.5 Temporal Variations in Magma Composition

A series of variation diagrams which show composition of Geyser Bight magmas as a function of age are given in Figure 4-5. There have not been major monotonic variations in chemistry over the 1.4 m.y. that lavas have erupted at Geyser Bight. However there are some minor trends that deserve comment. Lavas from central Umnak show a very slight decrease in FeO_t and CaO/Al_2O_3, and, perhaps, MgO over time. There is a very faint hint of concomitant increase in SiO_2. These changes are very slight, marred by the eruption of some silicic magmas early in the history of the central Umnak vents, and could well prove to be an artifact of the small number of analyses we have. These apparent trends are not likely to signal merely a slight increase in fractionation of a homogeneous magma batch because K_2O contents of 800 ka lavas are not higher than those of 1100 ka lavas. This suggests that these temporal variations, if real, reflect variations in the composition of parental magmas, as well as variations in the amount of fractionation.

Chemical changes within the lifetime of Mt. Recheshnoi are more pronounced, and are probably real. Figure 4-5 shows that over much of the 0.5 m.y. lifetime of Mt. Recheshnoi magmas have become more mafic, with a few notable exceptions described later. Over this time SiO_2 dropped from about 60% to about 53% and FeO_t, MgO, CaO, and CaO/Al_2O_3 increased. TiO_2 increased for about the first 200,000 years and then decreased, while K_2O remained steady for 200,000 years and then decreased. The lack of strict monotonic correlation between K_2O and SiO_2 suggests that there were variations in parent magma composition through time. The lack of monotonic correlation between

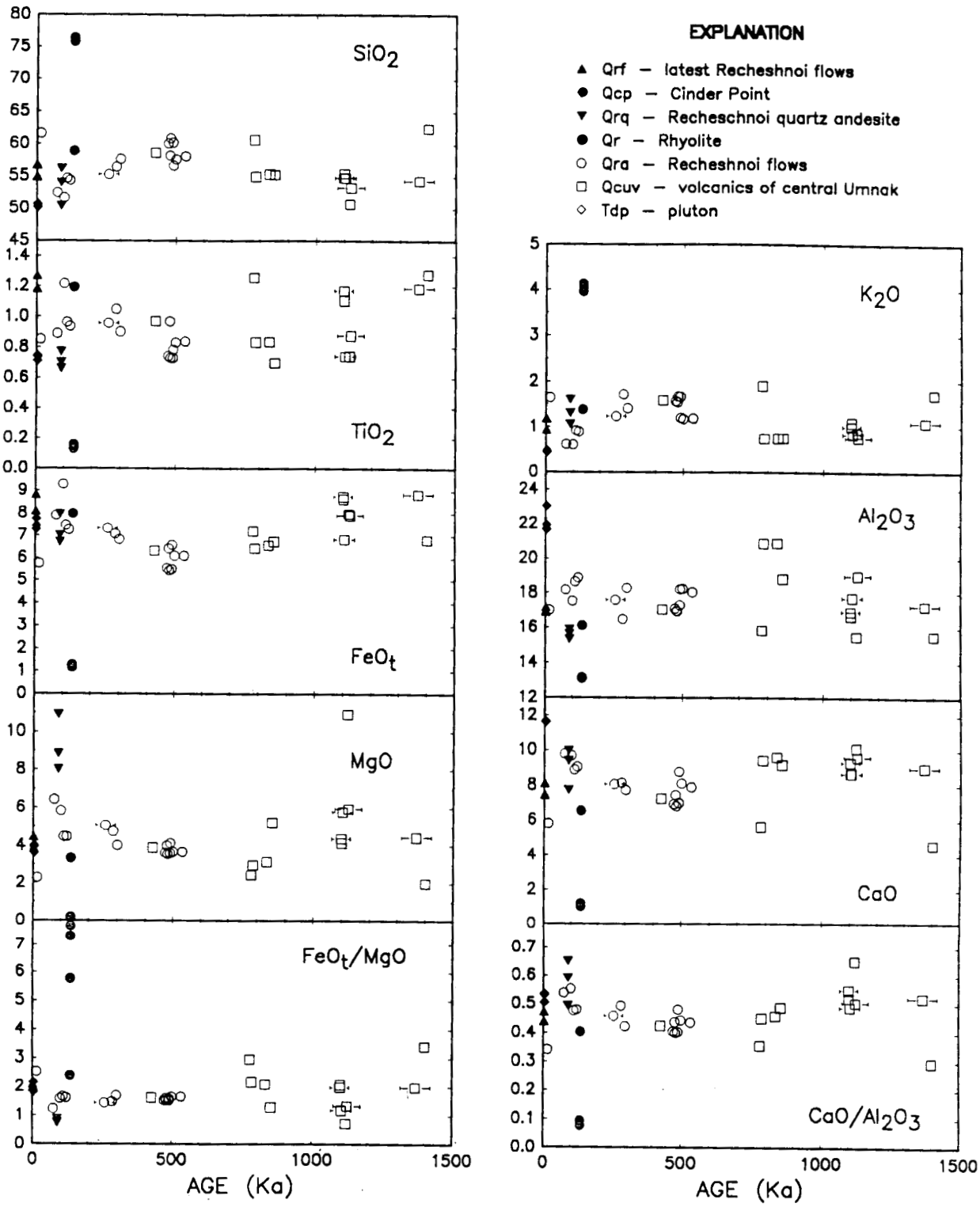

Figure 4-5. Temporal variation of the composition of volcanic rocks from Geyser Bight valley and the surrounding region.

TiO_2 and SiO_2 may reflect either variable parent magma composition or a slight change in magnetite stability (and thus probably oxygen fugacity) through time. It is impossible to quantify these processes with the data in hand. Also, as a cautionary note, we do not have samples from the northwest, west and southeast sides of the volcano. The temporal changes of magma chemistry with time may well be more complicated than our data set shows. There are also a few basalt flows from the Geyser Creek valley for which we do not have ages, and which are not plotted on Figure 4-5. These flows are presumably at least a few hundred thousand years old and may fall off the perceived temporal trend. These flows may represent the periodic influx of mafic magma into a system which is quasi-steady state, yet evolving towards more mafic average compositions through time. Periodic eruption of mafic magmas from steady-state systems has been observed elsewhere (e.g. Nye and Turner, 1990) and is not unexpected.

There are three exceptions to the trend towards more mafic compositions with time of Mt. Recheshnoi lavas. The first is the rhyolite, which erupted about 135 ka. Quenched andesite blobs within the rhyolite suggest that mafic magma was still present in the system as the rhyolite erupted. This andesite may conform to the overall temporal trend especially if corrected for minor contamination of the basalt with rhyolite. The second exceptions are the andesite flows from the east flank of the volcano (Qrf) which are more silicic than youngest lavas from the Mt. Recheshnoi central vent (57% compared to 52% SiO_2). These flows also contain inclusions of more mafic andesite which indicate that the entire system is not moving towards more silicic compositions. Note that in both the rhyolite and the young flank andesite the included blobs are quenched magma included within their host, as opposed to stoped conduit material or country rock. The third exception is felsic

andesite clasts in ashflows from young valley-filling ashflows in Russian Bay valley (Qral). The petrology and geochemistry of this unit is not well known.

All Recheshnoi samples which belong to the high FeTi group are young. Thus the most tholeiitic of Mt. Recheshnoi samples are young compared to the bulk of Recheshnoi lavas. Note however, that on a FeO/MgO vs. SiO_2 diagram Mt. Recheshnoi as a whole is very calcalkaline.

4.6 Evolution of the Magmatic System

The magmatic system most relevant to understanding the Geyser Bight geothermal system is that of Mt. Recheshnoi. The vents of central Umnak have been dormant for a half to three quarters of a million years and any magma chambers which were associated with them are probably fully crystallized and near the temperature of surrounding country rock at present.

Mt. Recheshnoi magmas have become more mafic with time, although some anomalously felsic magmas have also erupted within the last 150,000 years. This evolutionary trend is unlike those of the few other Aleutian volcanoes for which there are both abundant age and geochemical data. Mt. Spurr steady-state andesite magmas remain nearly constant in composition for the 250,000 year lifetime of that volcano, although mafic magmas were periodically erupted, most notably during and after avalanche caldera formation late in the history of the volcano (Nye and Turner, 1990). Early Mt. Wrangell lavas are mafic, but the lavas have remained nearly constant in composition over the last 500,000 years (Nye and Turner, unpub. data). Holocene Makushin magmas are on average more silicic than Pleistocene magmas, which are variable in composition. Myers and others(1985) and Myers and Marsh(1987), based on studies of two separate volcanoes of different sizes, and thus presumed

different ages, suggest that volcanoes may evolve from early calc-alkaline (and thus presumably andesitic) compositions to late tholeiitic (thus more basaltic) compositions. Mt. Recheshnoi may be an example of the type of volcano Myers proposes, although the magnitude of the compositional shift is less than he anticipates.

A possible model for the evolution of the Mt. Recheshnoi magmatic system follows. As new magma intrudes into the crust early in Recheshnoi's history it encounters relatively cool crust. Because of the large thermal contrast there is significant fractionation and therefore heat loss to the crust. Successive batches of melt enter and pass through the crust, fractionating and loosing heat. Through this process the crust heats, providing less thermal contrast, and thus decreasing fractionation of subsequent batches of rising melt. Therefore successive magmas are less fractionated and more mafic. Ultimately, the crust heats to the point where it undergoes partial fusion, producing the rhyolite. Once the crust starts to melt it generates a silicic component which can be mixed into incoming basaltic magmas to produce hybrid silicic magmas, such as the most recent of Recheshnoi's magmas. This model is very much like that of Myers and others (1985) in that it suggests that thermal maturation of the conduit system is important in volcanic evolution. It is unlike that of Myers and others (1985) in that it predicts increasing, rather than decreasing, chemical coupling with the crust.

TABLE 4-1.

Compositional data on samples from the Geyser Creek area and surrounding regions.

ID	88cnu51	88cnu19	88cnu19i	88cnu20	88cnu54b	88cnu55	88cnu14	88cnu17	88cnu18i
UNIT	Qcp	Qrf	Qrf	Qrf	Qrq	Qrq	Qr	Qr	Qr
Chemical composition									
SiO2	50.62	56.79	54.91	56.73	50.39	53.94	75.82	76.36	58.93
TiO2	0.75	1.18	1.27	1.18	0.77	0.70	0.15	0.13	1.19
Al2O3	21.67	16.97	17.16	16.87	15.35	15.91	13.16	13.11	16.14
FeOt	7.27	8.09	8.83	8.10	7.95	7.00	1.23	1.17	7.97
MgO	4.00	3.87	4.47	3.88	10.89	8.00	0.17	0.15	3.33
CaO	11.60	7.46	8.10	7.41	9.96	9.38	1.01	1.04	6.53
NaO	3.54	4.30	4.14	4.46	3.49	3.62	4.39	3.91	4.39
K2O	0.46	1.18	0.94	1.19	1.05	1.30	4.04	4.12	1.38
P2O5	0.10	0.16	0.18	0.18	0.15	0.13	0.03	0.01	0.14
MnO	na	na	na	na	na	na	na	na	na
LOI	na	na	na	na	na	na	na	na	na
Total	100.99	100.75	100.29	101.59	99.00	99.28	102.19	101.17	99.37
Fe2O3	8.10	8.98	9.75	9.07	8.68	7.67	1.39	1.31	8.72
Modal composition									
Gms	60	85	40	90	35	75	.	85	90
Plag1	+ +	+	+	=	=	.	.	+	+
Plag2	.	.	= =	= =	+	+	.	.	+
Ol	=	=	+	= =	+	+	.	.	.
Cpx	=	=	+	=	+	+	.	.	+
Opx	.	= =	.	=	.	=	.	.	.
Hb	.	.	.	.	+ +	.	.	.	.
Bi	.	.	.	.	.	.	.	+	.
Qz	.	.	.	.	.	= =	.	+	.
Oxide	= =	= =	.	=	.	=	.	= =	.
Comments	.	.	50% vesicles	.	.	gabbroic clots			

Whole-rock chemical composition is normalized to 100% anhydrous.
Original Fe2O3, total, and LOI reported.
Gms is estimated percent groundmass.
Plag1 is well formed and inclusion free.
Plag2 is resorbed, reversely zoned, or spongy
Proportions of minerals denoted by + + (dominant), + (common),
= (uncommon), = = (rare), and . (not observed).

TABLE 4-1. Continued.

ID	88cnu13	88cnu06	88cnu07	88cnu08	88cnu09	88cnu15	88cnu21	88cnu56	88cnu57
UNIT	Qra1	Qra	Qra	Qra	Qra	Qra	Qra	Qra	Qra
Chemical composition									
SiO2	61.61	55.27	.	.	51.74	.	50.70	56.44	58.18
TiO2	0.85	0.96	.	.	0.95	.	0.74	1.05	0.97
Al2O3	17.00	17.60	.	.	16.14	.	15.52	16.49	16.97
FeOt	5.75	7.32	.	.	8.04	.	7.97	7.07	6.43
MgO	2.28	5.07	.	.	8.08	.	10.93	4.76	4.01
CaO	5.79	8.07	.	.	9.84	.	10.11	8.15	7.45
NaO	4.93	4.32	.	.	4.19	.	3.05	4.13	4.27
K2O	1.64	1.24	.	.	0.85	.	0.87	1.71	1.54
P2O5	0.13	0.16	.	.	0.16	.	0.12	0.20	0.17
MnO	na	na	.	.	na	.	na	na	na
LOI	na	na	.	.	na	.	na	na	na
Total	100.14	101.05	.	.	100.66	.	100.84	100.47	99.21
Fe2O3	6.36	8.15	.	.	8.92	.	8.85	7.84	7.04
Modal composition									
Gms	70	65	50	70	75	60	40	70	50
Plag1	+	=	+ +	=	+	+ +	+	+	+
Plag2	+	+ +	=	+ +	=	.	.	=	=
Ol	.	=	= =	.	+	.	+ +	=	=
Cpx	+	+	+	+	=	+	=	+	+
Opx	.	=	+	+	= =	+	.	+	+
Hb	.	.	.	.	.	.	.	.	.
Bi	.	.	.	.	.	.	.	.	.
Qz	.	.	.	.	.	.	.	.	.
Oxide	=	= =	= =	.	.	=	.	=	=
Commentsglomerocrysts		.	.	clots	.	clots	.	.	.

Whole-rock chemical composition is normalized to 100% anhydrous.
Original Fe2O3, total, and LOI reported.
Gms is estimated percent groundmass.
Plag1 is well formed and inclusion free.
Plag2 is resorbed, reversely zoned, or spongy
Proportions of minerals denoted by + + (dominant), + (common), = (uncommon), = = (rare), and . (not observed).

TABLE 4-1. Continued.

ID	88cnu58	88cnu80	88cnu81	88cnu82	88cnu83	88cnu84	88cnu85	dt88-10	dt88-12
UNIT	Qra	Qra	Qra	Qra	Qra	Qra	Qra	Qra	Qra
Chemical composition									
SiO2	.	54.71	.	.	54.36	51.65	52.44	60.07	.
TiO2	.	0.96	.	.	0.94	1.22	0.89	0.74	.
Al2O3	.	18.65	.	.	18.87	17.53	18.17	17.11	.
FeOt	.	7.45	.	.	7.26	9.28	7.90	5.55	.
MgO	.	4.47	.	.	4.48	5.83	6.42	3.62	.
CaO	.	8.88	.	.	9.05	9.68	9.78	6.93	.
NaO	.	3.84	.	.	4.02	4.04	3.69	4.27	.
K2O	.	0.92	.	.	0.89	0.61	0.62	1.57	.
P2O5	.	0.12	.	.	0.13	0.16	0.10	0.14	.
MnO	.	na	.	.	na	na	na	na	.
LOI	.	na	.	.	na	na	na	na	.
Total	.	98.53	.	.	100.30	101.40	99.43	98.83	.
Fe2O3	.	8.09	.	.	8.03	10.36	8.65	6.06	.
Modal composition									
Gms	50	65	65	70	70	99	60	70	60
Plag1	+	+ +	+ +	+	+	=	+	=	+
Plag2	=	=	=	=	+	.	=	+	+
Ol	=	=	+	+	=	=	+	.	.
Cpx	+	+	=	+	=	= =	=	+	+
Opx	+	=	=	=	= =	.	.	=	=
Hb	.	.	.	.	.	.	.	.	.
Bi	.	.	.	.	.	.	.	.	.
Qz	.	.	.	.	.	.	.	.	.
Oxide	=	.	=	= =	= =	.	= =	= =	= =
Comments									

Whole-rock chemical composition is normalized to 100% anhydrous.
Original Fe2O3, total, and LOI reported.
Gms is estimated percent groundmass.
Plag1 is well formed and inclusion free.
Plag2 is resorbed, reversely zoned, or spongy
Proportions of minerals denoted by + + (dominant), + (common), = (uncommon), = = (rare), and . (not observed).

TABLE 4-1. Continued.

ID	dt88-13	dt88-14	dt88-15	dt88-16	dt88-17	88cnu02	88cnu03	88cnu04	88cnu05
UNIT	Qra	Qra	Qra	Qra	Qra	Qcuv	Qcuv	Qcuv	Qcuv
Chemical composition									
SiO2	60.84	60.16	56.64	58.08	57.58	54.95	55.21	55.35	60.65
TiO2	0.73	0.73	0.78	0.84	0.83	0.83	0.70	0.83	1.26
Al2O3	16.96	17.31	18.23	18.05	18.25	20.88	18.81	20.89	15.86
FeOt	5.45	5.50	6.58	6.10	6.10	6.43	6.73	6.57	7.20
MgO	3.56	3.61	4.14	3.67	3.68	2.97	5.22	3.14	2.43
CaO	6.81	6.99	8.78	7.89	8.12	9.44	9.19	9.60	5.65
NaO	3.85	3.93	3.51	4.03	4.12	3.62	3.28	2.74	4.85
K2O	1.67	1.66	1.20	1.19	1.18	0.75	0.76	0.75	1.90
P2O5	0.13	0.12	0.14	0.15	0.15	0.13	0.09	0.13	0.20
MnO	na	na	na	na	na	na	na	na	na
LOI	na	na	na	na	na	na	na	na	na
Total	99.01	100.45	97.52	99.41	100.24	98.34	98.93	97.93	101.18
Fe2O3	5.98	6.11	7.08	6.69	6.75	6.98	7.35	7.10	8.03
Modal composition									
Gms	60	65	70	75	75	65	50	55	95
Plag1	+	+	+	+	+	+	+	+	+
Plag2	+	+	=	+	+	.	=	=	.
Ol	.	.	.	.	.	+	.	+	.
Cpx	+	+	=	+	+	+	+	.	+
Opx	=	+	=	=	=	=	=	= =	+
Hb	.	.	+	.	.	.	= =	.	.
Bi	.	.	.	.	.	.	.	.	.
Qz	.	.	.	.	.	.	.	.	.
Oxide	= =	= =	= =	.	.	.	.	= =	.
Comments	.	.	.	.	.	.	.	.	.

Whole-rock chemical composition is normalized to 100% anhydrous.
Original Fe2O3, total, and LOI reported.
Gms is estimated percent groundmass.
Plag1 is well formed and inclusion free.
Plag2 is resorbed, reversely zoned, or spongy
Proportions of minerals denoted by + + (dominant), + (common), = (uncommon), = = (rare), and . (not observed).

TABLE 4-1. Continued.

ID UNIT	88cnu52 Qcuv	88cnu53 Qcuv	88cnu54 Qcuv	88cnu59 Qcuv	dt88-05 Qcuv	dt88-06 Qcuv	dt88-07 Qcuv	dt88-08 Qcuv	dt88-34 Qcuv
Chemical composition									
SiO2	55.48	54.78	.	58.58	54.73	.	53.24	.	.
TiO2	1.10	1.17	.	0.97	0.74	.	0.88	.	.
Al2O3	16.67	16.94	.	17.05	17.73	.	18.99	.	.
FeOt	8.64	8.75	.	6.33	6.83	.	7.90	.	.
MgO	4.16	4.39	.	3.90	5.79	.	5.94	.	.
CaO	8.70	9.32	.	7.24	8.69	.	9.61	.	.
NaO	3.99	3.47	.	4.18	4.54	.	2.56	.	.
K2O	1.10	1.00	.	1.59	0.84	.	0.75	.	.
P2O5	0.17	0.18	.	0.18	0.12	.	0.12	.	.
MnO	na	na	.	na	na	.	na	.	.
LOI	na	na	.	na	na	.	na	.	.
Total	98.84	98.02	.	99.23	98.50	.	100.12	.	.
Fe2O3	9.40	9.44	.	6.93	7.43	.	8.72	.	.
Modal composition									
Gms	95	90	99	50	60	95	85	80	99
Plag1	+	+	+	+	+	+	+	+ +	+
Plag2	+	.	.	=	=	.	=	.	.
Ol	.	=	.	= =	+	.	+	.	.
Cpx	+	+	+	.	+	.	.	.	+
Opx	+	.	.	.	+	.	.	.	.
Hb	.	.	.	.	.	.	.	.	.
Bi	.	.	.	.	.	.	.	.	.
Qz	.	.	.	.	.	.	.	.	.
Oxide	.	.	.	=	= =	.	.	.	.
Comments	.	clots	.	.	.	.	.	.	.

Whole-rock chemical composition is normalized to 100% anhydrous.
Original Fe2O3, total, and LOI reported.
Gms is estimated percent groundmass.
Plag1 is well formed and inclusion free.
Plag2 is resorbed, reversely zoned, or spongy
Proportions of minerals denoted by + + (dominant), + (common), = (uncommon), = = (rare), and . (not observed).

TABLE 4-1. Continued

ID	dt88-35	dt88-36	dt88-37	dt88-38	dt88-30	dt88-31	dt88-32	dt88-33	88cnu10
UNIT	Qcuv	Qcuv	Qcuv	Qcuv	Qcuv dike	Qcuv dike	Qcuv dike	Qcuv dike	Tdp
Chemical composition									
SiO2	.	54.37	62.48	.	.	.	.	.	59.67
TiO2	.	1.18	1.28	.	.	.	.	.	1.06
Al2O3	.	17.26	15.54	.	.	.	.	.	17.33
FeOt	.	8.85	6.81	.	.	.	.	.	5.90
MgO	.	4.46	2.00	.	.	.	.	.	3.43
CaO	.	9.01	4.61	.	.	.	.	.	5.81
NaO	.	3.57	5.07	.	.	.	.	.	3.67
K2O	.	1.09	1.71	.	.	.	.	.	2.77
P2O5	.	0.21	0.50	.	.	.	.	.	0.24
MnO	.	na	na	.	.	.	.	.	0.11
LOI	.	na	na	.	.	.	.	.	1.85
Total	.	98.88	99.41	.	.	.	.	.	100.02
Fe2O3	.	9.63	7.47	.	.	.	.	.	6.40
Modal composition									
Gms	95	80	99	98	98	90	85	98	.
Plag1	+	=	+	+	+	+	+	+	.
Plag2	+	+	.	.	.	.	=	=	.
Ol	.	+	.	.	.	.	=	?	.
Cpx	+	+	+	+	+	+	+	+	.
Opx	=	.	.	.	.	=	+	.	.
Hb	.	.	.	.	.	.	.	.	.
Bi	.	.	.	.	.	.	.	.	.
Qz	.	.	.	.	.	.	.	.	.
Oxide	.	.	.	.	.	.	.	.	.
Comments	.	.	.	.	.	.	.	ol altered	.

Whole-rock chemical composition is normalized to 100% anhydrous.
Original Fe2O3, total, and LOI reported.
Gms is estimated percent groundmass.
Plag1 is well formed and inclusion free.
Plag2 is resorbed, reversely zoned, or spongy
Proportions of minerals denoted by + + (dominant), + (common), = (uncommon), = = (rare), and . (not observed).

TABLE 4-1. Continued.

ID	88cnu11	dt88-01a
UNIT	Tdp	Tdp
Chemical composition		
SiO2	59.47	57.44
TiO2	1.26	0.86
Al2O3	17.05	17.59
FeOt	6.04	6.54
MgO	3.52	4.42
CaO	6.38	7.85
NaO	3.59	3.57
K2O	2.27	1.40
P2O5	0.29	0.18
MnO	0.12	0.14
LOI	1.16	0.85
Total	100.36	99.93
Fe2O3	6.61	7.15
Modal composition		
Gms	.	.
Plag1	.	.
Plag2	.	.
Ol	.	.
Cpx	see table 2-1	
Opx	for modes	
Hb	.	.
Bi	.	.
Qz	.	.
Oxide	.	.
Comments	.	.

Whole-rock chemical composition is normalized to 100% anhydrous.
Original Fe2O3, total, and LOI reported.
Gms is estimated percent groundmass.
Plag1 is well formed and inclusion free.
Plag2 is resorbed, reversely zoned, or spongy
Proportions of minerals denoted by + + (dominant), + (common), = (uncommon), = = (rare), and . (not observed).

5. THERMAL AREAS: DESCRIPTION, SPRING DISCHARGE, AND CONVECTIVE HEAT FLOW

5.1 Location

Six zones of thermal springs and small geysers are dispersed over an area of about 4 km^2 in the upper reaches of Geyser Creek valley at elevations ranging from 30 m to 110 m (Plate 2 and Figure 5.1). Letters designating spring groups follow the nomenclature established by Byers and Brannock (1949). Previous investigations of the geothermal springs at Geyser Bight include Byers and Brannock (1949), I. Barnes (1975 - U.S. Geological Survey, unpublished data, pers. comm., 1981), and Motyka and others (1981). Most of the hot springs emanate along Geyser Creek and its tributaries, and emerge in the valley floor and at the base of steep valley walls. Two small areas of steaming ground and weakly pressurized fumaroles are located at elevations of 275 and 310 m in a tributary valley at the headwaters of Geyser Creek (F1 and F2, Plate 1).

During geologic field mapping in 1988 a previously unreported fumarole field was discovered at an elevation of approximately 450 m on the lower northeast flank of the volcano Mt. Recheshnoi (F3, Plates 1 and 2). The field is about 4 km south of Geyser Bight valley and is separated from the valley by a broad ridge. The fumaroles lie near the head of a rugged canyon that drains towards Russian Bay. Fumarole temperatures measured in excess of 125°C. Weather conditions and lack of time prevented sampling of fumarole gases at F3.

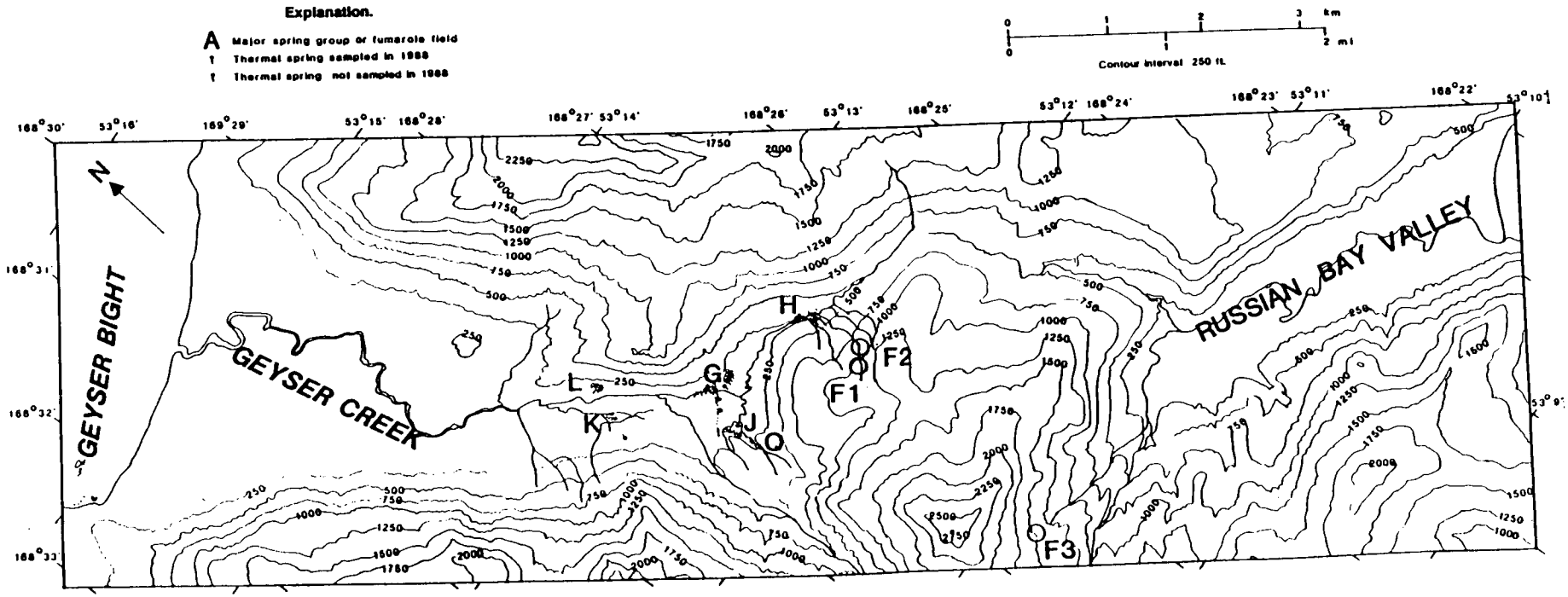

Figure 5.1 Location map for the thermal springs and fumaroles of Geyser Bight, central Umnak Island.

5.2 Spring Descriptions

Geothermal activity at Geyser Bight (Table 5.1) appears to vary over time with 1980 showing substantially less output than either 1947 or 1988. For the 1988 activity column in Table 5.1, the following conventions are used. The type of activity labeled seeps (s) generally has hot water quietly flowing from alluvium, colluvium, bedrock, or any combination thereof, at rates of 5 lpm (liters per minute) or less. Springs (sp) have larger flows than seeps. Pools (p) are small open bodies of water fed by a spring or by numerous indistinguishable seeps. Ebullient boiling springs (eb) are those in which gas and steam violently break the surface. Fountain (f) refers to springs in which, in addition to ebullition, hot water is ejected above the waters normal surface. Using White's 1967 definition, a geyser (g) is a "hot spring characterized by intermittent discharge of water ejected turbulently and accomplished by a vapor phase". Some authors also consider ebullition and fountaining to be a type of geyser activity. Some springs that were pulsing and almost continuous fountains in 1988 were described as geysers with 50 to 60 cycles per minute in 1980 (Motyka and others, 1981). Because the Geyser Bight geothermal area is relatively unknown, detailed descriptions of the thermal spring sites are provided here for future reference.

5.2.1 Site F1

Fumarole field 1 (Figure 5.2) is located at approximately 300 m (1000 ft) elevation in a slightly circular depression, mostly on the left bank of a creek informally referred to as Fumarole Creek. Immediately above F1 the temperature of Fumarole Creek is 9.2°C. The temperature of Fumarole Creek compared to other local snow fed creeks that have temperatures of 4°C indicates that the creek receives some geothermal heat input above F1. Visual

Table 5.1. Comparison of Geyser Bight spring characteristics 1947 to 1988.

Site	1988 Temp °C	1988 Flow[1] l/min	1988 Act	1980 Temp °C	1980 Flow l/min	1980 Act	1947 Temp °C	1947 Flow l/min	1947 Act
G1	81-102	70	f	100	20	g	101	260	sp
G2	102	25	f	79	5	g	88	6	sp
G3	101	20	f	100	16	g	100.5	18	sp
G4	97	15	f	92	5	s	98	36	sp
G5	u	0	eb	nr	nr		u	none	eb
G6	75-94	36	sp,eb	97	20	eb	95	80	sp
G7	not	found		not	found		82	85	sp
G8[2]	100	150	g	100	75	g	101	170	g
G8A	65-96	15	s,eb	92-98	nr	sp,s	nr	nr	
G9	102	36	f	99		sp	101	6	sp
G10	103	54	f	100		sp	99	170	eb,f
G11	88	18	sp	81		sp	77	170	sp
G12	51	u	p	nr	u	p	51	u	p
H0	nr	nr	sp	97	30	sp	nr	nr	
H1	102	400	f	100	300	g	102	660	g
H2	99-102	95	f	99	100	g,f	101	600	g
H3	48	150	sp	45	60	sp	53	none	
H4	102	400	g	100	45	eb	101	340	sp
H5	not	found		101	nr	g	101	85	sp
H6	104	50	eb	99	30	f,eb	100	66	sp
H7	101	135	sp	99	70	eb	90	260	g
H8	99	100	g	nr	nr		nr	nr	
H9	67	200	sp	nr	nr		nr	nr	
H10	97	150	f	nr	nr		nr	nr	
H11	71-96	165	g	nr	nr		nr	nr	
H12	75-81	5-30	sp,s	84	1	s	nr	nr	
H13	70	40	sp	nr	nr		nr	nr	
J1	80	10	p	82	nr	p	88	720	nr
J2	80	32	s	77	nr	s	nr	nr	
J3	55-80	41	sp,s	77-88	10	sp,s	nr	nr	
J4	65	20	p	69	5	p	nr	nr	
J5	90	25	g	92	15	g	nr	nr	
J6	85	25	p	83	15	p	nr	nr	
K1	61		p	62		p	70	170	
K2	50		p	59		p	58	85	
K1+K2		30			100				
K3	80	10	sp	nr	nr		nr	nr	
K3-seeps	63	50	s	nr	nr		nr	nr	
L	40-78	250	sp,s,p	45-85	200	p,sp,s	67-69	170	
Q	30-80	131	sp,s	70-75	25		nr	nr	
Total flow est.		3250			1150			4150	

[1] Most flows in 1988 were visually estimated. L, H7, G11, were measured with standard pygmy flow-meter.
[2] Flow for G8 is at maximum activity. See discussion in text.

Abbreviations: sp=spring, s=seep, f=fountain, g=geyser, eb=ebullient boiling, p=pool, u = unable to make measurement, nr = not reported

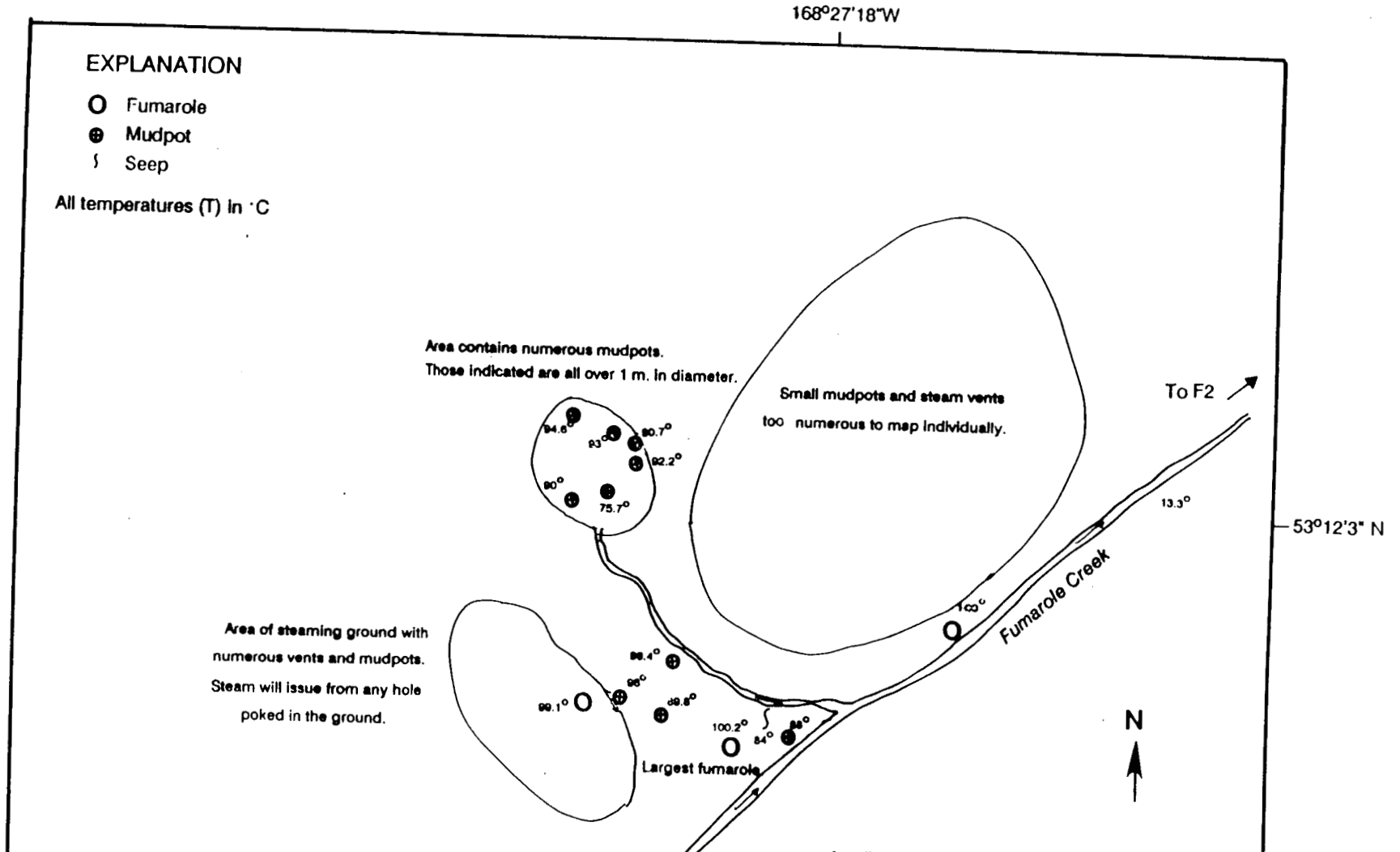

Figure 5.2 Details at Geyser Bight Fumarole Field 1.

estimates of creek flow are 400 lpm above and 450 lpm below F1; creek temperature below F1 is 19.5°C . The most prominent feature at F1 is a 100°C pressurized vent. A slight odor of H_2S is noticeable. Adjacent to this vent is an area of altered hot ground with active steam vents and mud pots, measuring approximately 6 by 8 meters.

5.2.2 Site F2

Fumarole field 2 (Figure 5.3) is located at approximately 275 m (900 ft) elevation and extends about 150 m along Fumarole Creek about 1/2 km downstream of F1. Fumarole Creek is 17°C above F2 and 21°C below it. Visual estimates of flow are 450 lpm above and 500 lpm below. The most prominent feature at F2 is a 102°C pressurized vent. F2 has low-chloride hot springs in addition to mud pots and fumaroles. About 20 to 30 m below the last steam vent of F2, lies a 20 m diameter fossil fumarole field on the left bank of Fumarole Creek.

5.2.3 Site F3

Fumarole field 3 (Figure 5.4) is located at approximately 425 m (1400 ft) elevation on a creek in the central portion of upper Russian Bay valley. The most prominent feature at F3 is a superheated, pressurized fumarole with a plume of over 30 m and a minimum temperature of 125°C. Rocks, 5 cm in diameter thrown into the vent were forcefully ejected by the fumarole jet. H2S smell is noticeable but not overpowering. The temperature of the creek draining the fumarole field is 7°C above and 43°C below the geothermal area. Two fossil fumarole areas are located about 10 m above the main active area, one on either side of the main creek. About 40 m east of the large fumarole is an area of altered steaming ground 40 m by 25 m with numerous active boiling point fumaroles.

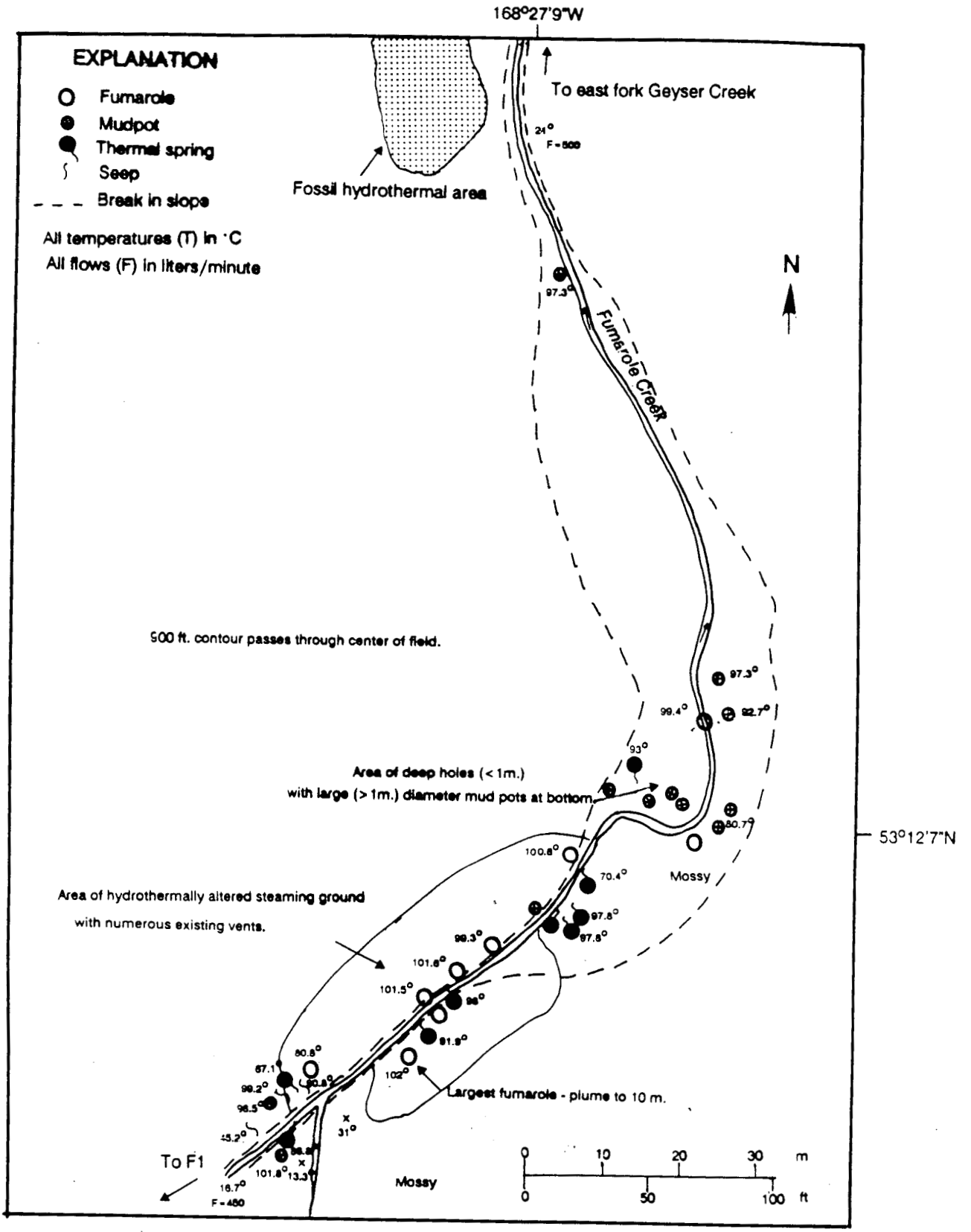

Figure 5.3 Details at Geyser Bight Fumarole Field 2.

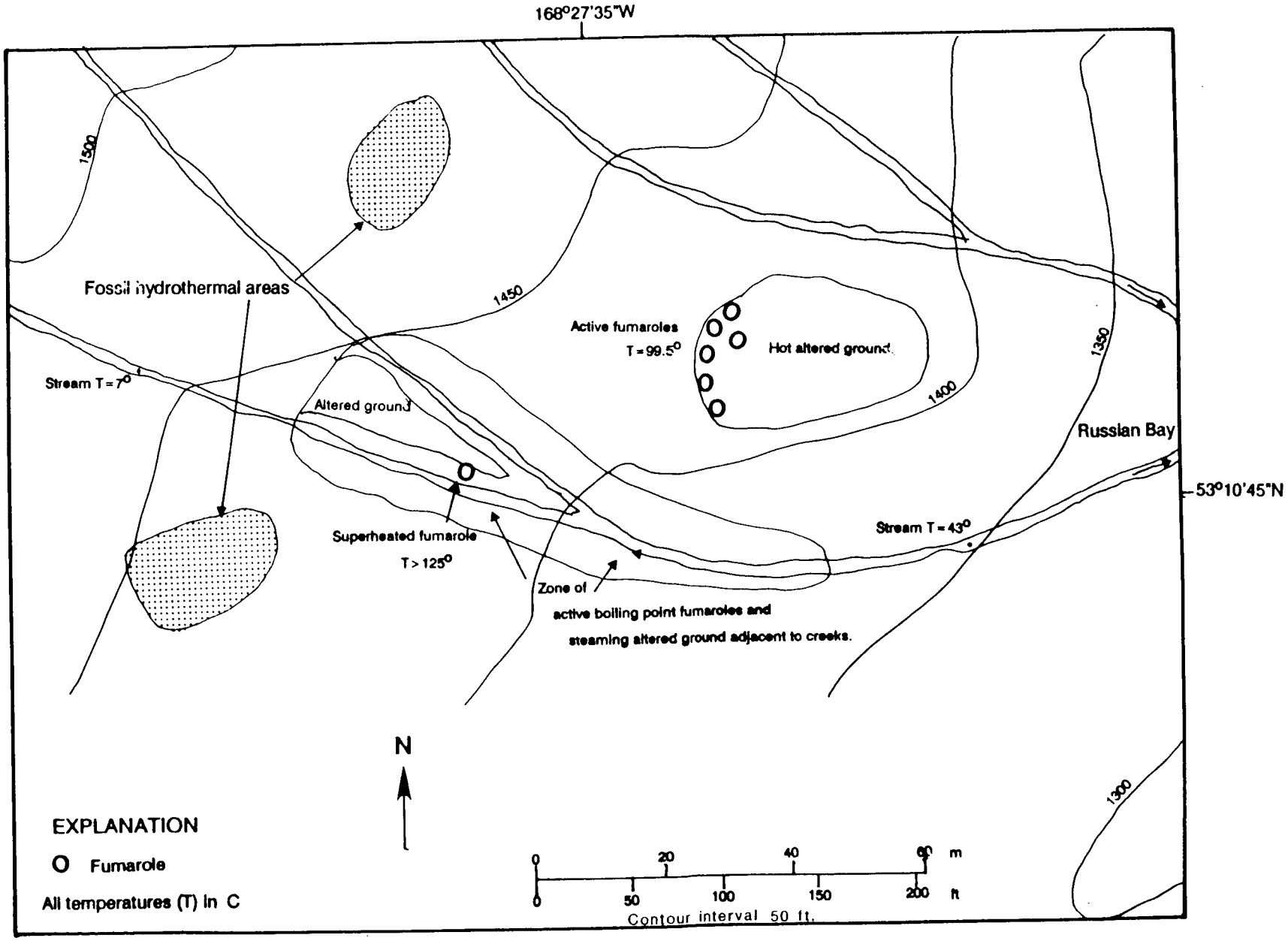

Figure 5.4 Details at Fumarole Field 3, upper Russian Bay Valley, central Umnak Island.

5.2.4 Site G

Site G (Figure 5.5) is located 5.5 km from Geyser Bight at the southeastern end of the main glacial valley. Two groups of thermal springs emerge at the base and on the lower slopes of the east valley wall. The thermal waters emanate from numerous small pools, orifices, and seeps in the cemented alluvium and colluvium. Several small steam vents also occur in the area. Fossil geothermal areas, the largest measuring 100 m by 50 m, indicate that the geothermal activity was either more extensive in the past or has migrated. Several warm seeps and numerous sinter covered rocks are located in an old channel across the east fork of Geyser Creek, towards site J.

The up-valley series of springs clusters at the base of a low ridge adjacent to two small ponds of warm water (Figure 5.6). Spring G1 consists of several vents at the upstream edge of the larger pond. Springs G1b, c, and e exhibit ebullient boiling and have fountains to 30 cm. Spring G1c has the largest flow and was sampled for water chemistry. In 1988 spring G1c was pulsing almost continuously; in 1980 it erupted every 1 to 3 seconds. G1a was fountaining with occasional bursts of steam. The pH of the thermal spring waters at G1 ranges from 6.8 to 9.2 reflecting the boiling and loss of acid gases.

Vigorously boiling fountains, springs G2, G3, and G4, plus several smaller vents lie above and 10 m distant from G1 (Figure 5.6). A silica apron up to 5 m wide extends down slope from this cluster and an area of steaming ground over 25 m in lateral extent lies immediately to the east. G5, a steaming vent over 2 m in diameter, lies further up slope. Water can be heard boiling below the surface but could not be reached with a 2 m probe. The ground in the immediate area is warm, moss covered, and has been altered to clays. Between

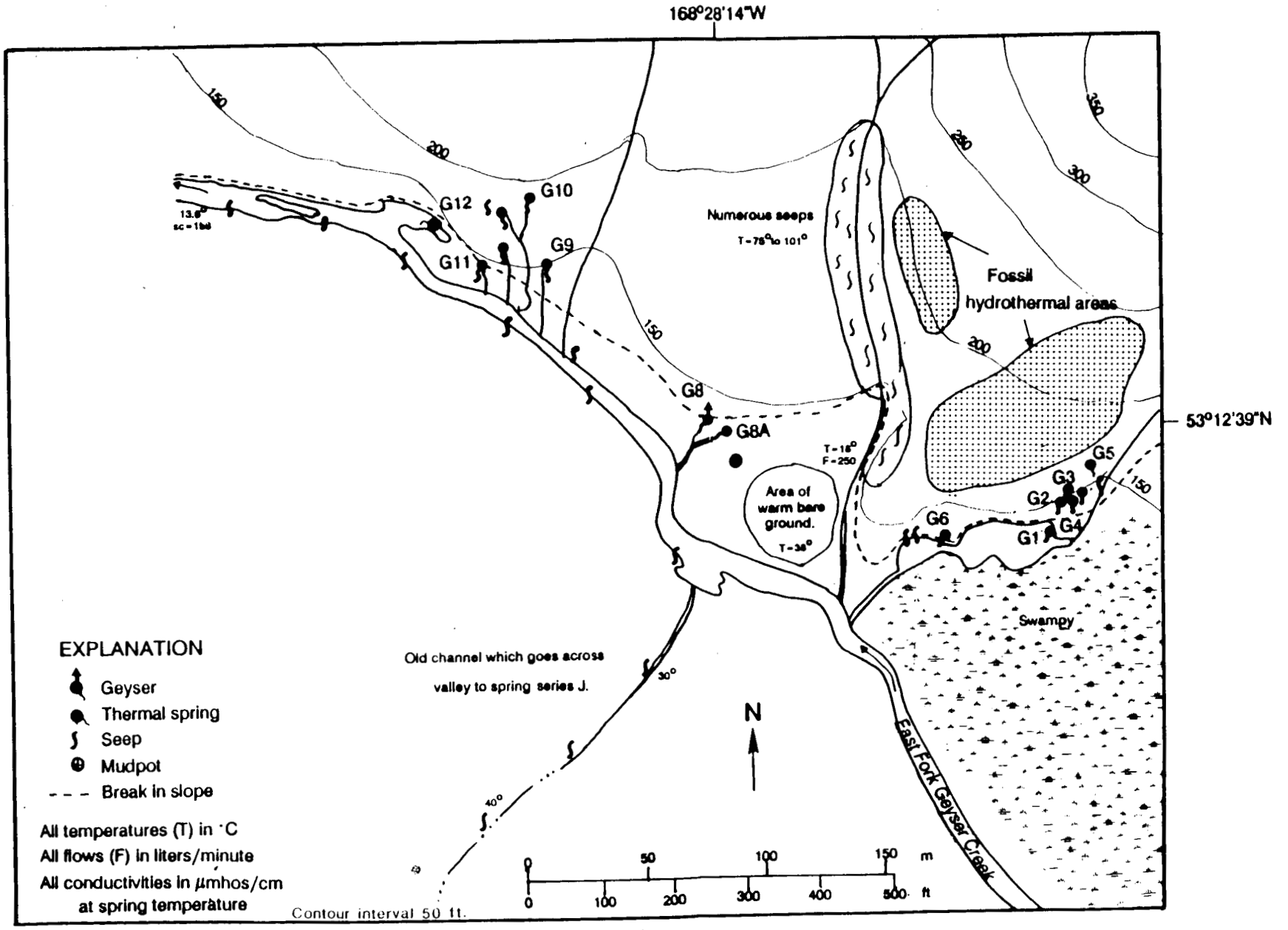

Figure 5.5 Overview of Geyser Bight spring series G.

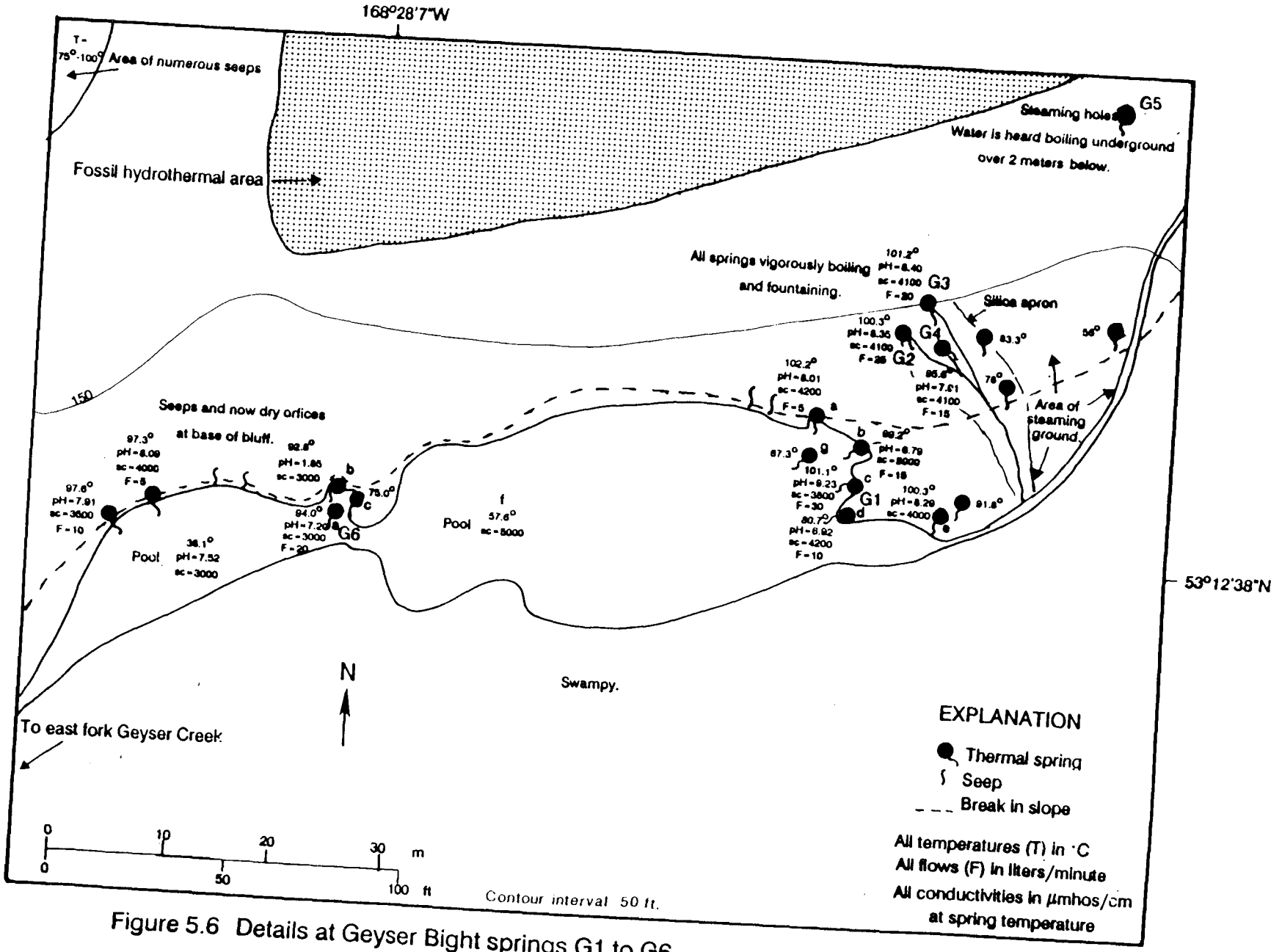

Figure 5.6 Details at Geyser Bight springs G1 to G6.

the two warm ponds, spring G6 emerges from a 50 cm diameter sinter cone. Its pH is 7.2 while 0.5 m away is a small bubbling vent with pH of 1.9. Several seeps with flows up to 10 lpm emanate along the shore of the smaller pond, and gas bubbling in the pond points to locations of additional vents.

Down-valley from G1-G6 is an area of diffuse geothermal activity (Figure 5.5). An unnamed creek has numerous seeps for 150 m of its length. Probably one of these had sufficient flow in 1947 to be called G7 by Byers and Brannock (1949). Between these seeps and the east fork of Geyser Creek is a 40 m diameter unvegetated area of warm bare ground with temperatures of 38°C. Nearby are two large mud pots, and 10 m farther is spring G8.

Spring G8 is a geyser that emerges in a bowl about 1 m in diameter composed of sinter-cemented rock (Figure 5.7). A typical eruptive cycle results in approximately 750 liters of water being discharged every 12 minutes for an average minimum flow of 60 lpm. The height of the fountaining was 60 cm in 1870 (Dall, 1870) and in 1947 but has decreased to 20 cm in 1988. A 5 m wide, 25 m long silica apron extends from the geyser towards the east fork of Geyser Creek. Figure 5.6 adjacent to spring G8 is a 4 m diameter cluster of acid springs with pH values from 1.5 to 5.9. Two are vigorously boiling, two are muddy, and all have low flows. Their combined discharge is about 15 lpm. These springs appear to be the result of steam and acid gases condensing into and warming near-surface meteoric waters.

Springs G9, G10, G11, and a warm pool G12 are located further downstream (Figure 5.8). Several vents also discharge directly into the east fork of Geyser Creek and along its banks. The creek bottom has algal growth at least 50 m below the last seep. Warm ground was found as far as 200 m downstream from G12. Springs G9 and G10 are fountaining and have siliceous sinter cones

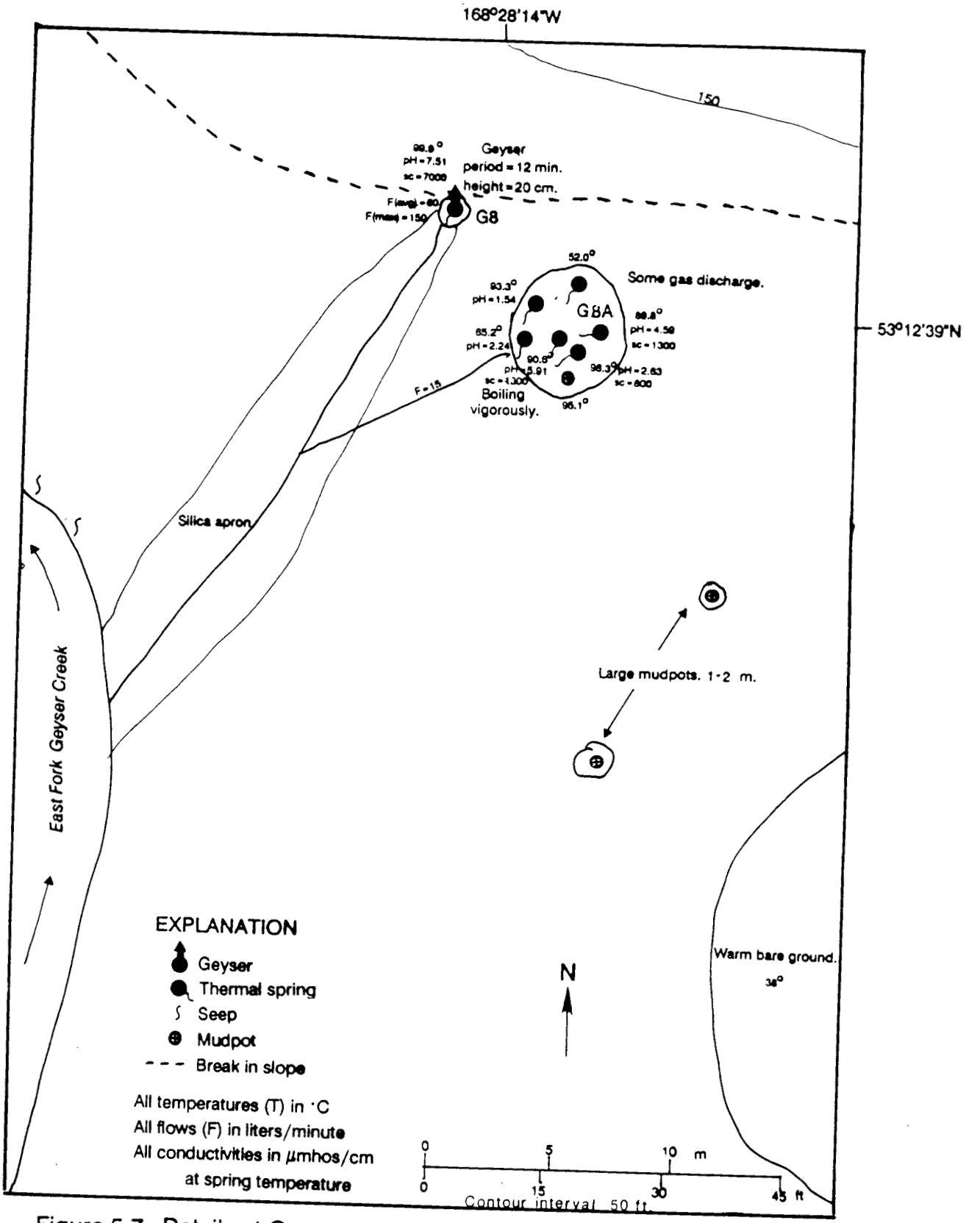

Figure 5.7 Details at Geyser Bight spring G8

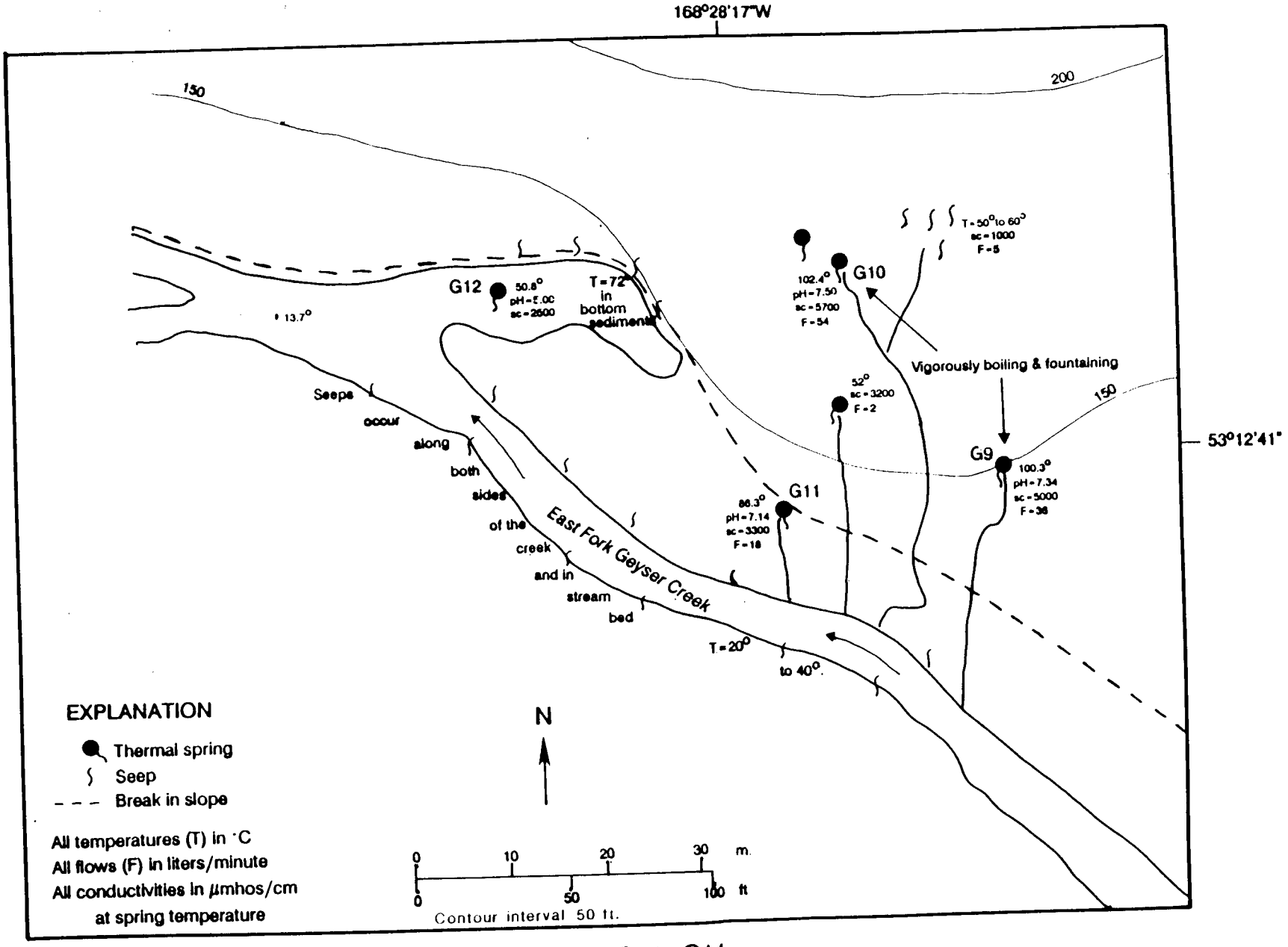

Figure 5.8 Details at Geyser Bight springs G9 to G11.

and terraces, while spring G11 emanates from a cluster of boulders. Water in pool G12 has a maximum temperature of 51°C but temperatures as high as 72°C were found in the bottom sediments.

5.2.5 Site H

Site H springs (Figure 5.9) lie along the east fork of Geyser Creek and in a narrow tributary valley at an elevation of about 100 m. The intensity of thermal activity at H has been irregular. In 1947 Byers and Brannock (1949) reported seven springs with total output of approximately 2000 lpm. In 1980 Motyka and others, (1981) reported eight springs but total output was only 650 lpm. In 1988 six additional springs plus numerous seeps were observed. A couple of previously reported vents were dry, but total output was at least 1900 lpm in 1988. The east fork of Geyser Creek measured 8.3°C above the H geothermal activity and 16.9°C below it.

The uppermost springs and seeps emerge from volcanic bedrock flanking a 15 m waterfall (Figure 5.10). Most of these vents are inaccessible because of cliffs but their presence can be inferred by dark green algae and steam. Springs also discharge directly into the creek as evidenced by gas bubbling up in a relatively calm area between two steps of the water fall. Temperatures, where they could be measured, range from 40 to 80°C. Flows ranged up to 40 lpm.

At the base of the waterfall a small creek, informally referred to as "H" Creek, enters the east fork of Geyser Creek from the south (Figure 5.10). The most active of the H springs line the banks of this creek. Above the highest visible seep, the temperature of "H" Creek is 16°C, which indicates that some hot water is seeping directly into the stream bed above the visibly active

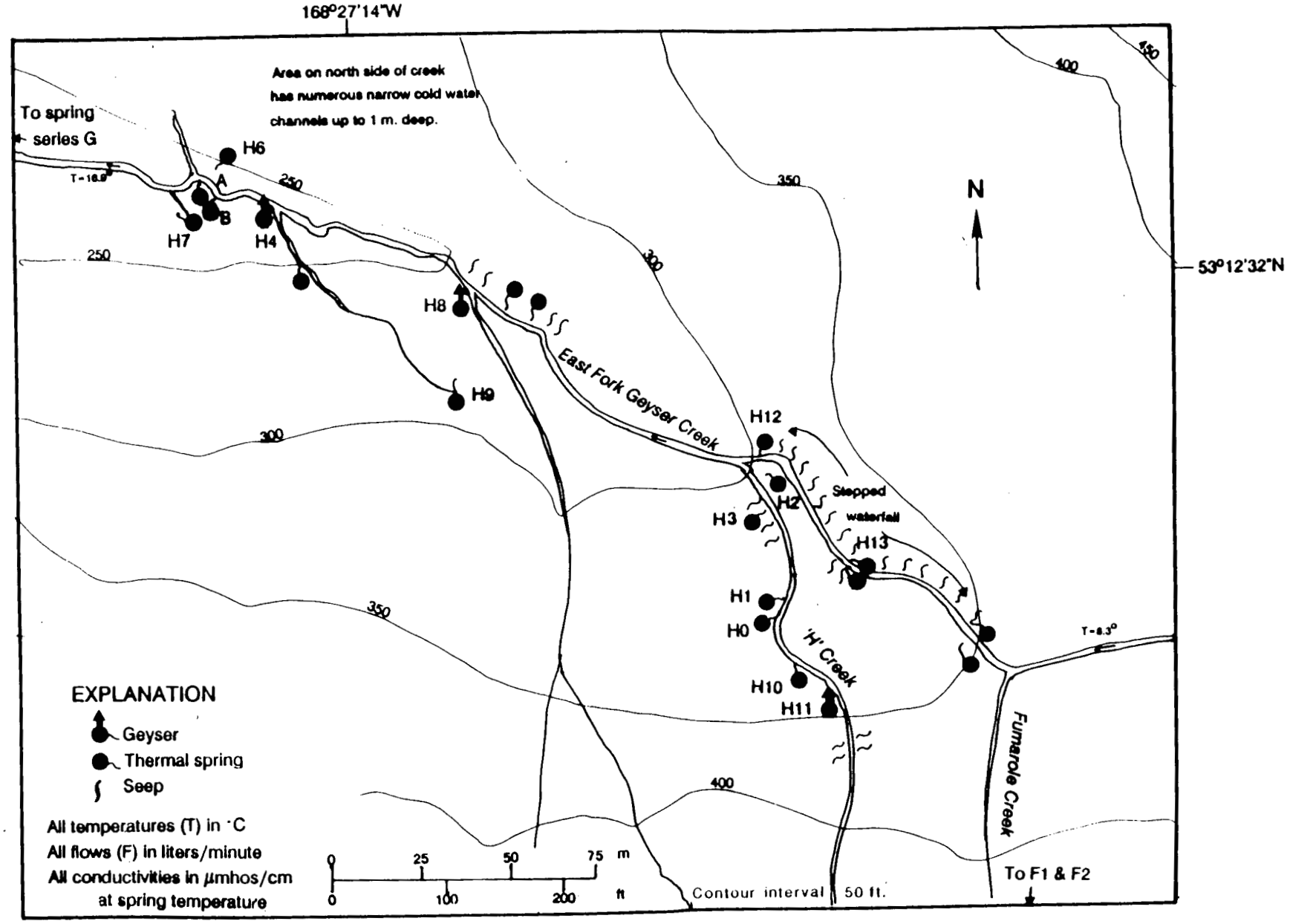

Figure 5.9 Overview of Geyser Bight spring series H

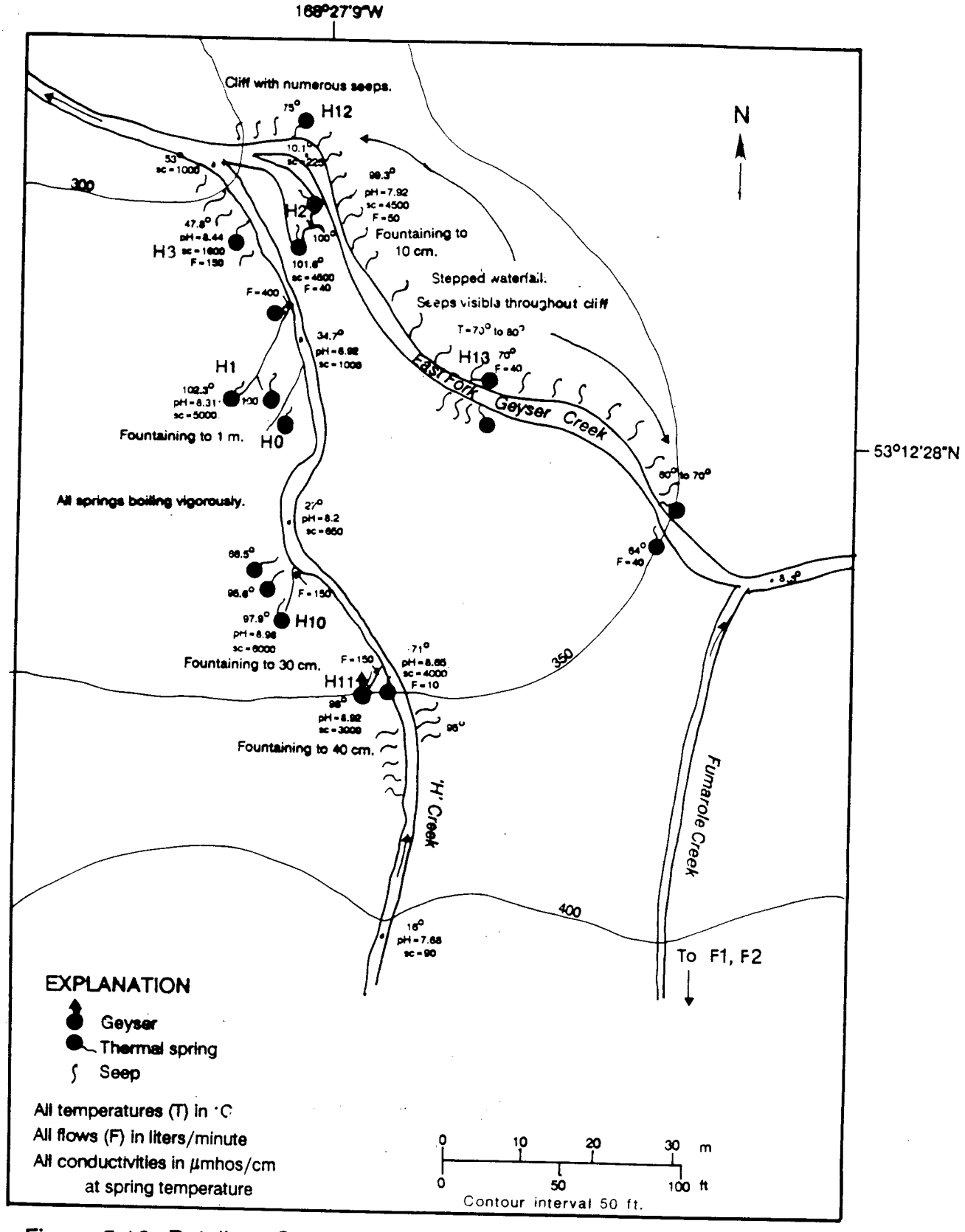

Figure 5.10 Details at Geyser Bight springs H0 to H3 and H10 to H13.

thermal zone. At the mouth of "H" Creek, the temperature is 53°C from the addition of boiling water from the visible springs. Except for H3 and HO, the other numbered springs along "H" creek exhibit ebullient boiling and fountaining.

Spring H2 is immediately upstream from the mouth of "H" Creek and along the east fork of Geyser Creek. Two vents, with flows of 40 to 50 lpm each, and several smaller spouting vents comprise this spring group. One of the larger vents discharges into a quiet pool and the other (H2) is constantly bubbling with a 10 cm fountain. Along "H" Creek itself, the first set of vents is labeled H3 (Figure 5.10). H3 and all other numbered springs along "H" Creek emanate from its west bank. The largest and most active spring along "H" Creek is H1, a set of three interconnected, 1 m diameter cauldrons set within a 10 m diameter patch of large, mostly volcanic boulders up to 2 m in diameter. The cauldrons contain vigorously boiling water with 70 cm fountains. The 12 m long channel which drains H1 contributes about one-third of the flow in "H" Creek. H1 was a geyser with period of 2.5 to 3.5 minutes in 1947, and a geyser with period of 1 minute in 1980, but was a continuously fountaining spring in 1988. Ten meters upstream from H1, spring HO emerges in a small, 1 m diameter bowl, perched about 5 m above "H" Creek. In 1980 this spring had a flow of 30 lpm but by 1988 its flow had diminished to a trickle.

H10 has an algae covered silica apron and is located about 20 m upstream from HO. The principal spring has a fountain of 30 cm in a 60 cm bowl located about 5 m above "H" Creek. Ten meters upstream, H11 emerges from the alluvium and colluvium. Located in a 1 m diameter bowl about 4 m from the "H" Creek, this geyser fountains to 40 cm with irregular periods on the order of one to

several minutes. H11 is the last of the large springs along this creek, but seeps with temperatures of 70 to 90°C are found for another 20 m upstream.

About 100 m downstream from the mouth of "H" creek and along the east fork of Geyser Creek lies a previously unreported area of geothermal activity (Figure 5.11). Along the north bank for a distance of 25-30 m numerous seeps discharge 40-60°C water at 2 to 20 lpm. Across the east fork of Geyser Creek, on the south side, H8 is normally a 1.3 by 0.5 m steaming pool of hot water with gas bubbling and no outflow. However, it was observed to erupt once in 1988 as a spectacular geyser with a 2 m fountain and water discharge of at least 100 lpm for about 10 minutes. Spring H9 emerges from colluvial cover about 15 to 20 m south of H8. Its outflow enters a narrow 40-50 cm wide channel, with several seeps and discharges into the east fork of Geyser Creek immediately upstream from H4.

H4 is a geyser of irregular period. On the day it was first sampled in 1988, H4 was boiling and fountaining continuously to 40 cm while discharging about 400 lpm of water during the five hours spent in the vicinity. Two days later H4 was at first observed to be dry. It then became active, geysering to 50 cm for 2 minutes before going dry. Three minutes later it geysered to 50 cm for a period of 3 minutes. Fountain height then decreased to 10 to 20 cm for 6 minutes before going dry again. After 11 minutes it geysered to 50 cm for 3 minutes again before decreasing to 10 to 20 cm. The fountain persisted at that level for another half hour, when the observer had to leave. The following day H4 had a 40 cm fountain and behaved as it had when first encountered.

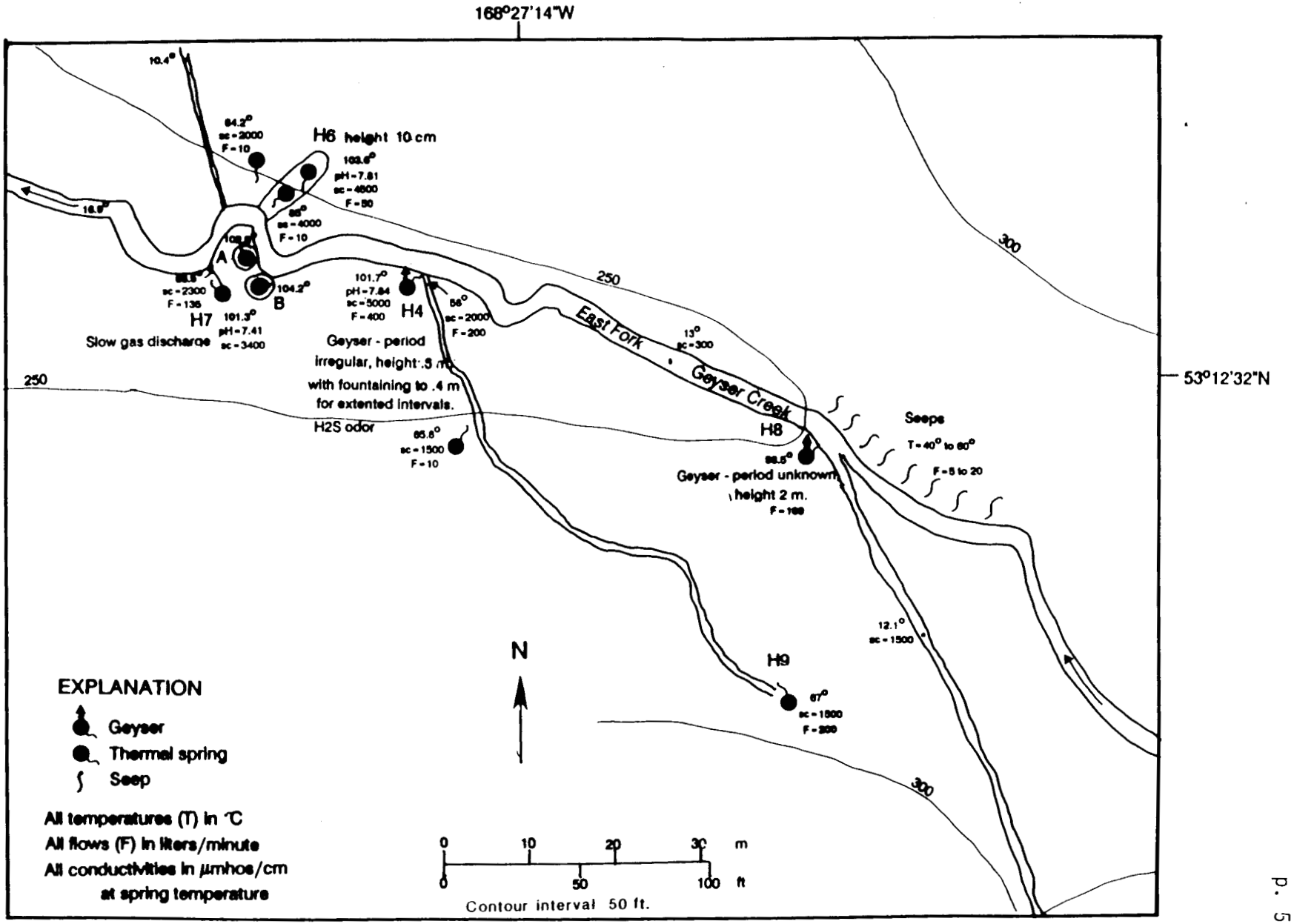

Figure 5.11 Details at Geyser Bight springs H4 to H9.

Downstream another 20 to 25 m is the last concentration of site "H" springs. A 10 by 15 m bare patch in the otherwise lush vegetation marks the area where the springs of H6 emerge from the cemented colluvium and glacial debris covering the valley on the north side of the creek. The main vent issues boiling water with a 10 cm fountain while a smaller vent 3 m away is quiet with gas slowly rising to the surface. On the south side, across from H6 are the two steaming pits called A and B in 1980. Both are about 2 m in diameter with water level 1.5 m below the surface. In 1980 the level of the water oscillated 25 cm while in 1988 it did not. Spring H7, situated 5 m away, changed from being an active geyser in 1980, to being a quiet pool with gas slowly bubbling to the surface. H5, which was a geyser in 1980, could not be found. The temperatures of A, B, and H7 were within a degree of each other in both 1980 and 1988, and are at or slightly above boiling.

5.2.6 Site J

Site J (Figure 5.12) is located in the southwest corner of Geyser Creek valley across from site G. The most prominent thermal spring at the site, J1, emanates from a 3 m dia., 5 m deep, funnel-shaped aquamarine pool set into the valley alluvium. A large silica apron extends east of the spring. Byers and Brannock (1949) estimated discharge from the pool at 720 lpm in 1947 but by 1988 it had decreased to 10 lpm. Low rumbling concussions could be heard and felt from beneath the ground surface in the vicinity of J1. The geometry, size, and temperature of the J1 pool suggest that J1 was once a geyser that has become inactive or is presently a geyser whose eruptive cycle has gone unobserved.

Other springs and seeps at site J are dispersed over a distance of 250 m along the slope break at the base of a low ridge. Above the currently active

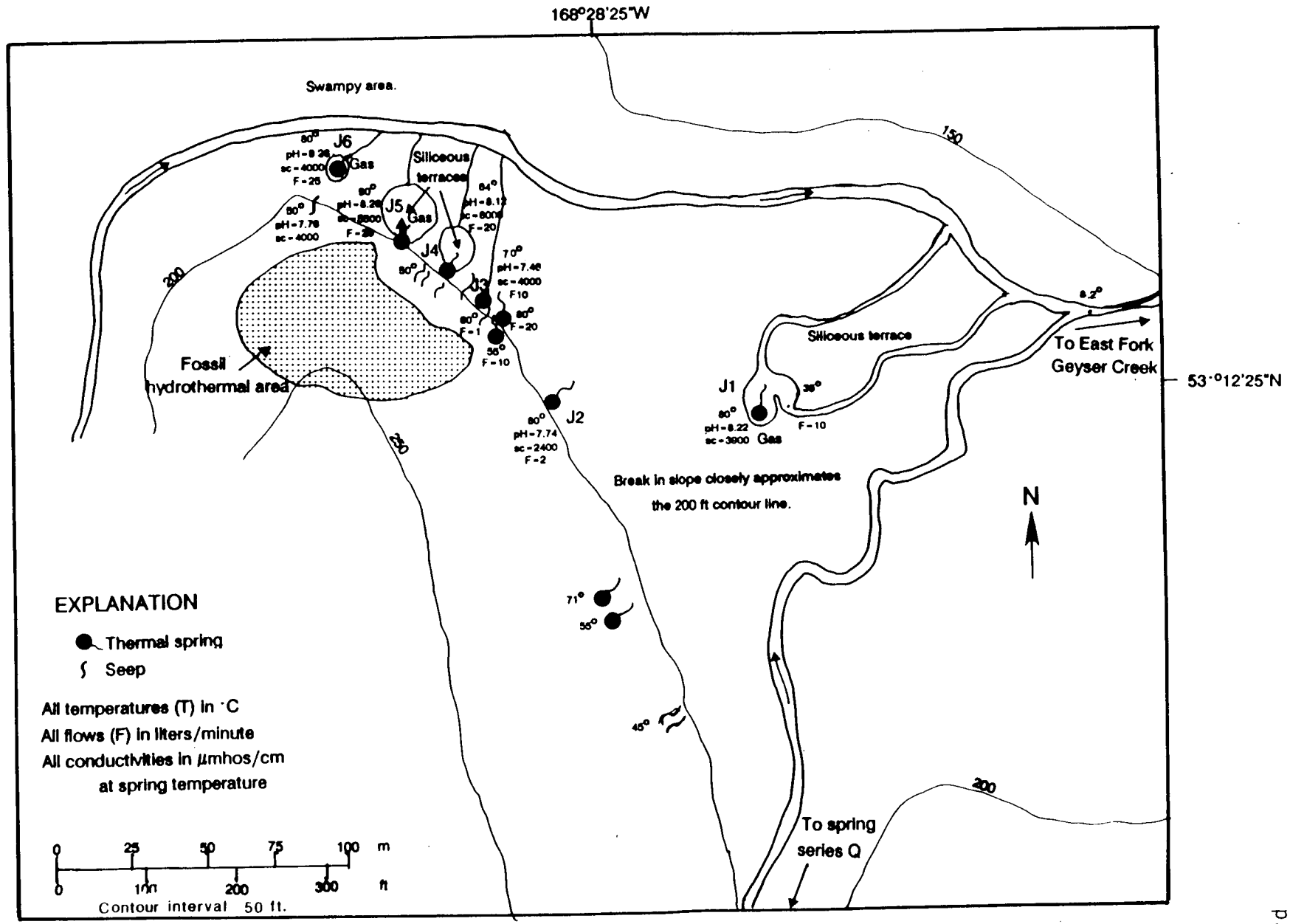

Figure 5.12 Details at Geyser Bight spring series J.

springs is a fossil hydrothermal area about 0.5 hectare in size. The active springs typically emerge from pools ranging from 0.5 to 2.5 m in diameter with deep funnel-shaped bottoms set into valley alluvium. Spring J6 emerges from a 1 m diameter vent in the center of a 4 m diameter pool set in the valley. Gas occasionally breaks the surface of the calm pool. An oblong pool 1 by 1.5 m at the head of a 20 by 20 m silica apron marks the location of geyser J5. Every hour or so gas and steam suddenly burst from the vent and the flow of water doubles to 50 lpm for about a minute. The temperature at J5 was 90°C but may increase during geysering. A puncture through the surface silica apron of J5 revealed a second silica surface 0.5 to 0.75 m beneath the upper one. The lower surface was irregular and may have been the bottom of an old pool. No water was seen between the two silica layers. The adjacent spring, J4, at 60°C, is cooler than J5 but similar to it in pH, conductivity, flow rate, the form of the pool from which it emanates, and the presence of a silica apron. A deep gurgling can be heard coming from beneath the surface in the vicinity of J4. The last spring emerging from a pool is J3 with a flow rate of 10 lpm. J2 is one of several seeps that lie 150 m farther along the slope break with temperatures decreasing with distance. Compared to other springs in Geyser Bight, site J is characterized by almost no algal growth. As with J1, geometry and pool size of several of the other J springs suggest they may also have been geysers or are currently geysers whose activity has not as yet been observed.

5.2.7 Site K

Site K (Figure 5.13) is located 4.8 km inland from Geyser Bight near the center of the valley. The springs flow directly out of the alluvium near the terminus of a large alluvial fan. At K1, 61°C water emerges in an oval-shaped

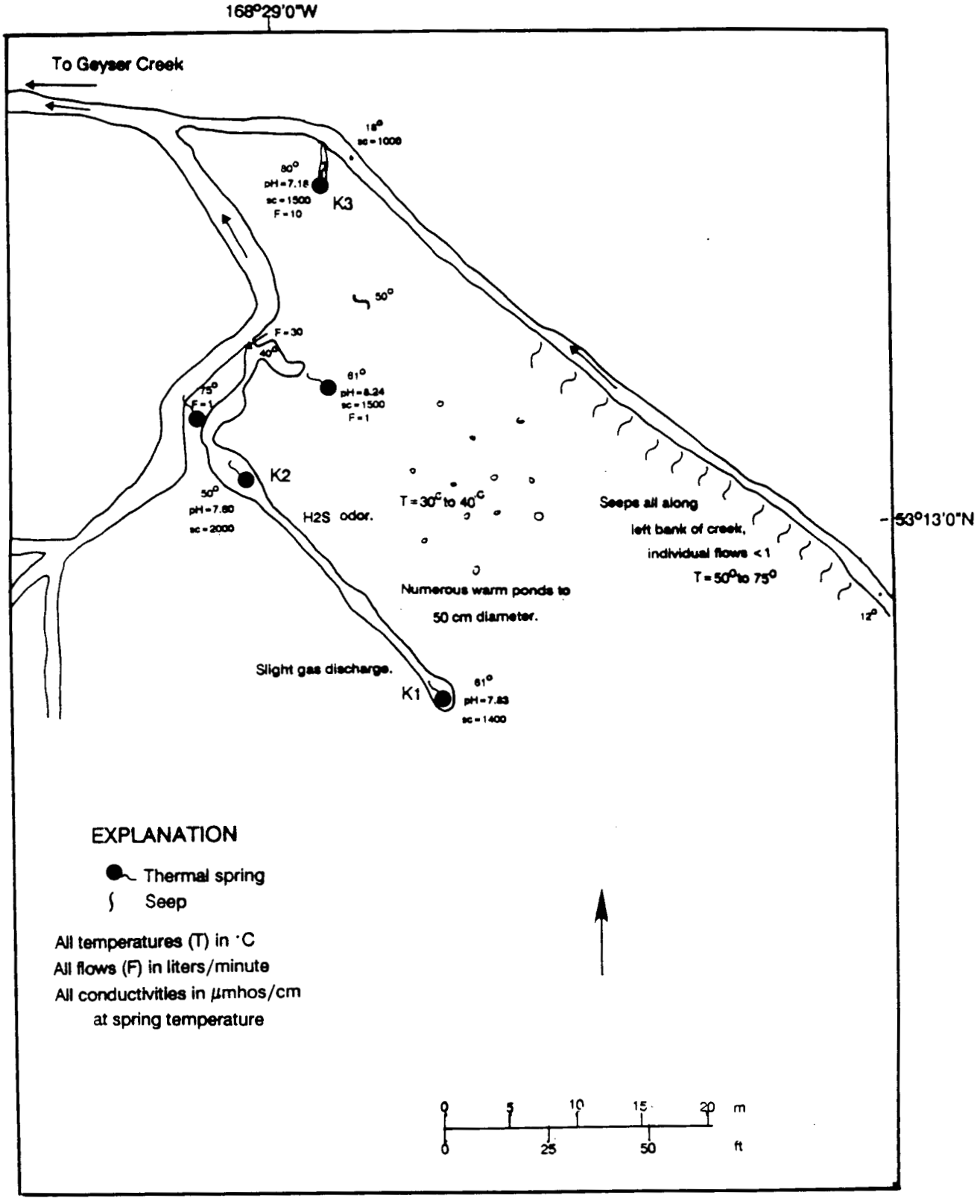

Figure 5.13 Details at Geyser Bight spring series K.

pool, 2.5 m wide, 4 m long and up to 1.5 m deep, and flows down a narrow channel into two successive large oval pools covered with a thick layer of dark algal growth. The lower pool, labeled spring K2, was 59°C in 1980, and was bubbling. A quiet 50°C pool clogged with algae was found in 1988. Overflow (100 lpm in 1980 and 30 lpm in 1988) from these pools and from a fourth small irregularly shaped pool with 40°C water spills into a nearby cold stream.

A second similarly sized cold stream joins this stream 20 m downstream from the outflow of K1 and K2. Spring K3 is found in the small delta between these two streams and drains into this second stream. The 30 cm diameter vent of K3 is hidden at the end of a 3 m long, 0.7 m wide and 1.25 m deep cut in the grass covered alluvium. This second stream has numerous seeps that range from 50° to 70°C emerging from its left bank. Stream water increases in temperature from 12 to 18°C as it passes through the area of seeps. Numerous small ponds to 0.5 m in diameter with temperatures of 30° to 40°C are found between this creek and the channel connecting K1 and K2. A slight odor of H_2S is evident at site K.

5.2.8 Site L

Hot-spring site L lies almost directly across from site K, in an indention on the northeast side of the valley (Figure 5.14). The concavity of the hollow in which the site is located, plus the warmth and muddiness of the soil in and around the springs suggest the area is the site of a small shallow slump caused by the injection of warm water. Several small springs emerge around the upper back wall of the depression and a few muddy seeps are at its center. Numerous vents, 36 to 86°C, discharge water directly into a 1 m deep, 20 m by 7 m pool. This pool supports abundant bacteria and algal flora.

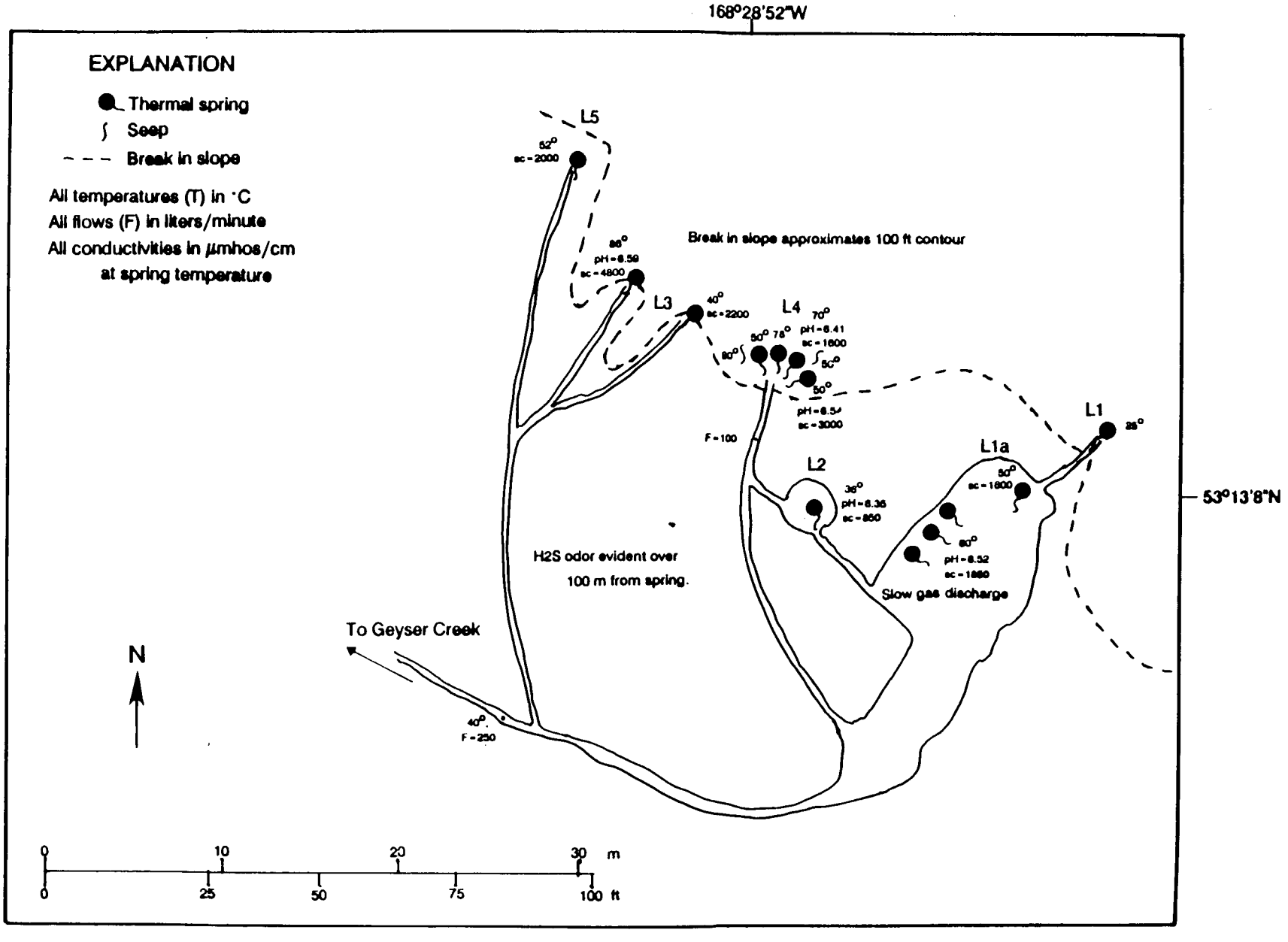

Figure 5.14 Details at Geyser Bight spring series L.

Spring L3 has the greatest flow. The most active site in 1980 was L1 but by 1988 this vent had cooled to 25°C with no water in its outflow channel. Combined discharge from site L totaled 250 lpm. This site has the strongest H_2S odor in Geyser creek valley. The odor is noticeable at least 100 m from the site.

5.2.9 Site Q

Two small springs and several seeps discharge in a narrow tributary valley located about 0.3 km above site J (Plate 2). They emerge from the valley alluvium for a distance of 50 m at the slope break and are found only on the west bank (Figure 5.15). Volcanic rock outcrops along the creek between sites J and Q and has signs of previous thermal spring activity. The most prominent springs, Q1 and Q2, are almost identical with temperatures of 80 and 79°C, flows of Figure 5.1430 and 25 lpm, similar conductivities, and pH. A slight H_2S odor is evident at the site. Above Q, creek temperature is 4°C, suggesting no additional geothermal activity up-valley.

5.3 Convective Heat Discharge by Spring Flow

The results of our 1988 thermal spring discharge measurements are given in Table 5.2. For comparison, thermal spring discharges measured by Motyka and others (1981) in 1980 are given in Table 5.3 and those by Byers and Brannock (1949) in 1947 are given in Table 5.4. Spring temperatures reported are the hottest measured at a specific site. The calculated heat discharged by spring flow given in Table 5.2 is referenced to the enthalpy of water at 10°C, the approximate average annual temperature in the central Aleutian Islands.

Because of problems with our flow meter, most of the 1988 discharges were visually estimated and may be subject to substantial error (25 - 50 %); those

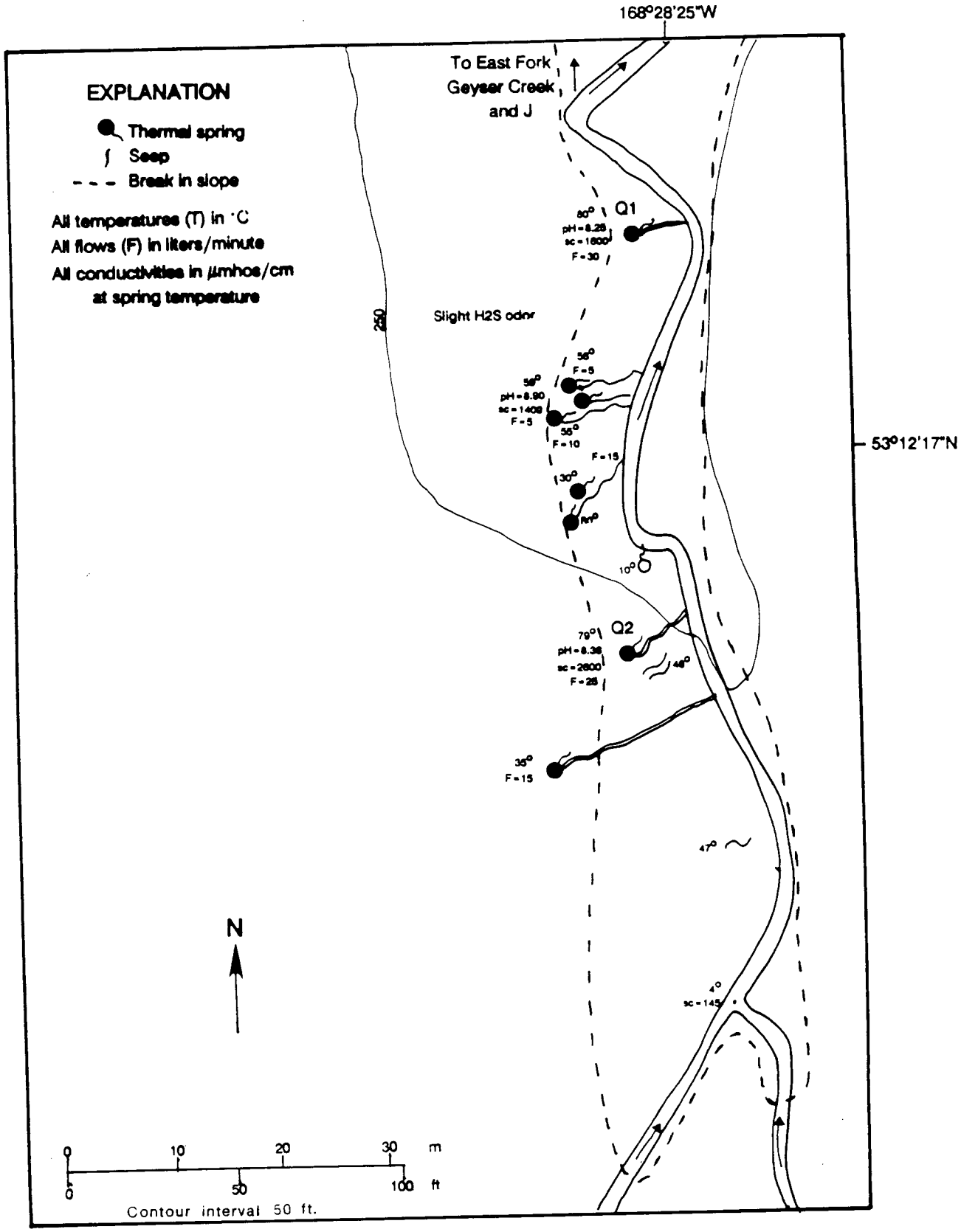

Figure 5.15 Details at Geyser Bight spring series Q.

Table 5.2. Convective Heat Discharge Geyser Bight Geothermal Area 1988.

Site[1]	Temp °C	Flow[2] l/min	Det.	Enthalpy[3] Joules/gm	Heat Discharge Kilowatts
G-1-A	102.2	5	E	386	30.8
G-1-B	99.2	15	E	373	89.6
G-1-C*	101.1	30	E	381	182.7
G-1-D	80.7	10	E	296	47.9
G-1-E	100.3	10	E	378	60.4
G-1-F-pool	57.6	1	U	199	3.3
G-1-G-pool	67.3	1	U	240	3.9
G-1-H	91.8	1	E	342	5.5
G-2	100.3	25	E	378	151.0
G-3	101.2	20	E	382	122.0
G-4	95.6	15	E	358	86.2
G-4-s	78.0	1	E	285	4.6
G-4.5	83.3	0	E	307	0.0
G-5-s	58.0	1	E	201	3.3
G-6-A*	94.0	20	E	352	112.9
G-6-B	92.8	0	E	347	0.0
G-6-Cs	75.0	1	E	272	4.4
G-6-Pool	36.1	1	U	109	1.8
G-6-s1	97.3	10	E	365	58.5
G-6-s2	97.6	5	E	367	29.4
G-7-crkblo	18.0	250	E	331	39.5
G-7-hi-s	101.0	25	E	381	152.1
G-7-lo-s	75.0	25	E	272	110.5
G-8-A1-s	65.2	2	E	231	7.6
G-8-A2-s	93.3	2	E	349	11.2
G-8-A3-s	52.0	2	E	176	5.8
G-8-A4-s	89.8	2	E	334	10.8
G-8-A5-s	96.3	2	E	361	11.6
G-8-A6-s	95.1	2	E	356	11.4
G-8-A7-s	91.0	2	E	339	10.9
G-8-Gey*	99.9	60	Mc	376	361.0
G-9	100.3	36	Mb	378	217.5
G-9.5	55.0	5	E	188	15.5
G-10	102.4	54	Mb	387	333.3
G-10.5-s	52.0	2	E	176	5.8
G-11*	86.3	18	Mb	319	92.8
G-12	50.8	1	U	171	2.8
Minimum Heat Discharge for "G" Springs					2498.3
H-1	102.3	400	E	386	2466.52
H-1s	100.0	5	E	377	30.1
H-1.5	99.7	100	E	375	600.4
H-2-A*	99.3	50	E	374	298.9
H-2-B	100.0	5	E	377	30.1
H-2-C	101.6	40	E	383	244.9
H-3	47.8	150	E	158	391.1
H-4-main*	101.7	400	E	384	2451.5

Table 5.2, con't. Convective Heat Discharge Geyser Bight Geothermal Area 1988.

Site[1]	Temp °C	Flow[2] l/min	Det.	Enthalpy[3] Joules/gm	Heat Discharge Kilowatts
H-4-s1	65.8	10	E	234	38.2
H-6-main*	103.6	50	E	392	312.4
H-6-s1	86.0	10	E	318	51.3
H-6-s2	64.2	10	E	227	37.1
H-7*	101.3	135	Mm	382	824.0
H-8	98.5	100	E	370	592.9
H-9	67.0	200	E	239	779.0
H-10-A	97.8			368	0.0
H-10-ALL	97.0	150	E	364	875.2
H-10-s1	95.6			358	0.0
H-10-s2	66.5			237	0.0
H-11	96.0	150	E	360	865.7
H-11-sa	71.0	10	E	255	41.6
H-11.5-s	71.0	10	E	255	41.6
H-12	75.0	50	E	272	221.1
H-13	75.0	40	E	272	176.9
H-W-topL	65.0	25	E	230	94.1
H-W-topR	64.0	40	E	226	147.8
H-RHS-flat	50.0	250	E	167	689.2
Minimum heat discharge for "H" Springs					12315.3
J-1	80.0	10	E	293	47.5
J-2	80.0	2	E	293	9.5
J-2-s1	71.0	5	E	255	20.8
J-2-s2	55.0	5	E	188	15.5
J-2-s3	46.0	2	E	151	5.0
J-3-A	70.0	10	E	251	40.9
J-3-B	55.0	10	E	188	30.9
J-3-C	80.0	20	E	293	94.9
J-3-D	60.0	1	E	209	3.4
J-4	64.0	20	E	226	73.9
J-4-s1,2,3	50.0	2	E	167	5.5
J-5*	90	25	E	335	134.8
J-6	85.0	25	E	314	126.8
Minimum heat discharge for "J" Springs					609.4
K-1	61.0			213	0.0
K-below1+2	55.0	30	Mb	188	92.8
K-2	50.0			167	0.0
K-2-s1	75.0	1	E	272	4.4
K-2-s2	61.0	1	E	213	3.5
K-3*	80.0	10	E	293	47.5
K-3-seeps	63.0	50	E	222	181.5
K-pools	40.0	10	U	126	20.8
Minimum heat discharge for "K" Springs					350.4

Table 5.2, con't. Convective Heat Discharge Geyser Bight Geothermal Area 1988.

Site[1]	Temp °C	Flow[2] l/min	Det.	Enthalpy[3] Joules/gm	Heat Discharge Kilowatts
L-1	25.0	0	E	63	0.0
L-1-a	50.0		U	167	0.0
L-1-Pool*	60.0		U	209	0.0
L-2	36.0			109	0.0
L-3-a*	86.0			318	0.0
L-3-b	40.0			126	0.0
L-4-a	50.0	20	E	167	55.1
L-4-b	78.0	20	E	285	92.3
L-4-c	70.0	25	E	251	102.3
L-4-d	50.0	20	E	167	55.1
L-5	52.0			176	0.0
L-ALL	40.0	250	Mm	126	519.1
Minimum heat discharge for "L" Springs					519.1
Q-1*	80.0	30	E	293	142.4
Q-1.2-s1	56.0	5	E	193	15.8
Q-1.2-s2	59.0	5	E	205	16.8
Q-1.2-s3	55.0	10	E	188	30.9
Q-1.5-s1	30.0	15	E	84	20.8
Q-1.5-s2	50.0	20	E	167	55.1
Q-2	79.0	25	E	289	117.1
Q-2-s	46.0	1	E	151	2.5
Q-2.5	35.0	15	E	105	26.0
Q-2++seeps	47.0	5	E	155	12.8
Minimum heat discharge for "Q" Springs					440.3
Minimum heat discharge for all Geyser Bight Springs					16732.8
Increase in enthalpy of creek water as it passes through fumarole fields F1 and F2:					
Crk abv F1	9.2	400	E	0	0.0
Crk blo F1	17.5	450	E	312	35.4
Crk abv F2	16.7	450	E	282	10.4
Crk blo F2	21.2	500	E	473	90.2

[1] Asterisk indicates water chemistry sample location.

[2] Seeps were given values of 1 l/min for the calculation. Some values refer to group of vents. Mm = measured with meter, Mb = measured by timing bucket filling, E = visual estimates, U = unable to estimate.

[3] Base temperature for calculations is 10 °C.

sites that were measured by catchment or flow meter are noted as such in Table 5.2. The heat discharge by spring flow calculated for 1988 (16.7 MW) is much greater than for 1980 (6.1 MW) partly because of the larger number of springs that were included in the 1988 calculations. Variations in spring flow may also be a contributing factor.

Convective surface heat discharge was also estimated from stream flow measurements made in 1981 and is included in Table 5.3. Geyser Creek flow was measured below the point of input of thermal waters draining from G and J (Plate 2). Stream water samples were collected at this site and from a site above H. The hottest and most chemically concentrated thermal spring waters at G (G8), J (J5), and H (H6) were taken to represent the undiluted thermal water discharging into the stream drainage. The average analyzed concentrations of the conservative elements Cl and B in these waters and in the stream waters above H and below G were then used in mass balance calculations to determine the hot water fraction. In calculating the convective heat discharge the hot water fraction was assumed to be at the surface boiling point. The estimated 13.3 MW of heat being discharged does not include contributions from spring groups K, L, and Q nor from any thermal waters that may be entering the creek below the point of flow measurement.

When the heat discharge from spring groups K, L, and Q is subtracted from the 1988 estimates, the result, 15.1 MW, compares reasonably well to the 1981 estimate of 13.3 MW determined by mass balance calculations. The 1988, 1981 and 1980 estimates are all substantially lower than the heat discharge by spring flow calculated using 1947 estimates of spring flow given in Table 5.4 (Byers and Brannock, 1949). Although Byers and Brannock (1949) do not report the method or precision of their measurements, the differences in flow rate in

Table 5.3. Convective Heat Discharge by thermal spring flow, Geyser Bight KGRA, 1980 and 1981.

Site	Temp °C	Flow l/min	Enthalpy Joules/gm	Heat Discharge Kilowatts
G1	100.0	20	419	134
G2	79.0	5	331	26
G3	100.1	16	419	107
G4	92.4	5	387	31
G6	97.3	20	407	130
G8	100.1	75	419	503
G9	99.3		416	
G10	100.0		419	
G11	81.0		339	
H0	97.3	30	407	195
H1	100.3	300	420	2016
H2	99.3	100	416	666
H3	45.2	60	189	181
H4	100.3	45	420	302
H5	101.8		427	
H6	99.9	30	419	201
H7	99.8	70	419	469
J1	82.0		343	
J2	77.2	1	322	5
J3	82.5	10	345	55
J4	69.0	5	289	23
J5	92.2	15	386	93
J6	83.9	15	352	84
K	60.5	100	253	405
L	82.3	200	347	1109
Q	72.5	25	304	121
Minimum heat discharge - all springs.				6856
Heat loss referenced to 10°C				6088

Heat loss computed from 1981 stream flow measurements and increase in chemical constituents using G8 chemistry for hot water fraction.

	Cl	B	Na	T
Hot water	630.	60	487	100
Cold water	6.2	0	5.2	4.8
Mixed	18.8	1.3	14.7	10
Hot water fraction:	0.0202	0.0217	0.0197	0.0546

Average of chemically determined fraction:	0.0205
Measured stream flow below G, lps:	1723
Hot water fraction, lps:	35.37
Heat loss referenced to 10°C, MW:	13.33

Table 5.4. Convective heat discharge by spring flow, Geyser Bight KGRA, 1947[1].

Site	Temp. °C	Flow l/min	Enthalpy Joules/gm	Heat discharge Kilowatts
G1	101.0	260	423	1760
G2	88.0	6	369	35
G3	100.5	18	421	121
G4	98.0	36	411	237
G6	95.0	80	398	509
G7	82.0	85	343	466
G8	100.5	170	421	1145
G9	100.5	6	421	40
G10	99.0	170	415	1129
G11	77.0	170	322	876
H1	101.5	660	425	4488
H2	101.0	600	423	4061
H3	53.0		222	
H4	101.0	340	423	2301
H5	101.0	85	423	575
H6	100.0	66	419	442
H7	90.0	260	377	1568
J1	88.0	720	369	4251
K	64.0	250	268	1072
L	68.0	170	285	774
Minimum heat discharge all springs.				25850
Heat loss referenced to 10°C.				23062

[1] Byers and Brannock (1949)

some cases appear too large to be explained by differences in measuring techniques and the variations in spring discharge appear to be real. As examples, flow meter measurement of spring discharge at H7 was 135 lpm in 1988 and 70 lpm in 1980 vs Byers and Brannock's report of 260 lpm in 1947; discharge from hot spring pool J1 was visually estimated at 10 lpm in 1988 vs 760 lpm in 1947. Geyser activity, particularly at H, was more subdued in 1980 than observed in 1988 or reported by Byers and Brannock (1949). Silica sinter is being actively deposited at many of the boiling point vents and also forms large aprons in outflow channels. Silica and other hydrothermal alteration deposits may also be periodically choking some of the spring and geyser conduits. Periodic vent opening and increase in discharge could be triggered by seismic activity or build up of steam pressure similar to that observed at Yellowstone National Park.

6. GEOCHEMISTRY OF GEOTHERMAL FLUIDS

6.1 Introduction

Reports of the Geyser Bight hot springs appear in Grewingk (1850) and in Waring (1917) and their existence was probably known to Aleut villagers at Nikolski since ancient times. Byers and Brannock (1949) conducted an extensive survey of the thermal spring areas during their reconnaissance geologic mapping of Umnak Island in 1946-48 and reported analyses on water samples from two of the springs. Samples from four thermal springs were also collected and analyzed by I. Barnes (pers. comm., U.S. Geological Survey, 1981) in 1975 as part of a USGS reconnaissance investigation of hot spring sites in the Aleutian arc.

In 1980 we sampled and analyzed seven Geyser Bight geothermal area thermal springs and measured spring discharges during a regional assessment of geothermal resources in the Aleutian Islands for the state of Alaska (Motyka and others, 1981). Our preliminary studies suggested that these hot springs are fed from multiple reservoirs, ranging in temperature from 160° to 190°C, which are in turn related to a deeper parent reservoir having a temperature as high as 265°C. In this fluid geochemistry study of the Geyser Bight geothermal area, waters from fourteen thermal springs and numerous surface waters were sampled and analyzed to more conclusively determine whether multiple reservoirs exist and to determine the geochemical, isotopic and temperature parameters of these reservoirs. These data are also used to examine chemical equilibria, to determine the source of waters charging the reservoirs, and to estimate heat loss by surface and near-surface thermal water discharge.

The results of this investigation confirm the existence of at least two chemically and isotopically distinct intermediate reservoirs with temperatures of 200° C and 165° C. Evidence for deep reservoirs at temperatures of 265° C and possibly 225° C also exists but whether these deep reservoirs are related or interconnected remains inconclusive.

6.2 Methods

6.2.1 Sampling Procedure

Thermal spring waters were collected as close to the issuing vent as possible. Surface waters were sampled directly from streams or creeks. The samples were normally filtered through 0.45 micron filters and consisted of either 500 ml or 1 liter each of filtered untreated and filtered acidified (HCl) waters; 100 ml 1:10 and 1:5 diluted samples for silica determinations; and 30 ml samples for oxygen-18 and deuterium isotopic analyses. At three springs (G8, H6 and L3) 500 ml of water were filtered through 0.1 micron filters and treated in the field with methyl isobutyl keytone (MIBK) for later aluminum analysis following methods described by Presser and Barnes (1974). At several sites (G8, H1, H4, J1 and L3) one liter of filtered water was collected and treated with formaldehyde for later determination of oxygen-18 composition of the sulfate species. One liter of unfiltered, untreated water was collected for tritium determinations from two springs (G8 and H4) and from two streams.

Gases were collected in 1980 and 1981 by immersing a plastic funnel in the pool of spring water. The funnel was placed over a train of bubbles and connected to an evacuated gas collecting flask with tygon tubing. The gas sample was taken by allowing the gases to displace water in the funnel,

purging the sampling line of air, then collecting the gas in the evacuated flask. Samples were collected in 50 to 100 cc flasks constructed from helium-impermeable Corning 1720 glass.

6.2.2 Analytical Procedures

All 1980 thermal spring water samples were analyzed at the DGGS water laboratory in Fairbanks. Procedures followed are presented in Motyka and others (1980).

1981 and 1988 stream waters: HCO_3, temperature, and pH were determined in the field following methods described in Presser and Barnes (1974). The remaining constituents were analyzed at the DGGS water laboratory in Fairbanks. Na, K, Li, and Sr were determined using a Perkin-Elmer atomic absorption spectrometer following procedures outlined in Skougstad and others (1979) and in the Perkin-Elmer reference manual. Ca, Mg and B were analyzed on a direct coupled plasma system. Silica concentrations were determined by the molybdate blue method. Sulfates were determined by the titrimetric (thorin) method; fluorides by specific ion electrode; and chloride by Mohr titration

1988 thermal spring waters: HCO_3, NH_3, and H_2S concentrations, temperature and pH were determined in the field following methods described in Presser and Barnes (1974). Rb and Cs were analyzed at the U.S. Geological Survey in Menlo Park using an atomic emision spectrometer. Ba and Al were analyzed at the DGGS water laboratory in Fairbanks on a direct coupled plasma system (DCP). The MIBK treated samples were used for the aluminum analysis. Because a laboratory move and equipment changes disrupted the analysis program at DGGS, the remaining constituents were analyzed by the University of Utah Research

Institute (UURI) water laboratory in Salt Lake City under a cooperative agreement. At UURI, major, minor and trace cation concentrations were determined using an inductively coupled argon plasma spectrometer (ICP). Sulfates were determined by the titrimetric (thorin) method; fluorides by specific ion electrode; chloride by Mohr titration; bromide by hypochloride oxidation and titration (UURI); and iodide by titration.

Gases were analyzed on dual-column gas chromatographs using both argon and helium carrier gases. The chromatographic analyses of gases collected in 1980 were performed at the U.S. Geological Survey, Menlo Park, California; gases collected in 1981 were analyzed at the Scripps Institution of Oceanography.

Stable isotope values of the water samples ($^{18}O/^{16}O$ and D/H) were analyzed by the Stable Isotope Laboratory, Southern Methodist University, Dallas, Texas. Procedures followed are outlined in Viglino and others (1985). Tritium concentrations were determined by the Tritium Laboratory, University of Miami, Miami, Florida. The $^{18}O/^{16}O$ values of sulfate species were analyzed at the U.S. Geological Survey, Menlo Park, California. Procedures followed are discussed in Nehring and others (1977).

6.3 Gas Chemistry

The gas flows from steam fields F1 and F2 located at the head of Geyser Bight valley were too diffuse to obtain useable samples in 1980, 1981 or 1988. Weather conditions and lack of time prevented sampling of the highly pressurized fumaroles discovered in 1988 at F3.

Gas samples were obtained from thermal spring G6 in 1980 and from an acid spring adjacent to G8 in 1981 (Table 6.1). Both samples consist primarily of nitrogen, carbon dioxide, and oxygen, the latter reflecting air contamination

Table 6.1. Gas chemistry and helium isotope analysis, Geyser Bight thermal springs. na = not analyzed.

	G6[a]	G8A[b]
Gas Chemistry, mole %:		
He	0.01	0.01
H_2	0.09	0.26
Ar	0.78	0.64
O_2	0.70	3.90
N_2	85.3	54.0
CH_4	0.04	na
C_2H_6	0.01	na
CO_2	13.45	41.2[c]
H_2S	<0.01	([c])
N_2 / Ar	109	84
$^3He/^4He$:		
R/R_a[d]	na	7.4
X[e]	na	70
R_c/R_a[f]	na	7.4

[a] Analysts: W.Evans, U.S. Geological Survey, Menlo Park and R.J. Motyka, ADGGS.
[b] Analysts: R. Poreda and J. Welhan, Scripps Institution of Oceanography, La Jolla and R.J. Motyka, ADGGS. Spring G8A is an acid spring adjacent to spring G8.
[c] Analyzed as $CO_2 + H_2S$.
[d] $R/R_a = {}^3He/{}^4He$ in sample over $^3He/^4He$ in atmosphere.
[e] $X = (He/Ne)_{sample}/(He/Ne)_{air}$
[f] Measured values of R/R_a corrected for atmospheric contamination by assuming that the neon is of atmospheric origin. $(R_c/R_a) = [(R/R_a)X - 1]/[X - 1]$.

during sample acquisition. The N_2/Ar ratios are nearly that of air indicating these constituents are probably mostly of atmospheric origin, from surface air contamination and from air dissolved in waters charging the hydrothermal system. Oxidation of H_2S in near-surface groundwaters could account for the apparent depletion of this gas in the G6 sample: a nearby thermal pool has a pH of 3.6. The carbon dioxide is most likely of thermal and perhaps also of magmatic origin as suggested by the helium isotope ratio.

The helium isotope ratio, $^3He/^4He$, of 7.4 reflects a probable magmatic influence on the Geyser Bight geothermal system. ^3He is considered to be of primordial origin and enrichments in ^3He with respect to atmospheric levels have been correlated with magmatic activity on a world-wide basis with the excess ^3He thought to be derived from the mantle (Craig and Lupton, 1981). The 7.4 value lies at the upper end of the range for helium isotope ratios found at other thermal sites in the Aleutian arc of active volcanism (5.0 to 8.0) (Poreda, 1983) and is nearly the same as the average of 7.5 found for summit fumaroles in circum-Pacific volcanic arcs (Poreda and Craig, 1989).

6.4 Water Chemistry

6.4.1 Results

The results of geochemical analyses of the 1988 Geyser Bight thermal spring waters and representative stream waters are given in Tables 6.2 and 6.3, respectively. Analyses from previous investigations are also included in Tables 6.2 and 6.3. These include data from Byers and Brannock (1949); I. Barnes (pers. comm., U.S. Geological Survey, 1981; Motyka and others, 1981) and previously unpublished data on DGGS stream samples collected in 1981. Comparison of these data show thermal water compositions have not changed

Table 6.2. Geochemical analyses of Geyser Bight hot spring waters collected in 1988. Previous analyses shown for comparison. Chemical concentrations in ppm and temperatures in degrees celsius. na = not analyzed.

Site	Date	T	pH	SiO_2	Ca	Mg	Na	K	Li	NH_4	Sr	Rb	Cs
DGGS and UURI 1988:													
G1	7-14-88	101	9.2	326	16	0.2	482	36	3.1	na	0.07	0.33	0.58
G6	7-14-88	94	7.2	176	20	0.9	269	18	1.8	na	0.09	0.18	0.29
G8	7-10-88	99	7.5	292	19	<0.16	485	35	3.6	1.2	0.14	0.34	0.58
G11	7-12-88	86	7.1	114	32	1.2	220	10	1.4	na	0.26	0.12	0.20
H2	7-22-88	98	7.9	142	28	0.5	311	15	2.1	na	0.27	0.13	0.24
H4	7-20-88	101	7.8	180	36	<0.16	411	20	2.9	1.8	0.31	0.19	0.33
H6	7-16-88	103	7.9	187	33	<0.16	407	19	2.9	1.4	0.29	0.20	0.33
H7	7-16-88	102	8.4	134	29	2.5	230	17	1.3	na	0.22	0.15	0.23
J1	7-24-88	80	8.2	264	20	<0.16	464	33	3.2	na	0.15	0.33	0.57
J5	7-24-88	90	8.3	254	22	<0.16	465	34	3.1	na	0.13	0.34	0.50
K3	7-26-88	80	7.2	134	29	2.5	230	17	1.3	na	0.22	0.14	0.29
L1	7-09-88	60	6.5	119	32	1.9	223	16	1.2	na	0.33	0.14	0.28
L3	7-08-88	86	6.6	159	41	0.8	330	23	1.8	1.8	0.54	0.20	0.35
Q	7-25-88	78	8.2	140	32	2.0	259	12	1.6	na	0.13	0.13	0.29
DGGS 1980:													
G6	7-26-80	97	7.5	178	22	1.2	248	17	1.8	na	0.07	na	na
G8	7-26-80	100	8.0	270	19	0.2	487	30	3.9	na	0.10	na	na
H1	7-25-80	100	7.3	170	33	0.3	355	16	2.8	na	0.23	na	na
H6	7-25-80	99	7.3	190	36	0.1	442	19	3.4	na	0.21	na	na
J1	7-26-80	82	7.6	272	19	0.0	447	31	3.5	na	0.08	na	na
K1	7-25-80	62	7.8	148	25	2.8	179	13	1.2	1.0	0.13	na	na
L1	7-25-80	85	6.9	160	39	1.4	280	20	1.8	1.0	0.24	na	na
Barnes, 1975:													
Gx	6-14-75	85	8.2	250	14	0.2	420	26	2.4	na	na	na	na
G8	6-14-75	102	8.3	255	20	0.1	480	32	3.2	na	na	na	na
J1	6-14-75	93	7.9	245	22	0.1	460	31	2.7	na	na	na	na
J4	6-14-75	65	7.7	224	22	0.1	460	33	2.6	na	na	na	na
Byers and Brannock, 1946:													
G1	8-17-46	100	7.5	303	15	0.1	441	33	3.0	na	na	na	na
H1	8-17-46	101	6.9	150	40	0.2	350	18	2.0	na	na	na	na

T, pH, HCO_3, H_2S, NH_4 = DGGS field measurements. Al and Ba analyzed at DGGS, Fairbanks. Rb and Cs analyzed at USGS, Menlo Park. All other constituents analyzed at UURI, Salt Lake City.

Table 6.2. Continued.

Site	Al	Fe	As	Ba	B	HCO_3	SO_4	Cl	F	Br	I	H_2S	TDS	Balance %
DGGS and UURI 1988:														
G1	na	<0.02	6.6	0.005	53	66	180	623	2.0	1.0	1.0	na	1764	2.7
G6	na	0.07	3.3	0.007	30	41	110	362	0.9	1.5	0.8	na	1015	1.8
G8	0.047	<0.02	6.4	0.004	56	62	174	657	2.1	2.4	1.1	0.4	1766	0.6
G11	na	0.05	2.6	0.012	24	75	93	288	0.9	1.0	0.6	na	826	2.3
H2	na	<0.02	4.7	0.009	40	35	124	412	1.0	1.3	0.9	na	1100	4.3
H4	na	<0.02	6.6	0.009	53	51	162	560	1.5	2.0	1.0	0.7	1464	2.5
H6	0.103	<0.02	6.5	0.008	51	52	149	556	1.4	1.9	1.2	0.6	1444	2.5
H7	na	<0.02	5.1	0.008	40	52	90	294	0.9	1.0	0.5	na	872	3.0
J1	na	<0.02	6.1	0.003	49	52	189	589	2.1	2.6	1.0	na	1650	4.4
J5	na	<0.02	6.5	0.003	52	39	206	598	2.0	1.9	0.9	na	1665	3.2
K3	na	<0.02	3.2	0.039	25	105	90	294	0.9	1.0	0.5	na	882	3.0
L1	na	0.30	3.2	0.032	26	90	79	295	1.1	0.9	0.6	na	846	4.7
L3	0.050	0.40	4.7	0.035	40	125	118	426	1.5	1.5	0.7	1.2	1214	4.3
Q	na	<0.02	3.3	0.019	29	72	118	343	1.2	1.2	0.6	na	979	1.1
DGGS 1980:														
G6	na	0.05	na	na	15	na	96	339	0.9	1.1	0.7	na	922	-
G8	na	0.05	na	na	60	72	170	630	2.3	2.2	1.1	na	1712	3.7
H1	na	0.03	na	na	51	na	131	492	1.3	1.7	1.1	0.3	1256	-
H6	na	0.04	na	na	58	na	154	591	1.6	1.9	1.2	na	1499	-
J1	na	0.05	na	na	50	55	168	591	2.4	2.1	1.0	na	1615	2.2
K1	na	0.07	na	na	18	133	63	225	0.9	1.2	0.5	na	747	-0.7
L1	na	0.08	na	na	30	130	90	370	1.6	1.1	0.7	0.5	1062	3.7
Barnes, 1975:														
G?	0.025	na	na	na	44	61	150	540	2.1	na	na	na	1478	2.7
G8?	na	na	na	na	36	52	170	640	1.2	na	na	na	1663	2.8
J1	0.018	na	na	na	49	46	180	610	2.2	na	na	na	1625	2.0
J4	0.012	na	na	na	48	44	180	610	2.2	na	na	na	1603	2.4
Byers and Brannock, 1946:														
G1	<0.5	<0.1	0.1	na	28	66	160	569	1.9	na	na	na	1586	3.1
H1	<0.5	<0.1	3.8	na	27	49	130	482	1.2	na	na	na	1228	4.6

T, pH, HCO_3, H_2S, NH_4 = DGGS field measurements. Al and Ba analyzed at DGGS, Fairbanks. Rb and Cs analyzed at USGS, Menlo Park. All other constituents analyzed at UURI, Salt Lake City.

Table 6.3. Geochemical analysis of stream waters 2in the Geyser Creek drainage. All analyses in ppm unless otherwise noted.

Site	SiO_2	Ca	Mg	Na	K	Li	Sr	B	HCO_3	SO_4	Cl	F
1981:												
abv H	23	2.3	0.9	5.2	1.3	<0.01	0.01	<0.1	na	0.4	6.2	0.1
blo G	20	2.9	0.9	15	1.2	0.07	0.01	1.3	na	5.3	18	0.1
1988:												
trib KL	18	1.8	0.8	5.4	0.8	0.01	0.02	0.1	11	2.4	6.3	0.05
blo KL	17	5.7	0.9	14	1.2	0.08	0.01	2.9	na	11	20	0.1
blo G	23	3.9	1.0	25	2.0	0.16	0.01	5.3	13	11	33	0.1
blo H	32	4.6	1.0	32	3.4	0.24	0.02	7.1	16	13	44	0.1
abv H	25	2.4	1.0	7.3	1.5	0.02	0.01	0.3	na	7.0	24	0.1
blo J	14	2.1	0.8	7.6	0.8	0.03	0.01	0.5	na	4.4	13	0.1
abv Q	12	1.8	0.8	5.1	0.7	0.01	0.01	0.2	na	2.4	7.6	0.04

significantly between 1946 and 1988. The slight variations in concentrations observed at resampled spring sites (eg, G8) can be attributed to slight differences in dilution ratios or, for boiling springs, the degree of adiabatic boiling. The thermal spring waters are all moderately concentrated Na-Cl waters, rich in boron and arsenic.

6.4.2 Compositional Trends

For concentrations present in Geyser Bight thermal waters Cl can be considered chemically conservative. Constituent-chloride ratios for the thermal spring waters are given in Table 6.4. Constituent concentrations are also plotted against chloride in Figs. 6.1 and 6.2. Na, Li, B, and SO_4, each plot along an approximately linear trend towards a dilute water end member. In contrast, the data for several other more reactive constituents (SiO2, K, Cs, Rb, and F) exhibit two distinct trends, one for down-valley sites (G, J, K, and L), the other for site H. These correlations suggest that the waters are related to a common deep aquifer but that during ascent to the surface the waters have partially or totally re-equilibrated to differing temperatures and wall-rocks in intermediate reservoirs. The observed variations in concentrations that the emergent spring waters display along each of these trends can be explained by dilution or boiling. A logical source of the dilution is meteoric water that infiltrates into the near-surface region beneath the springs. Point A on the constituent-chloride graphs represents such a water similar to stream samples unaffected by influx of thermal waters (Table 6.3).

Distinct compositional mixing trends toward local cold stream waters are evident in plots of Ca:Mg:Na and HCO_3:SO_4:Cl (Figs. 3a and 3b). The inverse correlation observed between Mg and Cl (Fig. 6.1e) is also indicative of

Table 6.4. Ratios of major and minor constituents to Cl and Rb/Cs ratios.

Site	SiO_2	Ca*0.1	Na	K*0.1	Li*0.01	Rb*0.001	Cs*0.001	As*0.01	B*0.1	HCO_3	SO_4	F*0.01	Br*0.01	I*0.01	Rb/Cs
DGGS and UURI 1988:															
G1	0.52	0.26	0.77	0.58	0.50	0.53	0.93	1.07	0.85	0.11	0.29	0.32	0.16	0.16	0.57
G6	0.49	0.55	0.74	0.50	0.50	0.50	0.80	0.91	0.83	0.12	0.30	0.23	0.41	0.22	0.62
G8	0.44	0.29	0.74	0.53	0.55	0.52	0.88	0.97	0.85	0.09	0.26	0.32	0.37	0.17	0.59
G11	0.40	1.11	0.76	0.34	0.49	0.42	0.69	0.90	0.83	0.26	0.32	0.31	0.35	0.21	0.60
H2	0.34	0.69	0.75	0.36	0.51	0.32	0.58	1.14	0.97	6.00	0.30	0.24	0.32	0.22	0.54
H4	0.32	0.65	0.73	0.35	0.52	0.34	0.59	1.18	0.95	0.09	0.29	0.27	0.36	0.18	0.58
H6	0.34	0.59	0.73	0.34	0.52	0.36	0.59	1.17	0.92	0.10	0.27	0.25	0.34	0.22	0.61
H7	0.46	1.02	0.78	0.59	0.44	0.51	0.78	1.73	1.36	0.18	0.31	0.29	0.34	0.17	0.65
J1	0.45	0.35	0.79	0.55	0.54	0.56	0.97	1.04	0.84	0.09	0.32	0.36	0.44	0.17	0.58
J5	0.42	0.37	0.78	0.57	0.52	0.57	0.84	1.09	0.87	0.07	0.34	0.33	0.32	0.15	0.68
K3	0.46	1.02	0.78	0.59	0.44	0.48	0.99	1.09	0.87	0.36	0.31	0.29	0.34	0.17	0.48
L1	0.40	1.11	0.76	0.54	0.41	0.47	0.95	1.08	0.91	0.31	0.27	0.37	0.31	0.20	0.50
L3	0.37	0.97	0.77	0.54	0.42	0.47	0.82	1.10	0.94	0.29	0.28	0.35	0.35	0.16	0.57
Q	0.41	0.94	0.76	0.34	0.47	0.38	0.85	0.96	0.87	0.21	0.34	0.35	0.35	0.17	0.45
DGGS 1980:															
G6	0.53	0.68	0.73	0.50	0.53	-	-	-	0.44	0.00	0.28	0.27	0.32	0.21	-
G8	0.43	0.31	0.77	0.49	0.62	-	-	-	0.95	0.12	0.27	0.37	0.35	0.17	-
H1	0.35	0.67	0.72	0.33	0.57	-	-	-	1.05	0.00	0.27	0.26	0.34	0.22	-
H6	0.32	0.61	0.75	0.34	0.58	-	-	-	0.99	0.00	0.26	0.26	0.32	0.20	-
J1	0.46	0.32	0.76	0.54	0.59	-	-	-	0.85	0.09	0.28	0.41	0.36	0.17	-
K1	0.66	1.12	0.80	0.62	0.52	-	-	-	0.84	0.59	0.28	0.40	0.54	0.22	-
L1	0.43	1.07	0.76	0.54	0.48	-	-	-	0.81	0.35	0.24	0.43	0.29	0.19	-
Barnes, 1975:															
Gx	0.46	0.26	0.78	0.48	0.44	-	-	-	0.81	0.11	0.28	0.39	-	-	-
G8	0.40	0.31	0.75	0.50	0.50	-	-	-	0.56	0.08	0.27	0.19	-	-	-
J1	0.40	0.36	0.75	0.51	0.44	-	-	-	0.80	0.08	0.30	0.36	-	-	-
J4	0.37	0.36	0.75	0.54	0.43	-	-	-	0.79	0.07	0.30	0.36	-	-	-
Byers and Brannock, 1946:															
G1	0.53	0.26	0.78	0.58	0.53	-	-	0.01	0.49	0.12	0.28	0.33	-	-	-
H1	0.31	0.83	0.73	0.37	0.41	-	-	0.79	0.56	0.10	0.27	0.25	-	-	-

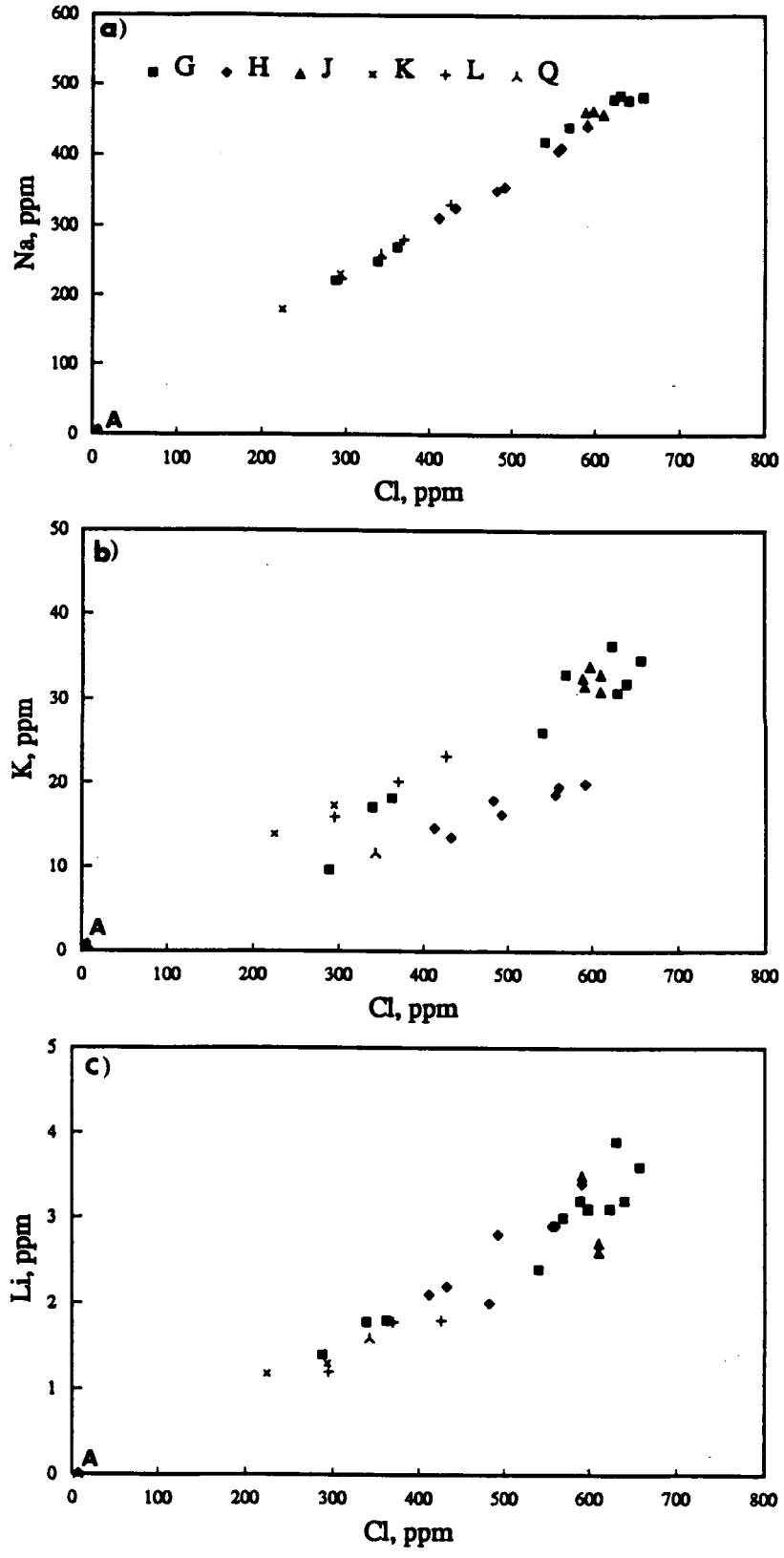

Figure 6.1. Constituent concentrations versus chloride: a) sodium; b) potassium; c) lithium.

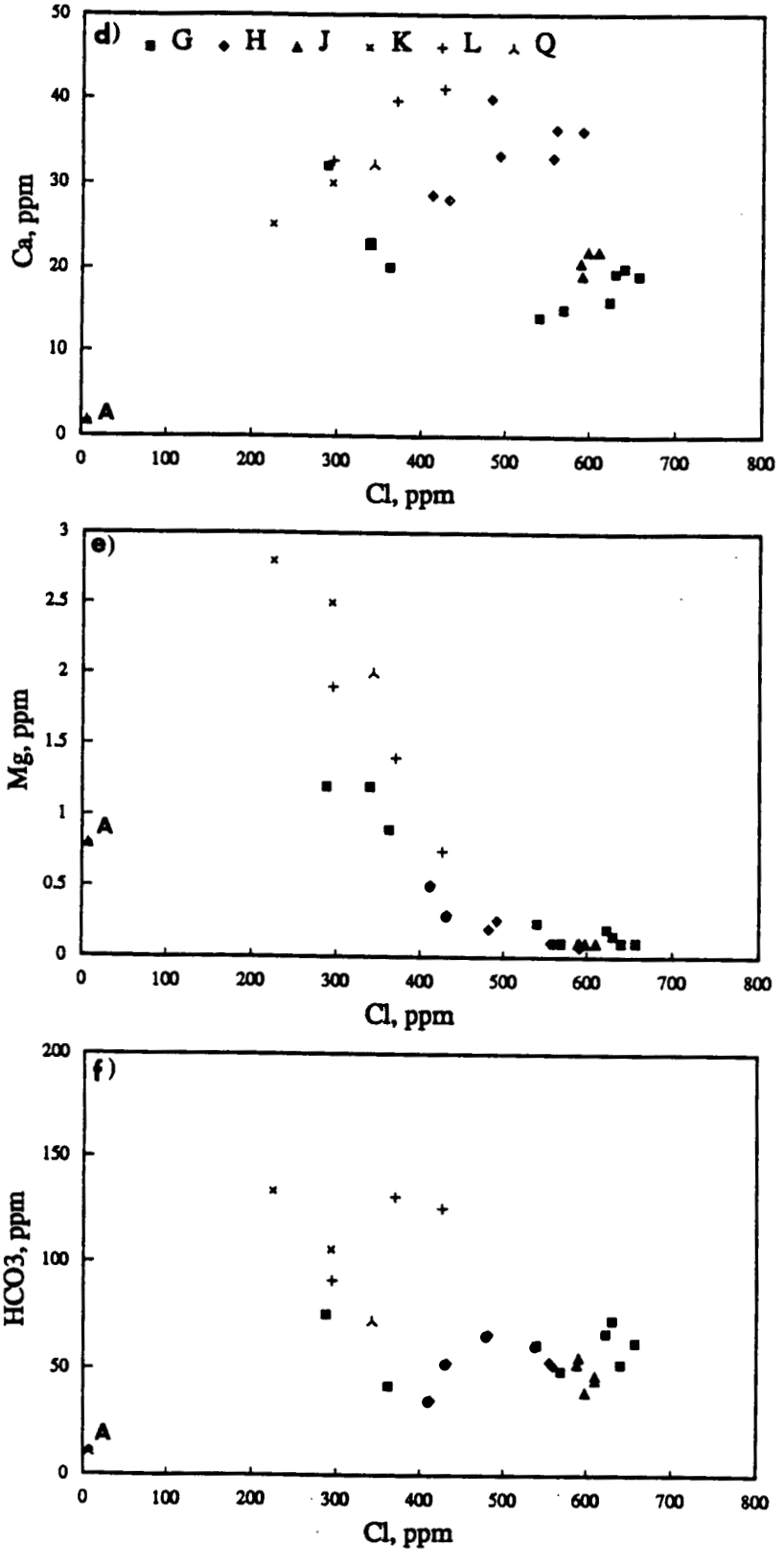

Figure 6.1, con't. Constituent concentrations versus chloride: d) calcium; e) magnesium; f) bicarbonate.

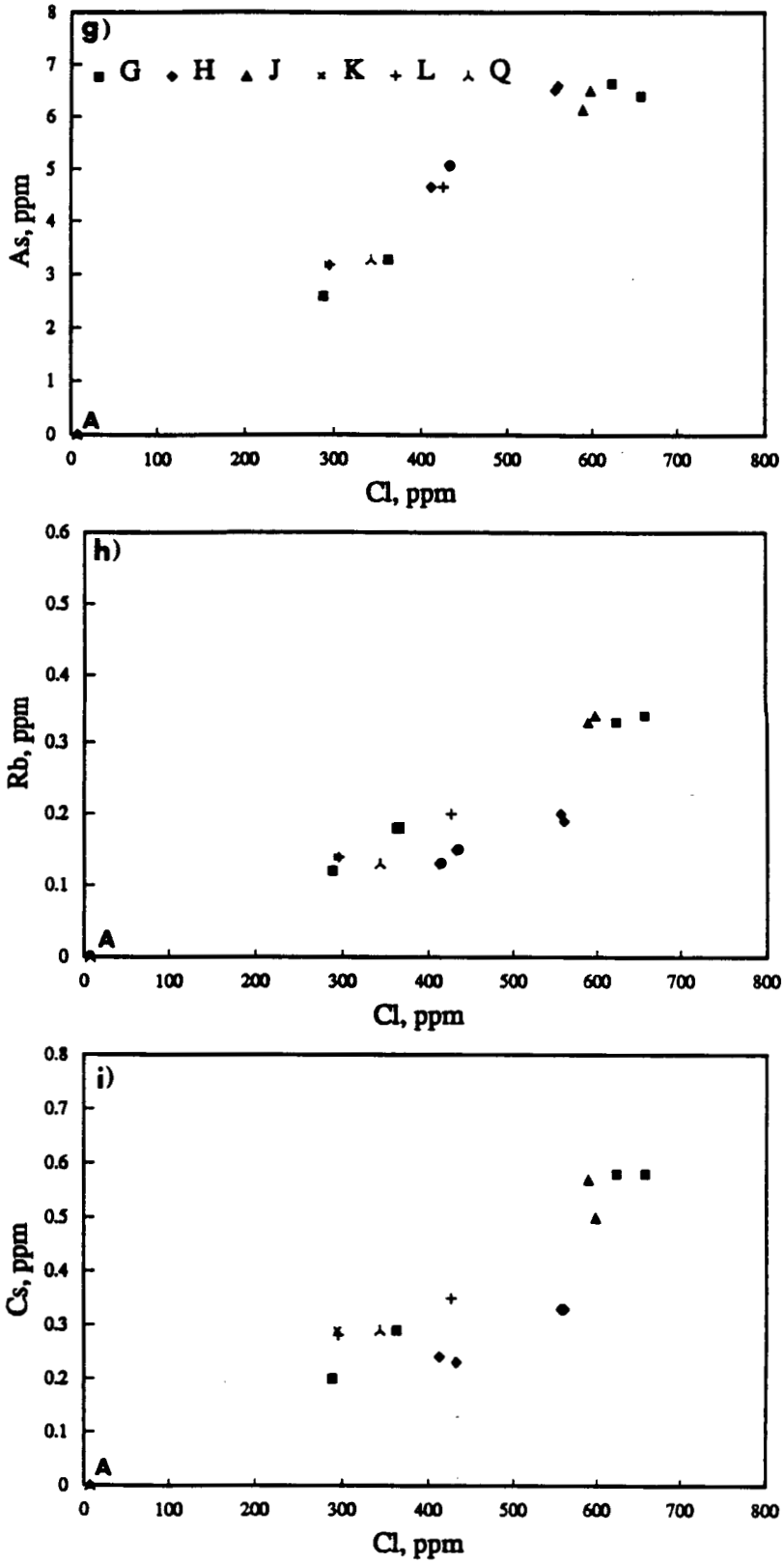

Figure 6.1, con't. Constituent concentrations versus chloride: g) arsenic.; h) rubidium; i) cesium.

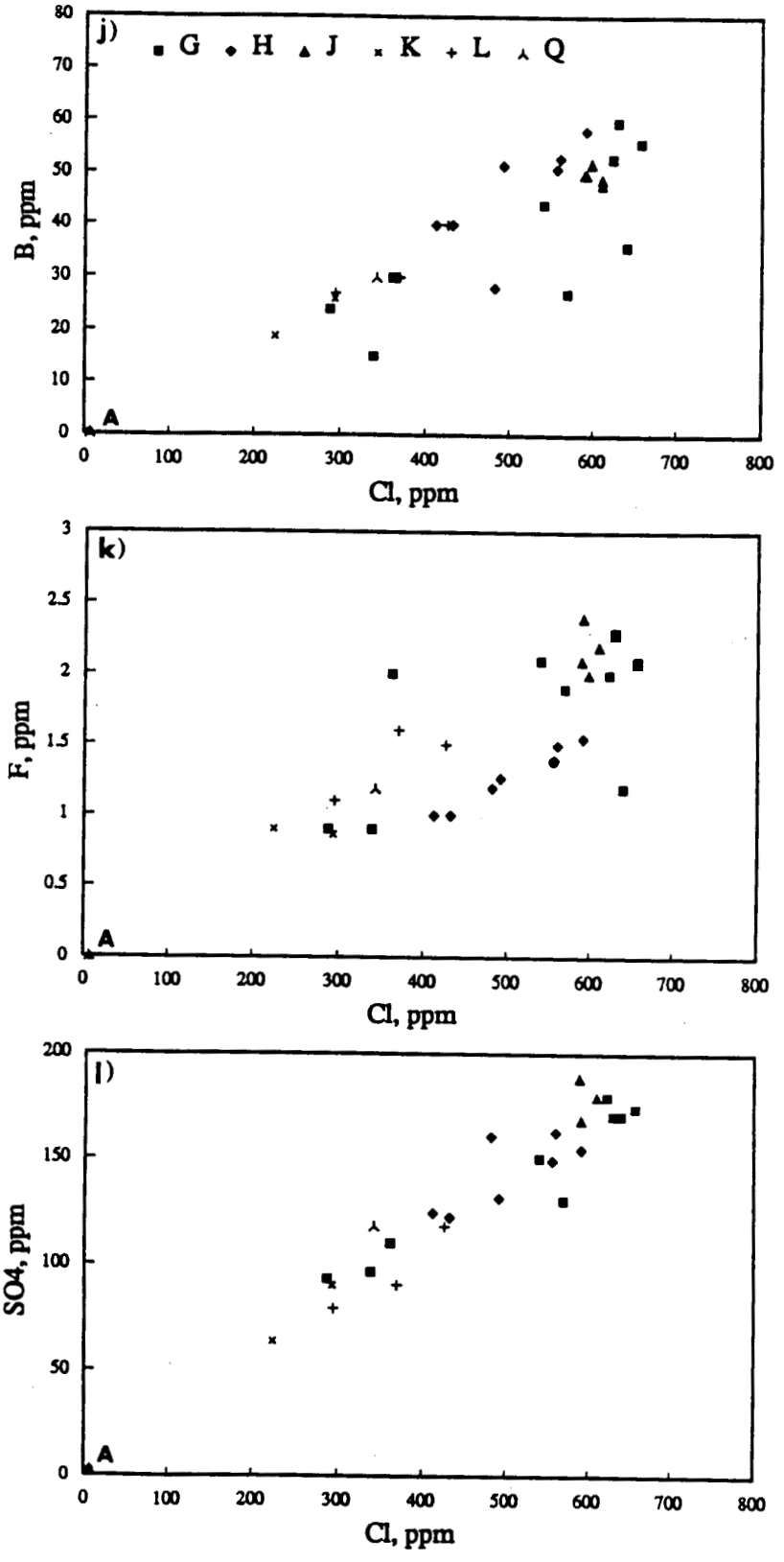

Figure 6.1, con't. Constituent concentrations versus chloride: j) boron; k) fluorine; l) sulfate.

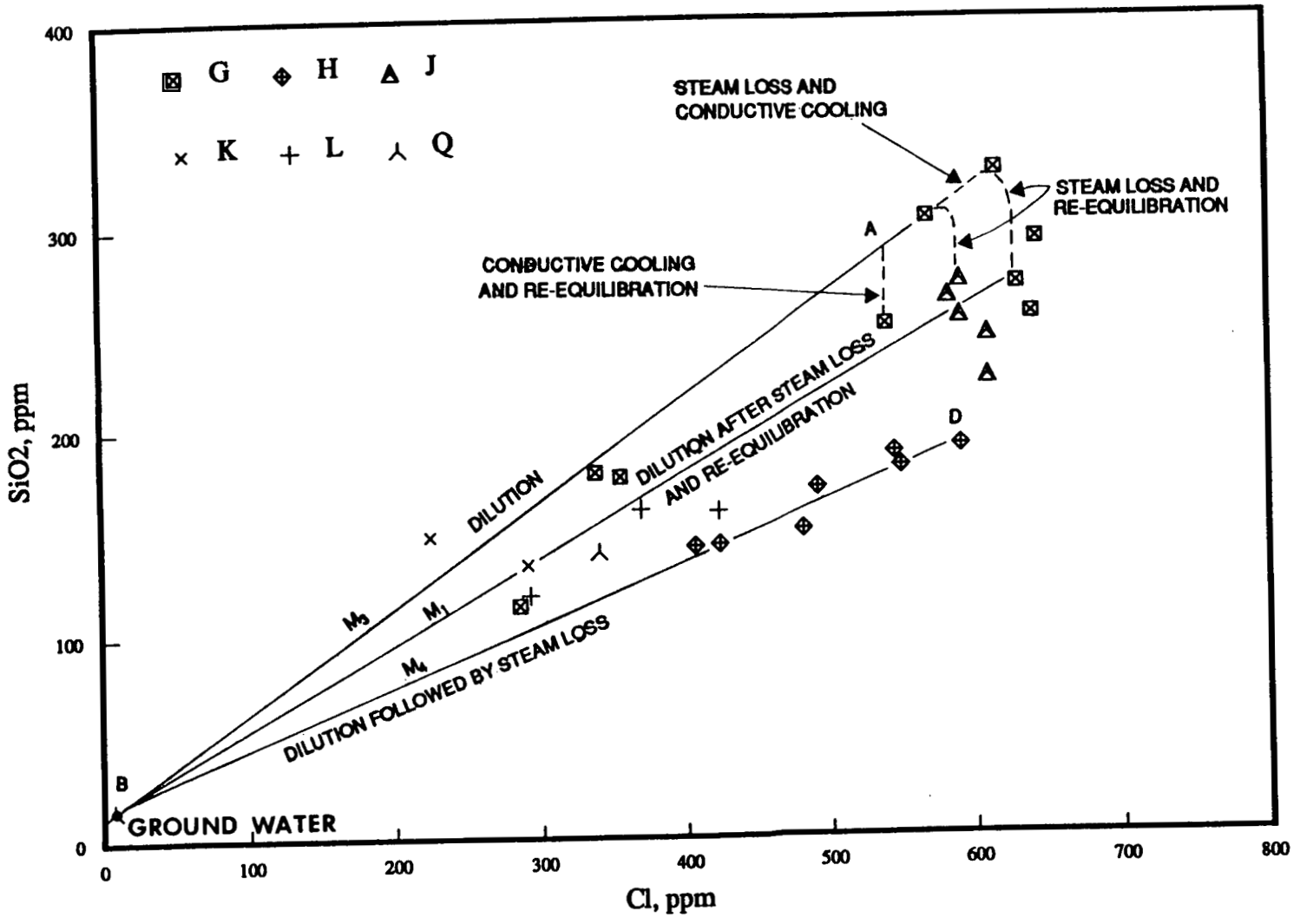

Figure 6.2. Silica versus chloride for thermal spring waters. The various dilution, conduction, steam-loss, and re-equilibration paths are discussed in the text under chloride-enthalpy analysis.

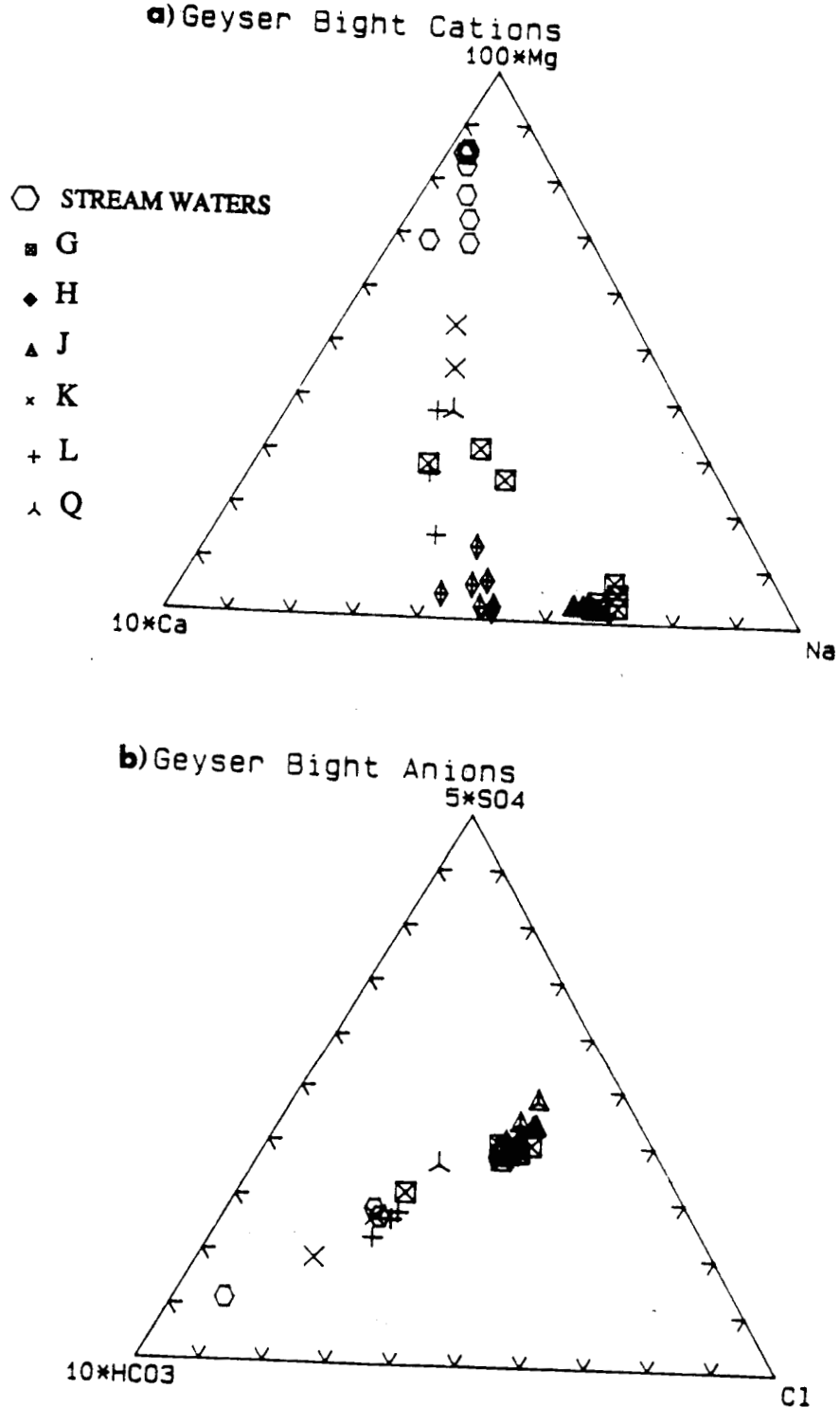

Figure 6.3. Cation (a) and anion (b) trilateral diagrams of Geyser Bight thermal springs and stream waters illustrating mixing trends between meteoric and thermal waters.

dilution of thermal waters. Because Mg is usually removed from high temperature thermal waters through hydrothermal reactions, the presence of Mg in thermal waters is commonly a sign of cold water mixing.

The constituent-chloride plots for Ca and HCO_3 are more scattered although they too appear inversely correlated with Cl (Figs. 6.1d and 6.1f). Spring waters at or above the boiling point have significantly less HCO_3 than lower temperature springs, probably due to the partitioning of dissolved CO_2 into the steam phase. The higher pH exhibited by the boiling springs is probably also due to the loss of CO_2 and other acid gases to the volatile phase which separates from the boiling water. Acid-sulphate springs which emanate near Spring G8 attest to this conclusion. Ca and HCO_3 in the boiling spring waters could also have been removed by precipitation of calcite as these waters are all near saturation with respect to calcite.

The Rb/Cl and Cs/Cl ratios for sites H and Q are lower than those for down-valley sites (Figs. 6.1h and 6.1i) but the Rb/Cs ratios are similar (Table 6.4), ranging from 0.45 to 0.68. Cs can be removed from thermal waters at temperatures less than about 200°C by analcime and other zeolites (Goguel, 1983; Keith and others, 1983). Thus the difference in Cs/Cl ratios suggests that the site H thermal spring waters are derived from a lower temperature environment than site G, J, K, and L waters..

Cs concentrations and Cs/Cl ratios for Geyser Bight thermal waters are similar to those found for thermal waters from Upper and Lower Geyser Basins at Yellowstone National Park (Keith and others, 1983). Keith and others (1983) have suggested that the Cs/Cl ratio may be useful in determining the host rock of the hydrothermal system. The Cs/Cl ratios for the Geyser Bight thermal waters are similar to data Keith and others (1983) selected as

representing equilibration within rhyolitic rock. Rhyolite is rare in the Aleutians. Based on Geyser Creek valley geology (Plate 1), rhyolitic reservoir rocks are not expected at Geyser Bight. The presence of a linear zone of 135 ka rhyolite domes about 4 km southwest of site H and 1.5 km southwest of fumarole F3, however, indicates that conditions appropriate for rhyolite generation existed in the recent past. Such conditions could exist today, although there is no evidence of a rhyolitic component in the youngest lavas erupted from Mt. Recheshnoi (see section 4).

6.4.3 Arsenic and Boron

As and B in Geyser Bight thermal waters deserve specific attention because concentrations of these constituents and particularly their ratios to Cl appear anomalously high when compared to other geothermal areas. Concentrations of both of these constituents increase linearly with Cl at Geyser Bight (Figs. 6.1g and 6.1j).

Although concentration of As in the Geyser Bight thermal spring waters (6.6 ppm) is similar to that found in geothermal well waters at the Makushin geothermal area on neighboring Unalaska Island (10 ppm) (Motyka and others, 1988), the As/Cl ratio at Geyser Bight is three times greater than at Makushin. Few of the volcanically hosted hydrothermal systems for which data are available have As concentrations as high as at Geyser Bight or Makushin (cf. Stauffer and Thompson, 1984). With one exception, the As/Cl ratio for the Geyser Bight waters (0.01) is greater than that reported for other geothermal systems. For example, the As/Cl ratio for Yellowstone thermal waters ranges from 0.003 to 0.005 (Stauffer and Thompson, 1984) while thermal springs at Lassen have As/Cl ratios of 0.005, except one spring which has a As/Cl ratio of 0.01 (Thompson and others, 1985). A principal source of As in

geothermal waters appears to be leaching of reservoir rocks. Arsenic occurs in minor to trace amounts in most rocks and averages about 0.5 ppm in the Geyser Bight pluton. Stauffer and Thompson (1984) concluded that at least 30 to 50 per cent of the As in the Yellowstone hot spring waters was derived by rock leaching. However, rock-water interaction appears insufficient to entirely explain elevated As concentrations found at Yellowstone, Lassen and some other volcanically hosted hydrothermal systems (Stauffer and Thompson, 1984; Thompson and others, 1985). Although a magmatic source for As in geothermal systems remains unproven it seems a likely candidate for explaining elevated As concentrations in these cases and perhaps for Geyser Bight.

Boron concentrations at Geyser Bight are also similar to the Makushin geothermal area (60 ppm). However, the B/Cl ratio is substantially higher, being over an order of magnitude greater at Geyser Bight than at Makushin (0.8 vs 0.02). Although B concentrations in geothermal waters are quite variable, ranging all the way up to 1,000 ppm for the Ngawha system in New Zealand, the B concentrations and B/Cl ratios observed at Geyser Bight are similar to or higher than found at most other geothermal systems. Elevated concentrations of B in some systems have been attributed to leaching of sedimentary formations (Stauffer and Thompson, 1984; Thompson, 1985). Although Byers (1959) reported albitized shales and sandstones in the vicinity of Geyser Bight, detailed geologic mapping did not uncover any unequivocally sedimentary units in the Geyser Bight area (cf 2.2.16). Boron concentration in the Geyser Bight pluton, the presumed reservoir rock, is only 7.5 ppm. In comparison, shales have an average concentration of 100 ppm (Krauskopf, 1979). Shales and sandstones exposed elsewhere on Umnak Island may still underlie the area but are not exposed. If so, hydrothermal fluids circulating through such rocks could have dissolved B and account for the elevated concentrations found in

the thermal spring waters. Alternatively, the excess B may have been derived directly from a degassing magmatic heat source. B has been shown to be selectively adsorbed on clay particles during circulation through both near-shore and deep sea pelagic sediments (Palmer and others, 1985). Boron, along with other volatile elements, would have been expelled from any subducted pelagic sediments and incorporated into magma rising from the region above the subducted slab into the shallow crustal regions.

6.5 Stable Isotopes

Results of stable isotope analyses of Geyser Bight meteoric and thermal waters are given in Table 6.5 and plotted in Figs. 6.4a and 6.4b. Two meteoric water lines are included: the first is the meteoric water line of Craig (1961) which is based on analyses of world-wide precipitation; the second is the Aleutian-Adak meteoric water line (A-AMWL) (Motyka and others, in preparation). The latter was derived from a combination of stable isotope values for 57 Adak weather station precipitation samples (data obtained from the International Atomic Energy Agency, Vienna (IAEAV)) and for 52 stream and precipitation samples obtained by the authors from various Aleutian Islands. Craig's meteoric water line is slightly steeper in slope than the A-AMWL and the two lines intersect at δD = -73 per mil and $\delta^{18}O$ = -10.3 per mil.

The Umnak Island meteoric water samples (which were included in deriving the A-AMWL) fall into two distinct groups with the 1980-81 samples plotting to the left of the meteoric water lines and the 1988 samples to the right (Fig. 6.4a). These differences cannot be attributed to systematic error in analyses as results for control samples were well within the analytical error limit of previously reported results. In addition, $\delta^{18}O$ results for the most chemically concentrated of the 1988 thermal spring samples are similar to

Table 6.5. Stable isotope compositions of Umnak Island thermal springs, streams, and meteoric waters, per mil.

Thermal Spring Waters

Site	$\delta^{18}O$	δD
1988:		
G1	-7.7	-67
G6	-8.3	-66
G8	-8.5	-68
G8A	-1.3	-56
G11	-8.8	-69
H2	-8.9	-71
H4	-8.7	-71
H6	-8.7	-72
H7	-9.4	-71
J1	-7.6	-67
J5	-7.9	-68
K3	-9.3	-71
L1	-8.9	-72
L3	-9.4	-72
Q	-9.0	-72
1980:		
G6	-9.0	-66
G8	-8.4	-67
H1	-8.2	-70
H6	na	-67
J1	-7.9	-63
K1	-9.3	-70
L1	-9.3	-68
1975:		
Gx	-8.2	-68
G8	-8.1	na
J1	-8.0	-67
J4	-7.1	-67

Streams and Meteoric Waters

Site	$\delta^{18}O$	δD
1988:		
H+	-9.6	-71
H-	-9.4	-74
G-	-9.6	-71
J-	-10.0	-77
Q+	-9.9	-74
KL-	-10.0	-74
Kl-side	-9.6	-70
RB-H	-11.4	-86
RB-M	-10.3	-78
RB-L	-9.7	-70
CS-H6	-9.9	-71
1981:		
above H	-10.6	-72
1980:		
rain	-5.5	-36
snow	-10.6	-71
Creek mouth	-11.0	-73
H1 stream	-10.3	-69
J1 cold spr	-10.8	-71
HSC, near E	-9.7	-68
Partov	-8.9	-59

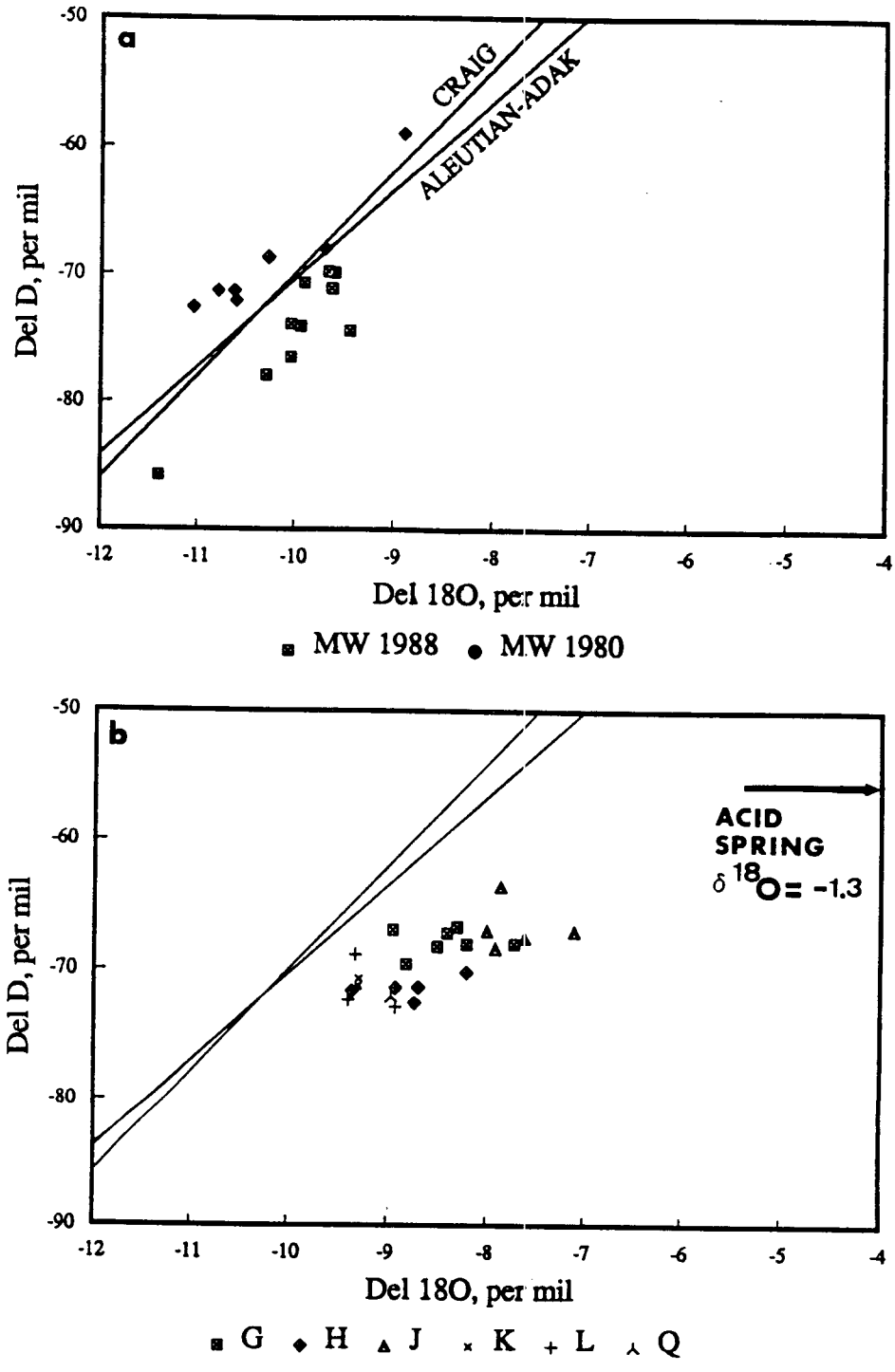

Figure 6.4. Stable isotope results: a) meteoric waters; b) Geyser Bight thermal waters. The Aleutian-Adak and Craig (1961) meteoric water lines are shown for comparison.

previously reported results for the same springs. The Aleutian Islands are subject to weather fronts originating from both the North Pacific Ocean and the Bering Sea. The differences in stable isotope values for these stream waters may be due to differences in prevailing meteorological conditions prior to and during the respective sampling periods.

Stream waters generally follow the well-known altitude effect associated with precipitation (see, for example, Gat, 1980) with streams at higher elevations correlating with lighter isotopic values. An example of this effect are samples RB-H, RB-M, and RB-L which were collected on the same day at elevations of 650 ft, 500 ft, and 150 ft, respectively (Table 6.5).

The isotope values for all the Geyser Bight thermal spring waters plot to the right of the meteoric water lines and the different spring groups have distinct isotopic signatures (Fig. 6.4b). Deuterium values for sites H, K, L, and Q are similar to or slightly heavier than the calculated average for local stream waters, while δD for G and J springs are all slightly heavier than the average stream water. In contrast to δD, $\delta^{18}O$ values for all the thermal springs are positively shifted with respect to local stream waters with the degree of shift correlating with Cl concentration. The greatest shift occurs for sites G and J which are 2 to 2.5 per mil heavier than the calculated average for local stream waters.

Near-boiling low Cl acid-springs occur at site G and have much heavier isotopic values then the surrounding high-chloride springs (Table 6.5). These acid-springs, which exhibit little flow, are likely surface and shallow ground waters that are heated by condensing steam and acid gases that are derived from the waters feeding the nearby high-Cl, near-neutral thermal springs. Their isotopic values are probably a result of continuous evaporative

fractionation of the lighter isotopes into the vapor phase. The comparatively heavier δD values for Spring G6 suggest these thermal waters may have a small component derived from such an acid-spring or that they have mixed with a heavier meteoric water. The 1980 δD value for J1 is also anomalously high compared to the other springs in the G and J groups. J1 is a large, open hot pool, with a low rate of flow, that may be subject to evaporative concentration of heavier isotopes.

Truesdell and others (1977) have shown how the original isotopic composition of boiling thermal spring waters can be calculated after allowing for fractionation processes which affect the compositions. However, a deep water composition (as determined from a well fluid) is required as a starting point for the treatment of the data and no such analysis is available for Geyser Bight. By using isotope values for site G waters as an end point, a range of starting point values can nevertheless be estimated. Changes in δD and $\delta^{18}O$ in the residual liquid as a water boils are a function of beginning and ending temperature and the degree to which the steam remains in contact with the liquid. Using data from Truesdell and others (1977), Fig. 6.5a illustrates the change in composition a thermal water would undergo as it ascends from a reservoir to emerge boiling at the surface with a δD value and Cl concentration similar to site G thermal spring waters. The paths correspond to two extreme cases: (a) SS, single-stage steam separation, and (b) C, continuous steam separation. The beginning point temperatures used in the analysis correspond to geothermometer estimates of reservoir temperatures discussed later. The estimated range of δD reservoir values lies within the range of values found for local stream waters. Similar correlations between deuterium of geothermal waters and local meteoric waters have led many investigators to conclude that geothermal systems are mainly recharged by

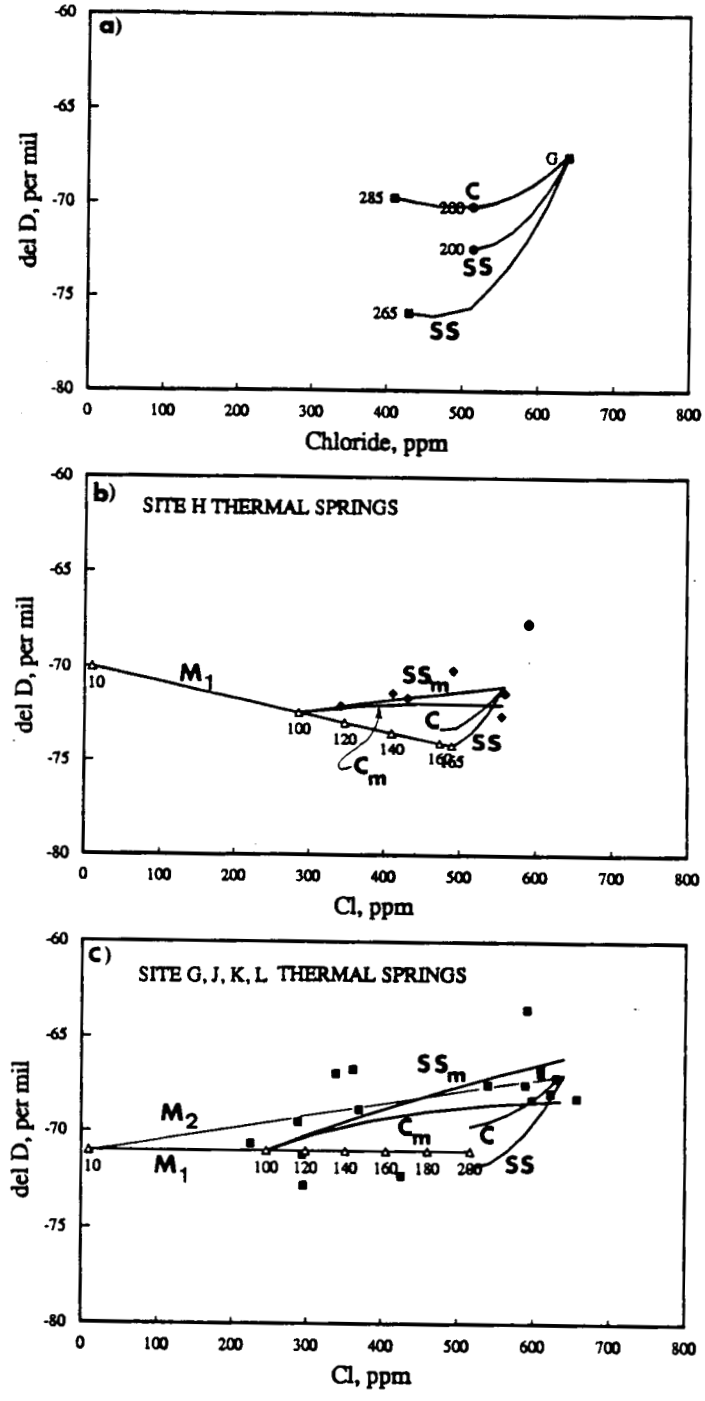

Figure 6.5. Possible compositional changes in thermal waters which ascend from reservoirs: a) at 285, 265, and 200°C and emerge boiling at the surface at spring G; b) at 165°C and mix with 10°C meteoric water to produce site H spring waters; and c) at 200°C and mix with 10°C meteoric water to produce spring waters at sites G, J, K, and L. Triangles mark end-point and mixed water compositions at various temperatures. SS and C indicate paths for single-stage and continuous steam separation, respectively. Lines SS_m and C_m show surface compositions of a mixed water following single-stage and continuous steam separation, respectively. See text for further discussion.

local precipitation (see Truesdell and Hulston, 1980 for review) and such is probably the case for the Geyser Bight geothermal area. A similar analysis for site H resulted in slightly lighter δD reservoir values compared to G and suggests that the zone of recharge for the reservoir feeding the H system lies at a higher elevation than that for the G/J reservoir.

Applying similar techniques to $\delta^{18}O$ vs. Cl gives "reservoir" values of $\delta^{18}O$ that are 0.6 to 1.0 per mil lighter than spring G8 and H4. The isotope boiling paths roughly parallel the meteoric water lines so that the apparent ^{18}O shift with respect to these lines remains at 2 to 2.5 per mil. Similar shifts in the ^{18}O content of geothermal waters to more positive values with respect to local meteoric waters have been observed at most high-temperature geothermal systems. These positive shifts have been attributed to ^{18}O exchange between the deeply circulating meteoric waters and reservoir wallrocks with the degree of shift depending on temperature and rock/water ratio (Truesdell and Hulston, 1980). Comparable shifts in δD do not take place because reservoir rocks contain little deuterium.

Nearly all of the H springs and many of the G springs are vigorously boiling at the surface. In addition, these and the other springs may also have been subject to dilution. Using techniques described by Truesdell and others (1977), the effects of mixing and boiling can be analyzed. Fig. 6.5b illustrates the case for site H spring waters. Here, M_1 is a mixing line between a hypothetical meteoric water having a temperature of 10°C, Cl concentration of 10 ppm, and δD value of -70 per mil and an ascending thermal water with T = 165°C, Cl = 490 ppm, and δD = -74 per mil. SS and C show compositions of waters which ascend to the surface without mixing and emerge as boiling spring waters for the cases of single-stage and continuous steam

separation, respectively. SS_m and C_m show the surface compositions of the residual liquid phase of waters which mix at depth along M_1 and then ascend to the surface for the cases of single-stage and continuous steam separation, respectively. This model adequately accounts for the δD and Cl compositions of spring Q and H springs sampled in 1988. Both 1980 H samples are heavier in δD than the 1988 samples suggesting that the diluting water may have had a different composition in 1980.

A similar analysis performed for G, J, K and L spring waters is illustrated in Fig. 6.5c. The value chosen for the reservoir water (δD = -72 per mil, Cl = 520 ppm) lies between the single-stage and continuous steam separation values determined for the case of a 200°C reservoir (Fig. 6.5a). M_1 is a mixing line between this deep thermal water and a hypothetical cold water (δD = -71 per mil, Cl = 10 ppm). M_2 illustrates a mixing line between the cold water and shallow thermal waters whose composition is similar to site G boiling spring waters.

This model suggests that the compositions of site G boiling spring waters are adequately explained as being the result of a steam separation process intermediate between single-stage and continuous without mixing with cold waters. Other springs in the area are below boiling. The isotopic values for some of these spring waters appear to be the result of mixing of fractionated thermal waters, similar to site G boiling water, with meteoric waters along M_2 rather than by mixing of meteoric waters with the deep thermal water along M_1, followed by boiling to the surface (SS_m and C_m). Data points for other down-valley, lower-temperature, and comparatively more dilute springs cannot be explained by this model and appear to have formed by mixing with a greater variety of meteoric waters.

6.6 Tritium

Results of tritium analyses of two Geyser Bight thermal spring waters and two streams are given in Table 6.6. Reviews of tritium in atmospheric waters and in groundwaters can be found in Gat (1980) and Fontes (1980), respectively. Tritium occurs in atmospheric waters as a result of both natural and man-made processes. It is produced naturally by the interaction of cosmic radiation with the upper atmosphere. Enormous amounts of man-made tritium were released into the atmosphere during the period of thermonuclear testing from 1952 to 1962. Although pre-1952 data is sparse, natural tritium levels in precipitation appear to range from about 4 to 25 tritium units (TU), depending on location (Gat, 1980) with an average of about 10 TU in temperate zone continental meteoric waters (Panichi and Gonfiantini, 1978). Average tritium concentrations in precipitation fluctuated widely following thermonuclear tests, reaching peak levels of over 2,200 TU in the northern hemisphere in the late spring of 1963 (Gat, 1980). Reported tritium concentration in precipitation at Adak Island for June, 1963 averaged 3,900 TU (data from IAEAV).

Since 1963, atmospheric concentrations of tritium have steadily declined through radioactive decay and precipitation of tritiated tropospheric waters, and average concentrations are beginning to approach pre-1952 levels. Tritium concentrations in precipitation undergo seasonal variations which are linked to exchanges between the stratosphere and the troposphere (Gat, 1980). Maximum concentrations occur in late-spring followed by a minimum in late-fall. As an example, in Anchorage in 1980 (the most recent year for which data are available) the weighted annual average tritium concentration dropped

Table 6.6. Results of tritium analyses, Geyser Bight waters. Tritium concentrations are in tritium units (TU). Analyses performed by Tritium Laboratory, U. of Miami.

Sample	TU	Std Dev
Hot Springs:		
88-H6	2.4	0.1
88-H6[a]	2.9	0.1
88-G8	0.0	0.1
Cold Streams:		
88-E Geyser Cr H+	9.6	0.3
88-Side Cr KL-	6.3	0.2

[a] Repeat analysis.

to 29 TU with a seasonal variation ranging from a winter minimum of 16 TU to a late-spring maximum of 51 TU.

Because of its relatively short half-life (12.3 yr), tritium is a good indicator of meteoric waters of relatively young age and has therefore been extensively used to estimate age and mixing of waters in groundwater and geothermal systems (see Fontes, 1980, and Panichi and Gonfiantini, 1978 for reviews). At Geyser Bight, tritium concentrations in G8 thermal spring waters are below detection (< 0.1 TU) indicating that the meteoric waters recharging the site G geothermal reservoir system must be at least 70 years in age. In comparison, thermal spring waters from H6 have a tritium concentration of 2.4 to 2.9 TU, one-quarter to one-half that of local stream water. Because of the surprisingly high concentration of tritium in H6 waters, a repeat analysis was requested and produced nearly identical results.

Interpretation of the elevated tritium concentration in the H6 waters remains ambiguous. The H6 tritium concentration could reflect mixing of meteoric waters of very recent age but analyses of water chemistry and stable isotope data do not support a 25 to 50 per cent admixture of near-surface meteoric waters in the H6 thermal spring waters. An alternate possibility is that recharge of the site H geothermal reservoir system is considerably more rapid than at G. A 1950 water with an initial tritium concentration of 10 TU would have decayed to about 2.5 TU by 1988. One further possibility is that small amounts of meteoric waters associated with periods of thermonuclear testing are intercepting and slightly diluting ascending thermal waters at deep levels. Northern hemisphere precipitation in 1954 with a peak tritium concentration of about 900 TU (Gat, 1980) would have decayed to concentrations of about 130 TU in 1988.

6.7 Geothermometry

6.7.1 Silica

Results of applying the silica geothermometer (Fournier and Potter, 1982) to Geyser Bight hot-spring waters are given in Table 6.7. Silica concentrations are plotted against vent enthalpy in Fig. 6.6 along with the quartz solubility curve. For pressures normally encountered in geothermal systems, silica concentrations in geothermal waters are a function of temperature, pH, and the controlling silica mineral phase. For the probable temperatures and host rocks for the Geyser Bight reservoirs (> 150°C; quartz monzonite to granodiorite), quartz can be considered the mostly likely phase controlling the dissolved silica concentration (Fournier, 1981).

For vigorously boiling springs, the quartz adiabatic geothermometer was applied. The effect of adiabatic cooling is illustrated in Fig. 6.6. Following the method of Fournier and Potter (1982), rays originating from a point representing separated steam at 1 atm pressure with an enthalpy of 2676 J/g and less than 1 ppm silica are drawn to points representing boiling springs G1 and H6. Intersection of these lines with the quartz solubility curve (A and D, respectively) mark the enthalpy and silica concentration of the parent water for the case of adiabatic cooling and single-stage steam separation at the surface. As this water ascends and cools adiabatically , boiling concentrates silica in the residual liquid phase. The case of continuous steam separation would provide slightly higher temperature estimates.

Fournier and Potter's (1982) quartz geothermometers are based on neutral or near-neutral solutions. For a pH greater than 7.5, the solubility of

Table 6.7. Silica and cation geothermometry applied to Geyser Bight hot spring waters. Temperatures in degrees celsius.

Site	T, spring	Quartz[a] Cond	Quartz[a] Adiab	Na-K[b]	Cation Na-K[c]	Na-K-Ca[b]
1988:						
G1	101	216	197	194	211	186
G6	94	171	161	186	203	168
G8	100	207	190	190	207	182
G11	86	145	139	156	174	140
H2	98	158	150	160	179	150
H4	102	173	162	160	179	152
H6	104	175	164	158	177	152
H7	103	158	150	152	171	145
J1	80	200	184	188	206	179
J5	90	197	182	192	208	181
K3	80	154	147	194	211	167
L1	60	147	141	190	207	164
L3	86	165	156	189	206	167
Q	78	157	149	157	176	144
1980:						
G6	97	172	162	187	204	166
G8	100	201	185	181	198	175
H1	100	169	159	158	177	149
H6	100	176	165	157	176	151
J1	82	202	186	189	206	180
K1	62	160	152	196	213	166
L1	86	165	156	190	207	166
1975:						
G?	85	196	181	179	197	174
G8	102	197	182	185	202	177
J1	93	194	180	185	203	176
J4	65	188	175	190	207	180
1946:						
G1	100	210	192	193	210	185
H1	101	161	153	166	184	153

[a] Fournier and Potter (1982).
[b] Na-K: Fournier equation; Na-K-Ca: Fournier and Truesdell equation (Fournier, 1981).
[c] Giggenbach (1988).

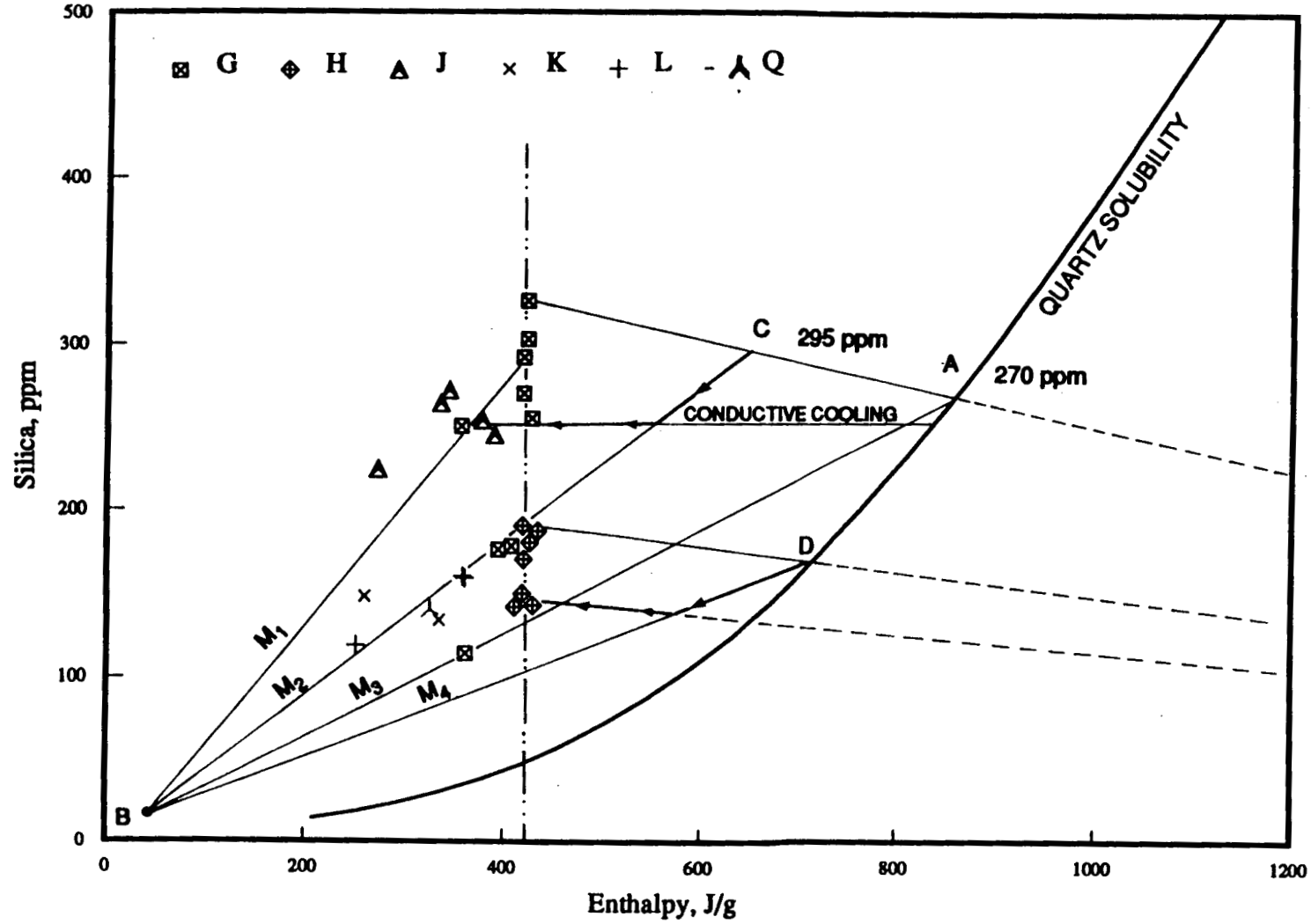

Figure 6.6. Silica concentrations versus vent enthalpy. Interception of dashed rays with quartz solubility curve at points A and D represent enthalpy and silica concentrations of parent waters for G and H springs respectively. M_1, M_2, M_3, and M_4 represent hypothetical mixing lines between a cold meteoric water (B) and various thermal waters (A, C, D, and G) and are discussed in the section on chloride-enthalpy analysis.

quartz increases with increasing pH and is most pronounced for temperatures between 100 and 250°C (Fournier, 1981). However, pH values of solutions in high-temperature geothermal reservoirs are likely to be below 7.5 because of the buffering of hydrogen ions by silicate hydrolysis reactions. The high pH values found for some Geyser Bight hot-spring waters probably result from the loss of CO_2 and H_2S as the water boils after leaving the high-temperature reservoir. Following the recommendation of Fournier (1981) for this situation, the silica concentration of the hot-spring water is assumed to reflect near-neutral pH reservoir conditions and no correction was applied to the observed silica concentration.

The silica geothermometer is based on absolute concentration, and subsurface dilution of ascending thermal water by cooler low-silica water can result in underestimating reservoir temperature. Dilution probably accounts for the lower temperatures predicted by the quartz geothermometer for non-boiling springs at site G, K, L, and Q. Solutions initially above 200°C can also become supersaturated with respect to amorphous silica and precipitation can take place as the waters ascend and cool adiabatically. The loss of dissolved silica in such a hot-spring water would also cause the quartz geothermometer to underestimate reservoir temperature. Site G boiling spring waters and site J waters have similar concentrations of Cl and Na, indicative of little or no dilution, but have varying SiO_2 concentrations, evidence that silica was lost from these waters by precipitation or re-equilibration (Fig. 6.1a and 6.1m). In contrast, hot-spring waters of group H show marked linearity between both SiO_2 and Cl and Na and Cl (Figs. 6.1a and 6.2). Here, dilution rather than precipitation appears to have affected the silica concentrations of some of the H site boiling hot-spring waters.

Using the results of the most concentrated spring waters, the minimum reservoir temperatures predicted by the quartz geothermometer are 200°C for groups G and J, and 165°C for H.

6.7.2 Cation

Three cation geothermometers were applied to the Geyser Bight hot-spring waters (Table 6.7). Because these geothermometers are based on ratios of constituents rather than absolute concentrations, they are less susceptible to dilution. Temperatures predicted by the Na-K geothermometer of Fournier (1981) are in excellent agreement with those temperatures predicted by the quartz geothermometer for spring waters having the highest silica concentrations. The Na-K-Ca geothermometer (Fournier and Truesdell, 1973) gives lower temperatures than the Fournier Na-K geothermometer with the difference ranging up to 20°C. In contrast, the Na-K geothermometer of Giggenbach (1988) predicts temperatures 15 to 20°C higher than the Fournier Na-K geothermometer.

The Na-K-Ca geothermometer was empirically derived specifically to deal with calcium-rich waters, particularly low-temperature thermal waters, because application of the Na-K geothermometer to such waters was found to give anomalously high calculated temperatures (Fournier and Truesdell, 1973). Calcium concentrations are generally low in all Geyser Bight hot-spring waters and calcium enrichment in Geyser Bight hot-spring waters appears to correlate with spring waters that are below boiling and considered to be of mixed origin. This correlation suggests the Ca enrichment may in part be associated with the dilution process. In addition, for the boiling springs, calcite was also found to be near saturation, suggesting $CaCO_3$ may have precipitated from these waters during their ascent. Such loss of Ca would affect the

reliability of the Na-K-Ca geothermometer. For thermal waters thought to be derived from high-temperature environments the Na-K method generally gives excellent results (Fournier, 1981) and is preferable for Geyser Bight. Using Fournier's Na-K geothermometer, reservoir temperatures of 190 to 194°C are estimated for site G and J thermal waters and 160 to 165°C for site H thermal waters In contrast, the Na-K-Ca geothermometer gives 175 to 186°C for sites G and J and 150 to 152°C for site H.

The Na-K geothermometers of both Fournier (1981) and Giggenbach (1988) are based on analytical data for a wide range of deep well discharges. The steeper temperature dependence of the Giggenbach Na-K geothermometer is due to his selection of data points representing only maximum Na/K ratios at a given temperature.(Giggenbach, 1988). The latter approach assumes that maximum Na/K ratios are more representative of full equilibration.

6.7.3 Sulfate - Water Oxygen Isotope

The results of applying the sulfate-water oxygen isotope geothermometer to the Geyser Bight hot springs are given in Table 6.8. The data include results for a sample obtained by I. Barnes (USGS) in 1975, three samples obtained by the authors in 1980 and two additional samples collected in 1988.

The data for spring G8 are the easiest to interpret because the lack of tritium in Spring G8 waters rules out mixing of young meteoric waters. Good correspondence exists between isotopic values for samples obtained in 1975 and 1980. Spring G8 is a boiling-point geyser and the presence of warm ground and acid-springs nearby indicate that steam separation from the spring conduit is intermediate between single-stage and continuous. Following the

Table 6.8. Sulfate-water isotope geothermometer applied to Geyser Bight hot spring waters. Temperatures in degrees celsius.

Site	T, spring	$\delta^{18}O$-SO_4	$\delta^{18}O$-H_2O	T1	T2	T3
1988:						
H4	102	-2.3	-8.7	248	221	228
L3	86	-3.5	-9.4	262	225	235
1980:						
H1	100	-2.0	-8.2	254	225	232
J1	82	-4.1	-7.9	333	265	287
G8	100	-4.2	-8.4	315	263	279
1975:						
G8	102	-4.1	-8.1	322	264	282

Geothermometer temperatures computed using formulas and tables from McKenzie and Truesdell (1977): T1 = conductive cooling, T2 = single stage steam removal, T3 = continuous steam removal.

All $\delta^{18}O$-SO_4 and $\delta^{18}O$-H_2O of spring G8, 1975 analyzed by N. Nehring and C. Janik, U.S. Geological Survey, Menlo Park. Remaining $\delta^{18}O$-H_2O analyzed by Stable Isotope Laboratory, Southern Methodist University. $\delta^{18}O$ in per mil WRT SMOW.

recommendation of McKenzie and Truesdell (1977), the appropriate range to be chosen as the reservoir temperature is then 263 to 282 °C.

Spring J1 is a large open, hot pool whose water is geochemically very similar to G8 water. Compared to G8, J1 has the same $\delta^{18}O$ value for dissolved sulfate but is slightly heavier in $\delta^{18}O$ for H2O. As discussed previously, the slightly heavier isotopic composition could be attributed to evaporative concentration. As J1 is below the boiling point the conductive cooling temperature, T1, would ordinarily be chosen as the SO_4-H_2O geothermometer estimate. However, this temperature for J1 seems excessively high when compared to that found for G8. As at G8, warm marshy ground is found near the J springs, suggesting that steam may be separating from the spring conduit at depth. There is the intriguing possibility that J1 is actually a geyser but with a relatively long period. Chloride concentration of J1 is slightly lower than G8 suggesting that a small amount of cold water may be diluting the thermal water and quenching residual boiling below the pool. If so, then the range 265 to 287°C, given by T2 and T3 are more applicable. These latter temperatures are in much better agreement with G8 results.

Spring L3 is below the boiling point and has a chloride concentration substantially below that of G8. As discussed previously, based on similarities of constituent/chloride ratios, L3 is likely a diluted version of G-type water. Examination of Na vs Cl (Fig. 6.1a) suggest mixing of about 35 per cent cold meteoric water with G8 type water to produce L3 water. No boiling springs, acid or otherwise, occur near L3 and it is likely that boiling of the ascending deep thermal water is completely quenched by near-surface mixing of cold meteoric water.

Dilution complicates interpretation of the L3 SO_4-H_2O geothermometer because the near-surface mixing of meteoric water obscures the calculation of the $\delta^{18}O$ value of the deep thermal water. Surface stream waters sampled near spring groups K and L in 1988 had $\delta^{18}O$ values of -9.6 and -10 per mil while the average for all stream waters samples was -10.2 per mil. These values are 1.5 to 2 per mil lighter than $\delta^{18}O$-H_2O values for the most concentrated spring waters at Geyser Bight. Dilution of deep thermal water with meteoric water would then result in the mixed water having a lighter $\delta^{18}O$ value than the thermal water. The T1 conductive SO_4-H_2O geothermometer for the L3 spring water $\delta^{18}O$ value therefore provides only a minimum estimate for the deep thermal water temperature. This estimate of 262°C compares well with the lower range of G8 and J1 estimates.

Results of isotopic analysis of the two H springs samples are consistent with each other (Table 6.8). Compared to G and J spring waters, the $\delta^{18}O$ values for dissolved sulfate are about 2 per mil heavier, although the $\delta^{18}O$ values for these H spring waters are similar. The difference in isotope values for dissolved sulfate is probably not attributable to formation of sulfate by oxidation of H_2S at low temperatures. No odor of H_2S was detected at site H and hot spring waters analyzed from site H have nearly identical SO_4/Cl ratios (Fig. 6.1k), indicating that oxidation of H_2S is probably unimportant (McKenzie and Truesdell, 1977). We suggest two possibilities to explain the differences in $\delta^{18}O$ values for dissolved sulfate: 1) there are two deep reservoirs with different temperatures; or 2) $\delta^{18}O$-SO_4 partially re-equilibrates while the waters reside in lower temperature reservoirs at intermediate depth.

Tritium analyses indicated the presence of young meteoric water in the H spring system but the data were insufficient to determine the amount of mixing or whether mixing was responsible for the high tritium value. As with spring L3, any addition of near-surface meteoric water to ascending thermal water would tend to produce a spring water with $\delta^{18}O$ values lighter than the thermal water. The temperatures predicted by the SO_4-H_2O geothermometer for the H springs are therefore minimum estimates. Both H springs sampled are at boiling so the applicable temperature range is 221° to 232°C.

6.7.4 Assessment of Geothermometers

Accuracy of chemical and isotopic geothermometers depends on a number of conditions: availability of constituents used in the geothermometer, full equilibration between the thermal water and the constituents, no re-equilibration, precipitation, or additional reaction with wallrock upon ascent, and no mixing with other waters. All or none of these conditions may actually be met in real systems. In reviewing the Geyser Bight geothermometers, we find that the temperatures predicted by two traditionally used geothermometers, i.e., the quartz geothermometer and the Na-K cation of Fournier, are in excellent agreement with each other for the Geyser Bight hot-spring waters that have the highest concentrations of dissolved solids, eg., G1, G8, J1, H6, and H4, and probably represent minimum estimates of temperatures for subsurface aquifers. For springs issuing below boiling point at sites G, J, K, and L, the Fournier Na-K temperature exceeds the quartz conductive geothermometer by several to tens of degrees Celsius. Because the quartz geothermometer is more susceptible to dilution, this discordance probably reflects near-surface mixing of cold meteoric waters with thermal waters (Fournier and Truesdell, 1974). Mixing at H is not as clearly

indicated by comparison of Na-K and quartz geothermometers. Results for the most concentrated springs H6 and H4 show Na-K temperature to be identical or slightly lower than the quartz adiabatic temperature. For the more dilute springs suspected to be of mixed origin (H1, H2, and H7), the Na-K temperature is similar to or slightly higher than quartz temperature.

For the pH and temperature range of most deep geothermal waters, the rates of the sulfate oxygen isotope exchange reaction are very slow compared to silica solubility and cation exchange reactions (Fournier, 1981; Truesdell and Hulston, 1980). Once equilibrium is attained in the deep reservoir, there is little re-equilibration of the oxygen isotopes of sulfate as the water cools during movement to the surface, unless that movement is very slow. Therefore, temperatures predicted by the SO_4-H_2O oxygen isotope geothermometers, which are substantially higher than the cation and silica temperatures, may reflect temperatures in deep reservoirs at Geyser Bight.

Assuming that this is the case at Geyser Bight, geothermometry then suggests that thermal waters initially reside in deep reservoirs with a minimum temperature of 265°C. Thermal water from these deep reservoirs ascend to reservoirs at intermediate depths where cations and silica re-equilibrate to temperatures of 200°C for waters emerging at sites G and J and other down-valley sites and to temperatures of 165°C for waters emerging at site H and perhaps site Q. Residence time in these intermediate reservoirs must be on the order of several months or more to achieve new cation equilibrium. Residence and travel time for site H waters may have been sufficiently long enough for partial re-equilibration of the sulfate oxygen isotopes.

6.8 Chemical Equilibria

Proper evaluation of chemical equilibrium in subsurface aquifers requires information on dissolved constituents, gas partial pressures (CO_2, H_2S), aquifer pH, and wallrock characteristics. Such information, which is normally obtained from a well, is lacking for Geyser Bight, and aquifer conditions must be inferred from available surface thermal spring chemistry. Aquifer chemical composition can be estimated by adjusting for the concentration of constituents caused by boiling, but lack of information on the volatile phases and on the possibility that calcite has precipitated hinder accurate calculation of aquifer pH and aquifer Ca concentration, parameters which are critical in evaluating mineral stabilities. Nevertheless, with reasonable assumptions, some reservoir fluid-mineral equilibria can still be estimated.

An activity diagram showing the principal phases in the system Na_2O-K_2O-Al_2O_3-H_2O at 200°C is shown in Fig. 6.7. Stability fields for albite, potassium feldspar (K-feldspar), and muscovite (K-mica) at 150°C are also shown for comparison. Log activities for Geyser Bight waters calculated using 1988 thermal spring chemistry show that the most concentrated waters from sites G and J are in equilibrium with both albite and potassium feldspar. The more dilute springs plot on or near the extension of the albite-potassium feldspar equilibrium line into the field of muscovite stability. In contrast, site H thermal spring waters plot closer to the 150°C equilibrium line. Points G8-B and H6-B, which illustrate the effects of adjusting concentrations but not pH for steam losses, are only slightly displaced on the albite-potassium feldspar equilibrium line. The effect of decreasing pH to more realistically reflect probable aquifer conditions is to displace points G8-B

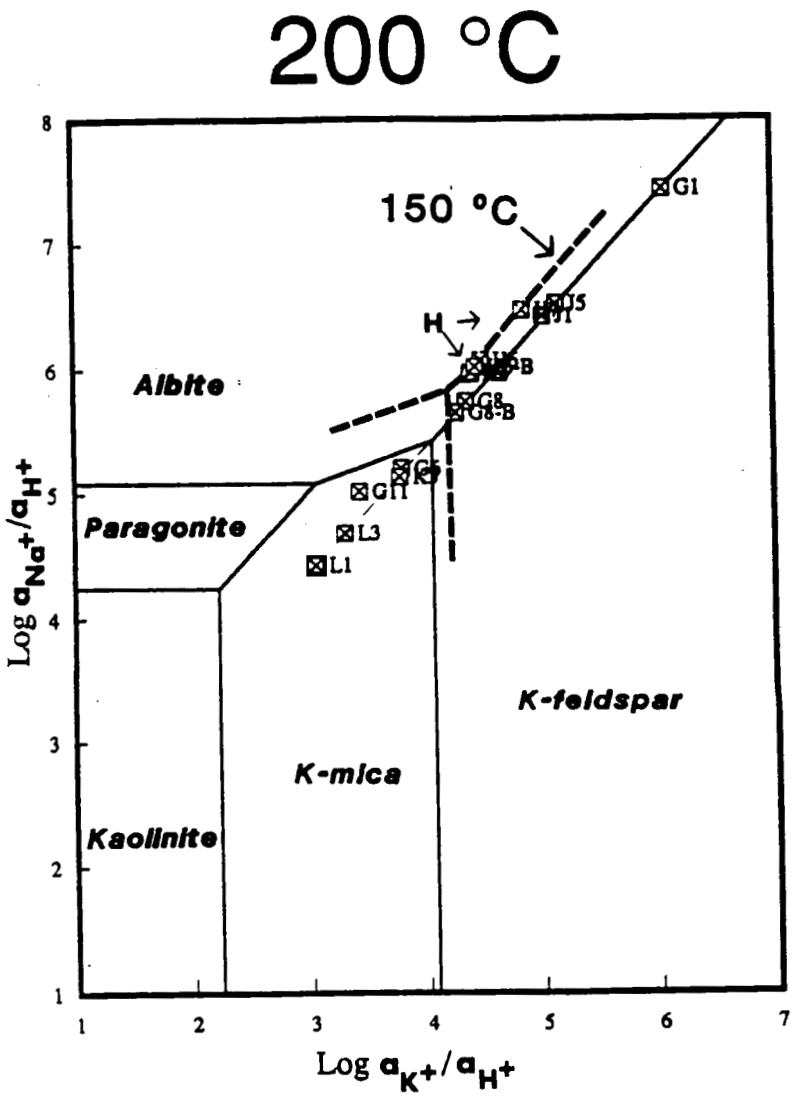

Figure 6.7. Activity diagram of the Na_2O-K_2O-Al_2O-H_20 system at 200°C showing principal mineral phases, with 150°C overlay.

and H6-B further toward muscovite stability. Calculated pH at the albite-potassium feldspar-muscovite 200°C triple point is 7.2.

It is readily apparent in the trilateral plot of Na-K-√Mg shown in Fig. 6.8a that thermal waters at site H vs the down-valley sites have equilibrated at different temperatures. This diagram and its application to geothermal systems are described by Giggenbach (1988). The "full-equilibrium" curve in Fig. 6.8a represents compositions of waters in full equilibrium with the mineral system albite-potassium feldspar-muscovite-clinochlore-silica at the temperatures indicated. The boundary between partially equilibrated and immature waters shown in Fig. 6.8a is somewhat arbitrary and serves only as a rough guideline (Giggenbach, 1988). The isotherms correspond to the equilibrium equations

$$L_{kn} = \log (C_K/C_{Na}) = 1.75 - (1390/T) \quad (1)$$

for the pair K-Na and

$$L_{km} = \log (C^2_K/C_{Mg}) = 14.0 - (4410/T) \quad (2)$$

for the pair K-Mg, where C is in mg/kg and T in °K as derived by Giggenbach (1988).

Magnesium concentrations in thermal waters are highly temperature dependent with hotter temperatures favoring depletion of Mg from the water through hydrothermal reactions. For more mature thermal waters Mg is commonly present in only trace quantities. The effect of increasing or decreasing Mg is to move the points down or up respectively, parallel to the K-Na isotherms.

In Fig. 6.8a the spring waters from group H plot on or near the 180 °C isotherm while those from groups G, J, L and K lie on or between the 200 and 210°C isotherms. The K-Mg system adjusts to cooling temperature more rapidly than the K-Na system, and spring waters that plot below the "immature water"

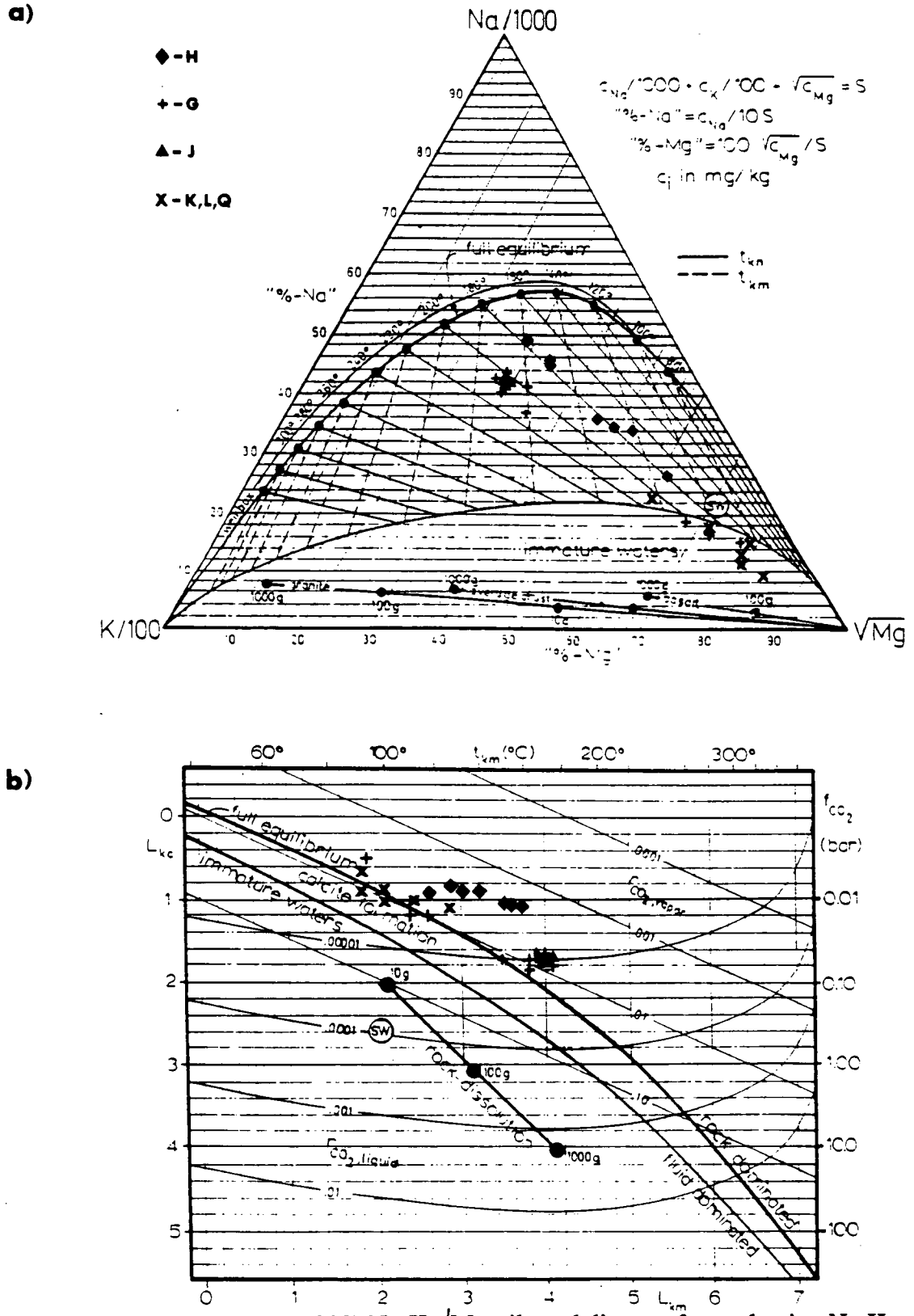

Figure 6.8. a) Giggenbach's (1988) Na-K-√Mg trilateral diagram for evaluating Na-K and K-Mg equilibration temperatures; b) Giggenbach's (1988) graphical CO_2 geobarometer.

line probably reflect the dissolution of Mg in the shallow environment as the waters cool conductively or, more likely, cool by mixing with colder ground waters.

Giggenbach (1988) has also devised a CO_2 "geobarometer" based on K and Ca concentrations:

$$L_{kc} = \log (C^2_{K+}/C_{Ca++}) = \log f(CO_2) + 3.0 \quad (3)$$

Equation (2) is used to correlate CO_2 fugacities with their likely equilibration reference temperatures because K and Mg are more likely to equilibrate at similar rates and under similar conditions as the K-Ca-geobarometer. Giggenbach's graphical representation of this geobarometer based on end-member mineral phases assumed to control CO_2 fugacities in geothermal systems is reproduced in Fig. 6.8b with data points for Geyser Bight geothermal area thermal springs superimposed. Based on data from explored systems, Giggenbach (1988) concluded that the geobarometer is only reliable for data points close to the full equilibrium line; those plotting above this line are likely to come from a rock-dominated, CO_2-deficient environment. Using this criteria, site G waters appear the most suitable for application of this geobarometer. Assuming equilibrium with calcite, the graphically predicted $f(CO_2)$ is about 0.1 bar for G1 and G8 waters. The $f(CO_2)$ corresponding to equilibrium with calcite at the predicted Na-K and quartz geothermometer temperature of 200°C suggested by the equilibrium curve would be about 1.0 bar.

Assuming these values for $f(CO_2)$ and assuming that calcite is at saturation at the predicted geothermometer reservoir temperature of 200°C, an estimate of reservoir pH can be made by using the reaction (Henley and others, 1984):

$$CaCO_3 + 2H^+ = Ca^{++} + H_2O + CO_2 \quad (4)$$

The calculated pH range of 6.1 to 6.6 compares well with pH values found in wells at explored geothermal systems; eg., the Makushin geothermal system on neighboring Unalaska Island has a reservoir pH of about 6.1 (Motyka and others, 1988). Figures 6.9a and 6.9b are SiO_2-Ca activity diagrams at 200°C for various zeolites and clays with Makushin water plotted for comparison. The range for Geyser Bight water was plotted using the reservoir pH estimated from site G water and spring G8 Ca concentration adjusted for boiling. The low end of the pH range suggests that the reservoir fluid is in equilibrium with prehnite, laumontite, and kaolinite.

6.9 Model of Hydrothermal System

6.9.1 Chloride-Enthalpy Analysis

Thermal water ascending from a deep reservoir may cool by boiling, by conduction of heat to surrounding rock, by dilution with colder waters, or by a combination of these processes, depending on the depth of the reservoir, channel geometry, pathway taken, the rate of flow, the coefficient of thermal diffusion through surrounding rock, and the initial temperature (Fournier, 1979). During ascent, its chemical and isotopic composition can be affected by water-rock reactions, re-equilibration, precipitation, mixing, and boiling. The emergent hot-spring waters can, and commonly do, have compositions and enthalpies significantly different from the original parent thermal water. Despite these complexities, chemical compositions of hot spring waters can still be useful for deriving information on underground conditions. Cl-enthalpy and SiO_2-chloride diagrams, when used in conjunction with other evidence, are particularly useful tools for tracing the origins of spring waters. compositions and for determining underground temperatures,

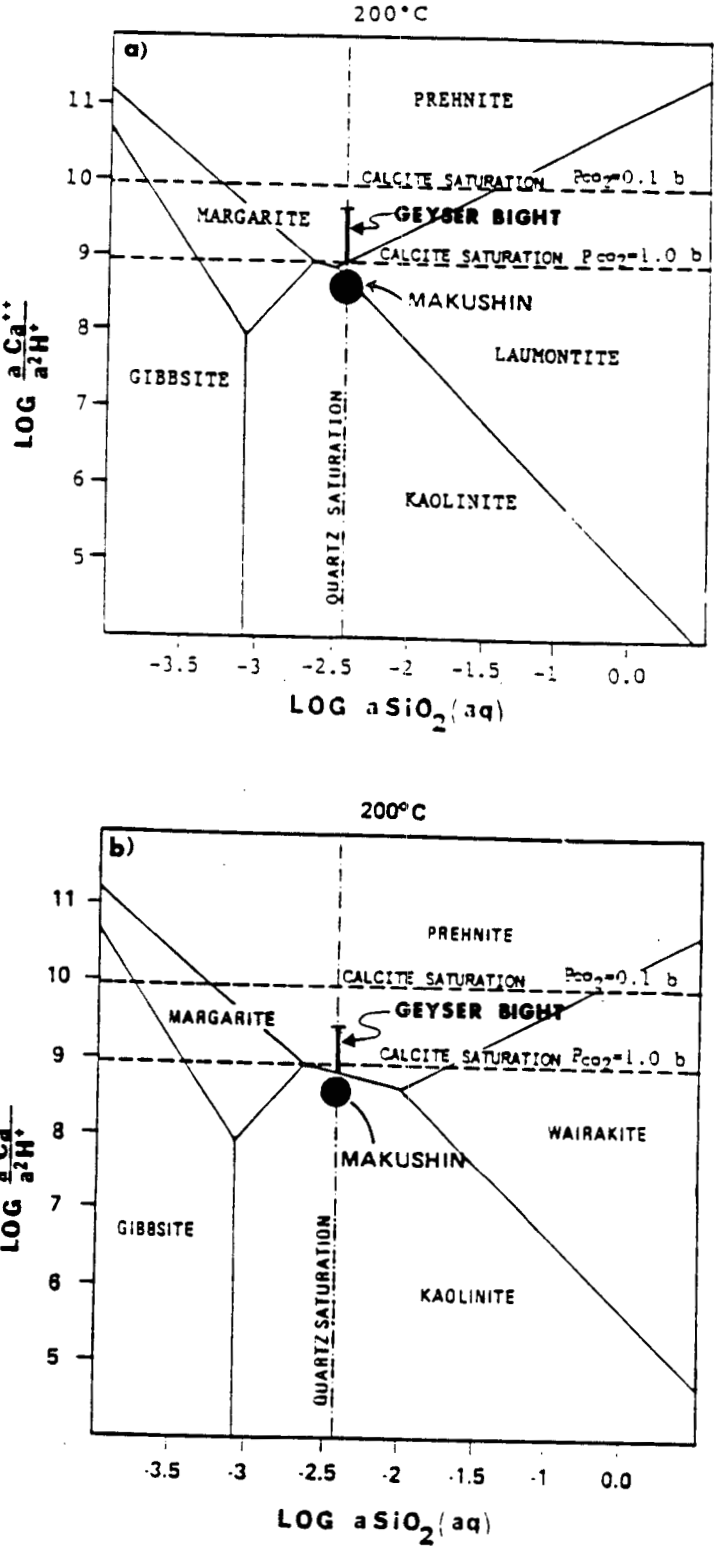

Figure 6.9. Silica-calcium activity diagrams at 200 °C for various zeolites. Makushin test well results shown for comparison.

salinities, and boiling and mixing relationships. Figure 6.10 shows Cl concentrations of sampled Geyser Bight hot spring waters plotted as a function of enthalpy at the measured vent temperature. In our analyses we seek consistency between these diagrams and 1) geochemical and isotopic compositions; 2) SiO_2-enthalpy relationships; 3) geothermometry ; 4) chemical equilibria; and 5) rates of spring discharge.

Truesdell and others (1977) calculated the maximum rates of mass flow for conductive cooling without boiling, and the minimum rates of mass flow for adiabatic cooling with negligible conductive cooling for water moving vertically from different initial depths. Waters were assumed to start at 200°C and emerge at 100°C. Conduits were assumed to be small diameter cylinders. The results of these calculations, some of which are shown in Table 6.9, are particularly useful for our assessment of the Geyser Bight hydrothermal system in as much as geothermometry and chemical equilibria indicate that many of the boiling and near-boiling spring waters originated from an aquifer or aquifers at 200°C. Although the reservoir depths at Geyser Bight are unknown, given the degree of thermal activity observed at the surface, it is reasonable to assume that the reservoir depths are unlikely to be much greater than 1 km. As a comparison, the depth to the hot-water reservoir at the Makushin geothermal area on neighboring Unalaska Island as determined by drilling is about 0.6 km.

6.9.1.1 Sites G, J, K, and L

We first analyze the origin of spring systems located in the upper part of the Geyser Creek valley floor. As discussed previously, based on constituent ratios, these springs appear to be geochemically related. As the starting point we use spring G8. G8 has the highest concentration of Cl and dissolved

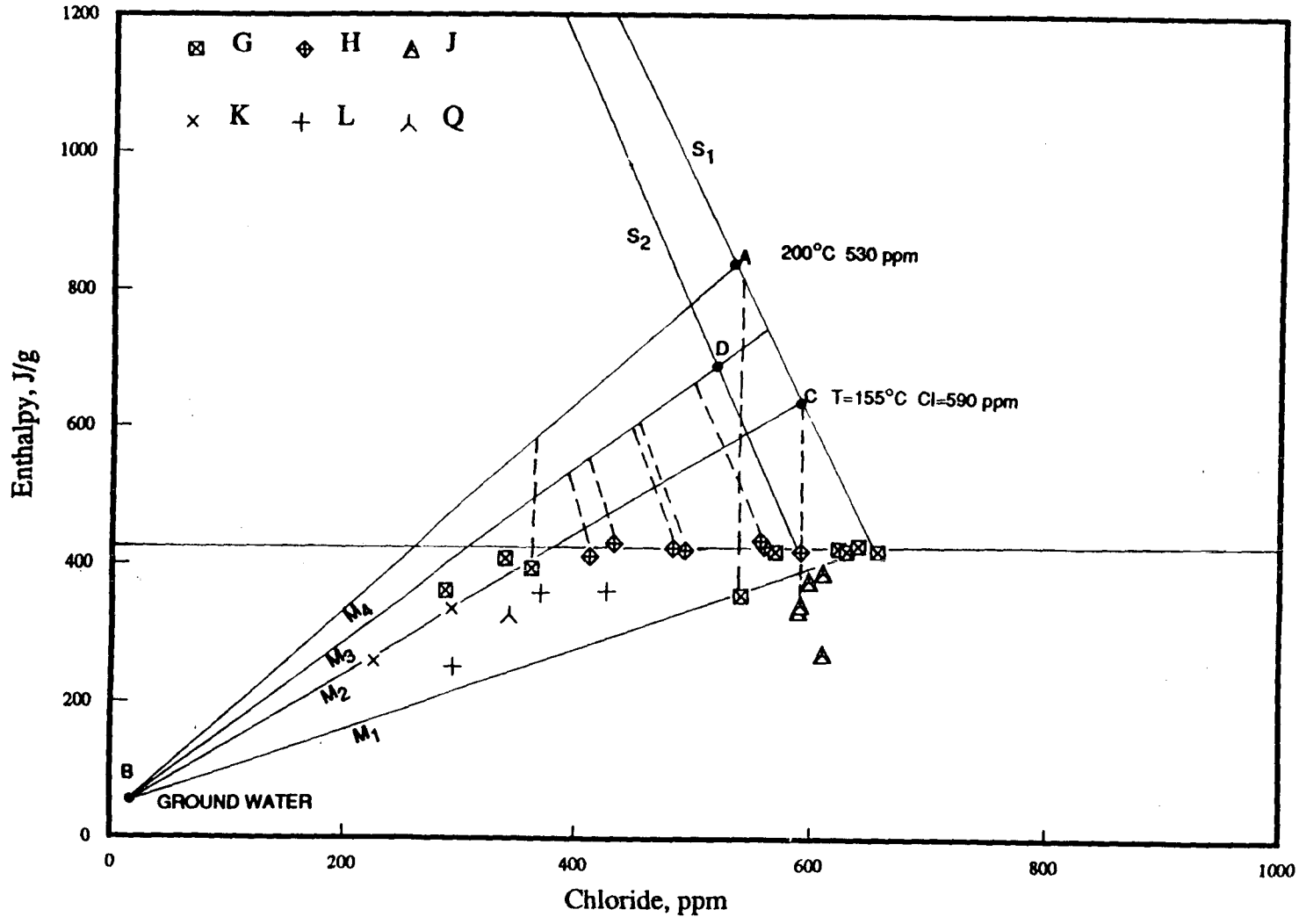

Figure 6.10. Chloride concentrations of thermal waters versus vent enthalpy. Lines S1 and S2 show enthalpy and chloride concentrations of the residual water phase as a thermal water cools adiabatically upon ascent to the surface. M_1, M_2, M_3, and M_4 represent hypothetical mixing lines between a cold meteoric water (B) and various thermal waters (A, C, D, and G) as discussed in the text. Dashed lines represent hypothetical cooling by conduction and boiling and are discussed in the text.

solids of the entire suite of samples, and its chemistry is therefore likely to be closest to the deep thermal water. Lack of tritium eliminates mixing of cold meteoric waters as a factor in interpreting the concentrations and enthalpy of the 1988 G8 spring waters. Our assessment of quartz and cation geothermometers indicated site G thermal waters were derived from an aquifer with an estimated minimum temperature of 200°C. Flow rate of the G8 spring was estimated to be 150 lpm in 1988. Compared to Table 6.9, conductive cooling of the G8 thermal water is unlikely to be a significant factor for depths less than about 0.75 km. This leaves boiling as the sole process by which these waters have cooled. The boiling curve S_1 in Fig. 6.10 represents the evaporative concentration of chloride in the thermal water as a function of enthalpy as it adiabatically cools and emerges as spring G8('88). Point A on this curve corresponds to the Cl concentration and enthalpy at the estimated reservoir temperature of 200°C.

Spring Gx and the springs sampled at site J issue at below boiling (80 to 90°C), are comparatively rich in Cl and SiO_2, and have relatively low Mg. The location and flow rate of spring Gx sampled by the U.S. Geological Survey in 1975 (I. Barnes, pers. comm.) is not known. Flow rates of site J springs (< 30 lpm) indicate these springs could have cooled by conduction. Perpendicular projection of a line from Gx, simulating conductive cooling, intersects the G8 ('88) boiling curve at an enthalpy equivalent to 195°C which is consistent with the predicted reservoir temperature and the silica-enthalpy diagram (Fig. 6.6). Perpendicular projections from the J springs intersect the G8 boiling curve at enthalpies well below point A suggesting J waters would have first boiled to point C, then conductively cooled to the surface. Alternatively, the site J and Gx spring waters could have formed by near-surface dilution of G8 water with groundwater along the path M_1, followed in some cases by

Table 6.9. Maximum rates of mass flow in a conduit of circular cross-section for waters to cool by conduction without boiling and minimum rates of mass flow for waters to cool adiabatically with negligible conductive cooling. All waters are assumed to come from a reservoir at 200°C and emerge at 100°C. Data from Truesdell and others (1977).

Depth (km)	Conductive cooling (kg/minute)	Adiabatic cooling (Kg/minute)
0.5	13	117
1.0	26	234
1.5	40	355

conductive cooling. The latter explanation appears more consistent with silica-enthalpy and deuterium-chloride relationships. Conductive cooling should have produced waters having deuterium values similar to deep thermal waters. Instead, Fig. 6.5c shows these waters have δD values similar to site G boiling spring waters. Mixing rather than conductive cooling is favored by analysis of SiO_2 vs enthalpy diagram for site J springs (Fig. 6.6) and is also consistent with our interpretation of the SO_4-H_2O oxygen isotope results for spring J1.

The remaining spring waters at these sites and further down-valley are below boiling. Concentrations of most constituents in these waters are substantially lower than spring G8 water (Table 6.2). One exception is Mg (0.9 to 2.8 ppm) with the increase in Mg correlating with decreasing chloride (Fig. 6.1e). The temperatures predicted by the Na/K geothermometer for these springs are also significantly higher than the quartz conductive geothermometers. The combination of these factors is strong evidence that these springs are a mixture of ascending thermal waters and shallow groundwaters. Two mixing lines, M_2 and M_3, are illustrated on the Cl-enthalpy and SiO_2-enthalpy diagrams to account for these springs (Figs. 6.10 and 6.6). Cl and SiO_2 concentrations of 10 ppm and 15 ppm, respectively, and a temperature of 10°C, were chosen for the cold water end-member, point B, in these mixing models. These values are similar to cold stream waters entering Geyser Creek valley unaffected by input of thermal waters (Table 6.3). M_2 extends to point C on the G boiling curve (enthalpy = 650 J/g), a hypothetical thermal water end-member that coincides with the perpendicular projection from J1 on the chloride-enthalpy diagram; M_3 extends to point A. The corresponding chloride and silica concentrations and temperatures for the hypothetical

thermal water end-members are 590 ppm, 290 ppm, 155°C, respectively, for point C, and 530 ppm, 260 ppm, and 200°C, respectively for point A.

Many of the dilute hot springs lie on or near M_2 on both the Cl and SiO_2 - enthalpy diagrams, suggesting their compositions and temperatures are fixed mainly by mixing. However, these springs have relatively low rates of flow and conduction may have also played a part in cooling the ascending waters. Those springs that plot below line M_2 may have cooled additionally by conduction or by mixing with a different end-member.

M_3 illustrates mixing between the assumed 200°C reservoir water and groundwater. Spring waters formed by mixing along this line would have had to cool appreciably by conduction to produce the dilute springs. Both M_2 and M_3 mixing relationships appear to be generally consistent with stable isotope values (Fig. 6.5c) with some springs correlating with a deep thermal water end member and others with a shallow fractionated thermal water. The variation in δD for the dilute springs suggests that they were formed by mixing with groundwaters having different δD values.

The preceding paths for formation of the G, J, K, and L thermal springs are illustrated on the SiO_2-Cl diagram (Fig. 6.2). A deep water originating at point A cools adiabatically and by conduction to produce spring G1 waters. Continued steam loss and re-equilibration of SiO_2 leads to formation of G8. Site J and Gx springs form either by conductive cooling from the point A steam-loss line or by near-surface dilution of G8 waters or both. SiO_2 would have had to have re-equilibrated to varying degrees following dilution and conductive cooling to account for the remaining dilute springs.

6.9.1.2 Site H

Application of chloride-enthalpy analysis to site H springs results in a comparatively simple boiling and mixing model (Fig. 6.10). Our geothermometry showed that site H spring waters were derived from a reservoir with a minimum temperature of 165°C. As with the down-valley sites, sulfate-water oxygen isotope geothermometry predicts even higher temperatures at deeper levels (225°C). The most concentrated spring of our sample suite is 1980 H6 and its values for Cl and SiO_2 were used to derive the composition of the parent thermal water for site H springs. Although H6 ('80) has a relatively low rate of flow (50 lpm), conductive cooling is unlikely to be an important factor given the much lower initial temperature in contrast to the values used to generate Table 6.9. The boiling curve S_2 in Fig. 6.10 represents the evaporative concentration of chloride in the thermal water as a function of enthalpy as it adiabatically cools and emerges as spring H6 ('80). Point D on this curve corresponds to the chloride concentration (520 ppm) and enthalpy at the estimated reservoir temperature of 165°C. The point corresponding to the 'deep' reservoir is also shown on this curve.

All the remaining springs sampled at site H can be explained as forming through a combination of mixing of point 'D' type thermal water with groundwater B (line M_4), followed by adiabatic cooling. Na/K temperatures for these spring waters are nearly uniform, indicating they originated from a common reservoir. All the sampled springs were at or near boiling point and had relatively high rates of flow, factors which eliminate conduction as a major cause in the cooling of these waters. H6 and H4 had nearly identical compositions in 1988 and appear to be slightly dilute versions of H6 ('80). The presence of measurable Mg in H2 and H7 spring waters also indicate these springs have a cold water component and must have cooled at least in part by mixing. This mixing-boiling model for the formation of site H springs is

consistent with both the SiO_2-Cl and SiO_2-enthalpy diagrams (Figs. 6.6 and 6.2) and with the δD-chloride considerations for the 1988 samples (Fig. 6.5b).

6.9.2 Thermal Water Relationships and Reservoirs

The preceding analysis offers a contrast in the style of cooling of the ascending thermal waters. At site H, dilution appears to occur at deeper levels followed by boiling as the mixed water rises to the surface. At the down-valley sites, some steam loss appears to occur at deeper levels before mixing, with dilution primarily occurring in the near surface region.

The proximity of Site H to the down-valley sites and the linear correlation of the more conservative chemical constituents with Cl suggest all these spring waters are related at depth. Tritium analysis showed H6 ('88) to have a component of modern water but ambiguities in interpreting tritium make it difficult to estimate the amount. In Fig. 6.10, type 'D' waters could have formed from type 'A' waters by boiling along S_1 then mixing along path M_4, or by first mixing along path M_3 followed by boiling along S_2. In either case, residence in the 'D' reservoir must have been long enough for potassium, silica, and other more reactive constituents to re-equilibrate to new temperature and wallrock conditions. Travel and residence time for the thermal waters may also have been long enough for the SO_4-oxygen isotope ratios to begin re-equilibrating to lower temperature conditions.

Figure 6.11 presents a conceptual model of the reservoir system at the Geyser Bight geothermal area as suggested by the preceding analysis. In it we show a 'deep' reservoir (R_1) housed in a fractured quartz diorite to quartz monzonite pluton with a temperature of 265°C underlying the geothermal area that is recharged by deeply circulating water of meteoric origin. Chloride

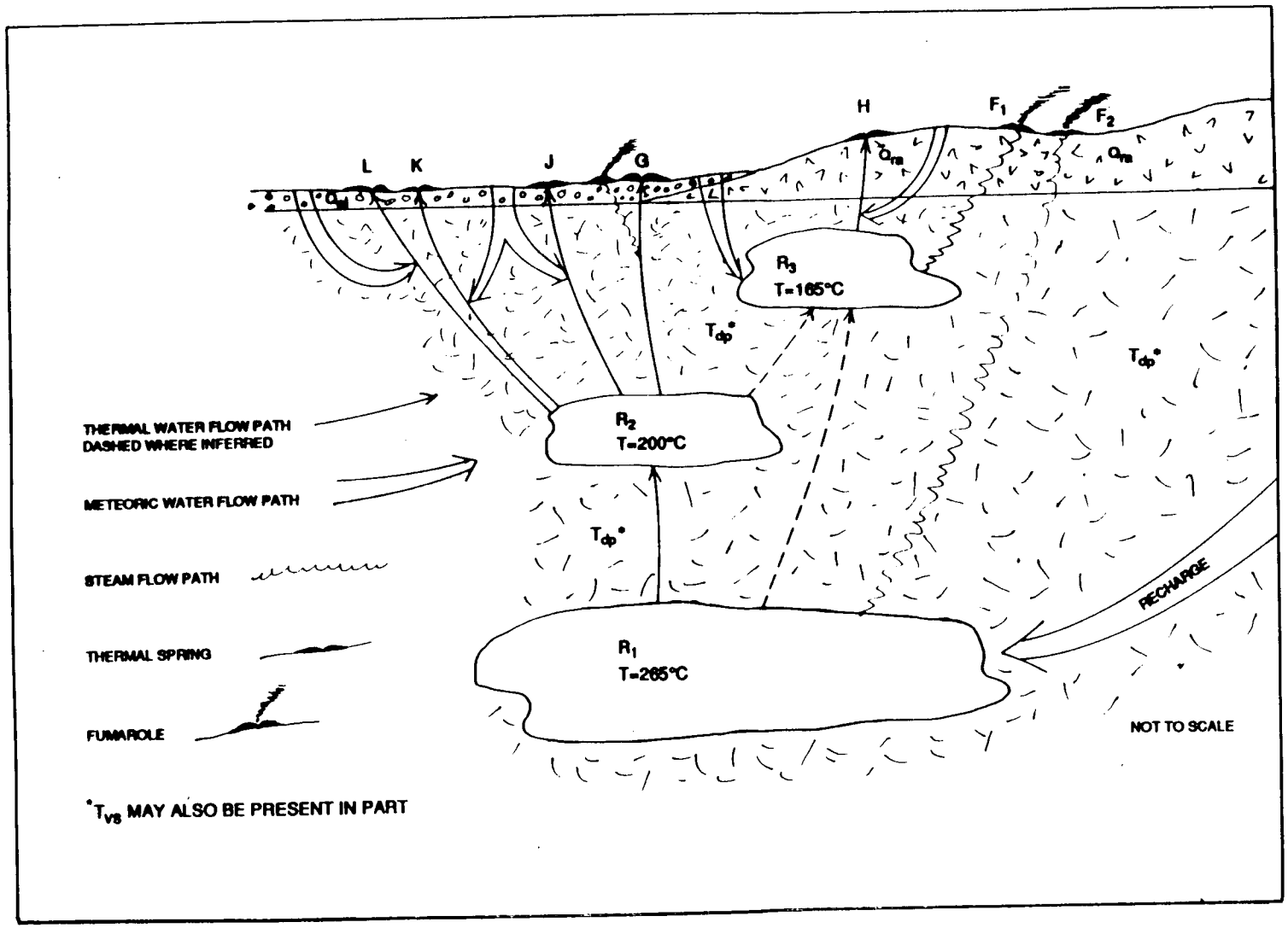

Figure 6.11. Conceptual model of reservoir system at the Geyser Bight KGRA. Rock units are defined on Plate 1 and in section 2.2.

concentrations in this reservoir would be on the order of 450 ppm. Waters ascend from this deep reservoir to a reservoir at an intermediate depth (R_2) where they re-equilibrate to a temperature of 200°C. Some of the water from this intermediate reservoir further migrates into a shallower reservoir (R_3) where it mixes with meteoric groundwaters and re-equilibrates to a temperature of about 165°. Alternatively, waters may ascend directly from R_1 to R_3 and mix with deeply infiltrating meteoric waters. Following re-equilibration, waters from R_3 continue to ascend, further mix with meteoric groundwaters, and boil to the surface to emerge as springs and geysers at site H.

At R_2, following re-equilibration, some waters ascend directly to the surface and emerge as boiling springs and geysers (eg. G8). A portion of the ascending thermal water branches off, mixes with a small amount of groundwater near the surface which quenches boiling, and then cools conductively to form J springs. A third fraction cools primarily by mixing with cold groundwaters in the near-surface region to emerge as dilute warm springs throughout the valley. As the deep thermal water ascends and boils, some or all of the steam may separate in the subsurface, heating marshy areas and perched groundwater tables and producing acid springs. Steam may also separate at deeper levels and migrate directly along fractures to produce the fumaroles above the valley floor.

The chemistry of Q spring waters appears to have attributes of both H type (similar K/Cl) and G/J type (similar Rb/Cl and Cs/Cl) thermal waters. Q spring waters may be derived from a reservoir intermediate between the other two or perhaps are a mixture of waters from both reservoirs.

7. SUMMARY AND CONCLUSIONS

The Geyser Bight geothermal area is a zone of hot springs and fumaroles located on the flank of Mt. Recheshnoi, a large calcalkaline stratocone on central Umnak Island (Figure 1-1). Geologic basement consists of volcanic and marine volcanogenic rocks of probable Oligocene age (McLean and Hein, 1984). These rocks are only gently deformed and lightly metamorphosed. One or more quartz-diorite to quartz-monzonite stocks have intruded the basement in the Geyser Bight area. K-Ar dating of one sample at 9.5 Ma establishes a much younger plutonic event than is represented by the Oligocene stocks described by McLean and Hein (1984) from southwestern Umnak. Our mapping shows that plutonic rock occurs much further up Geyser Creek valley than previously mapped by Byers (1959), thus increasing the probability that plutonic rock hosts the geothermal reservoir system.

The valley walls are composed of volcanic material, primarily lava flows, which were erupted first from several unnamed vents to the northeast, and then from Mt. Recheshnoi, to the southwest (Figure 2-1). Since about 500 ka the primary source of lava has been Mt. Recheshnoi. The most recent flows are mid-Holocene andesite from flank vents on the upper slopes of Mt. Recheshnoi.

Two flank volcanic units are of special interest. These are the Russian Bay valley rhyolite and the quartz-bearing andesite above Hot Springs Bay. These units document the presence of small volumes of silicic melt in the volcanic system. These are notable in their rarity. There are only four other reported rhyolite localities among late Quaternary volcanoes from the Alaska Peninsula or Aleutian Islands. Dacite is more common throughout the Aleutians.

The Russian Bay rhyolite is not likely to come from a large, well established, upper crustal rhyolitic chamber. It is probably the result of heating and partial melting (or "sweating") of the upper crust by repeated passage of more mafic magma. Such a process may also be responsible for the observed magmatic evolutionary trends at Mt. Recheshnoi, which become generally more mafic with time. This may reflect progressive heating of the crust, which would produce decreased thermal contrast between magma and crust, and thus decreased cooling and fractional crystallization of the magma (Myers and others, 1985; Myers and Marsh, 1987).

Geyser Bight has one of the most extensive areas of thermal activity known in Alaska, and includes numerous boiling springs, steam vents, and three regions of fumarolic activity. One fumarole, discovered in 1988, is superheated with a temperature in excess of 125°C. Geyser Bight is the only area in Alaska with documented geysers. In 1988, at least 5 springs were observed to geyser. Vent geometries suggest that some of the other springs are also geysers whose eruptive cycles have as yet been unobserved, or have been geysers and are now inactive.

Thermal spring activity appears to have declined significantly since 1947. Using data from Byers and Brannock (1949) we estimate that convective heat discharged by spring flow was 25 MW in 1947 vs. 16.7 MW in 1988. The decline in spring activity may be due to the choking of spring vents through deposition of silica, calcite and other hydrothermal minerals. Declining activity probably does not reflect cooling of the reservoirs because water chemistry and geothermometry results are essentially unchanged between 1947 and 1988.

Most of the thermal spring activity occurs at the head of Geyser Creek Valley. Chemical and isotopic data acquired in this study provide strong evidence that the thermal spring waters are derived from two intermediate depth reservoirs with minimum temperatures as estimated by geothermometry of 200°C and 165°C, respectively. These reservoirs in turn appear to be related to an underlying parent reservoir with a minimum estimated temperature of 265°C. The 3He/4He ratio of 7.4 found in gases emanating from the thermal springs provides evidence for a magmatic influence on the hydrothermal system. The 7.4 value is nearly the same as the average value found for summit fumaroles in circum-Pacific volcanic arcs.

The most likely reservoir rock is the highly fractured quartz monzonite-to-diorite pluton which is exposed in lower Geyser Creek valley. Reservoir recharge is likely through deeply infiltrating meteoric waters that have isotopic compositions similar to surface stream waters. Tritium concentrations indicate thermal waters feeding spring G8 are over 70 years in age. Thermal waters feeding spring H6 are either younger in age or have been diluted by near-surface meteoric waters. Examination of chemical equilibria suggests that the waters in the reservoir feeding sites G and J are in equilibrium with the mineral assemblage albite + K feldspar + muscovite + clinochlore + quartz ± prehnite ± laumontite ± kaolinite ± analcime.

The site G boiling spring waters have low to moderate concentrations of Cl (650 ppm) and total dissolved solids (1760 ppm), but are rich in B (60 ppm) and As (6 ppm) compared to most other geothermal systems. Variations in spring water chemistries can be explained through boiling and steam loss, and/or mixing of ascending thermal water, derived from one or the other of the intermediate reservoirs, with infiltrating meteoric waters. The As/Cl ratios

in Geyser Bight thermal spring waters are among the highest reported for geothermal areas. The source of B and As is unknown but may be in part of magmatic origin.

Using the areal extent of thermal activity at the surface as a reference, the USGS estimated the area of the subsurface reservoir to be 6.3 km^2 (Mariner and others, 1978). This estimate can be considered a minimum, given our discovery of a superheated fumarole field on the lower east flank of Mt. Recheshnoi which suggests the reservoir(s) may extend another 4 km to the southwest of Geyser Creek valley. Using the assumptions regarding thickness of unexplored reservoirs (1.7 km) and methods established by the USGS (Brooks and others, 1978) for estimating geothermal reserves, we estimate that for a reservoir temperature of 200°C and an assumed depth to mid-reservoir of 1 km, the accessible resource base is approximately 5.4×10^{18} J. This energy base is sufficient to produce up to 132 MW of electrical power for 30 years. The corresponding estimates for a reservoir temperature of 265°C and a depth to mid-reservoir of 3 km are 7.3×10^{18} J as the accessible geothermal energy base and up to 225 MW of extractable electrical power for 30 years.

We believe that the probability of finding a high-temperature, hot-water reservoir at Geyser Bight is excellent. We recommend that follow-up work include a program of geophysical exploration and exploratory drilling to determine depth and extent of reservoirs. The accessibility of the resource from the sea (5 km) and the nearly certain probability of intercepting a hot water reservoir with temperatures of at least 200°C make Geyser Bight one of the most promising areas for geothermal resource development in the Aleutians. Because of its remoteness from population centers, the site would be best

developed for energy intensive industries which could locate and operate in the Aleutian Chain.

8. REFERENCES CITED

Baker, D.R., and Eggler, D.H., 1987, Compositions of anhydrous and hydrous melts coexisting with plagioclase, augite, and olivine or low-Ca pyroxene from 1 atm to 8 kbar: application to the Aleutian volcanic center of Atka: American Mineralogist, v. 72, p. 12-28.

Black, R.F., 1975, Late-Quaternary Geomorphic Processes: Effects on the Ancient Aleuts of Umnak Island in the Aleutians: Arctic, v. 28, p. 159-169.

Brook, C.A., Mariner, R.H., Mabey, D.R., Swanson, J.R., Guffanti, M., and Muffler, L.J.P., 1978, Hydrothermal convection systems with reservoir temperatures greater than or equal to 90°C: *in* Assessment of Geothermal Resources of the United States - 1978: U.S. Geological Survey Circular 790, p. 18-85.

Byers, F.M., Jr., 1959, Geology of Umnak and Bogoslof Islands, Alaska: U.S. Geological Survey Bulletin 1028-L, 369 p.

Byers, F.M., Jr., 1961, Petrology of three volcanic suites, Umnak and Bogoslof Islands, Aleutian Islands, Alaska: Geological Society of America Bulletin, v. 72, p. 93-128.

Byers, F.M., Jr., and Brannock W.W., 1949, Volcanic activity on Umnak and Great Sitkin Islands, 1946-1948. American Geophysical Union Transactions, v.30, no.5, p. 719-734.

Coe R.S., Globerman, B.R., Plumley, P.W., Thrupp, G.A., 1985, Paleomagnetic results from Alaska and their tectonic implications, *in* Howell, D.G., ed., Tectonostratigraphic Terranes of the Circum-Pacific Region: Circum-Pacific Council for Energy and Mineral Resources, Houston Texas, p. 85-108.

Craig, H., 1961, Isotopic variations in meteoric waters: Science, v. 133, p. 1702.

Craig, H. and Lupton, J.E., 1981, Helium-3 and mantle volatiles in the ocean and oceanic crust, *in* The Oceanic Lithosphere, v. 7, The Sea, John Wiley and Sons, New York, p. 391-428.

Dall, William H., 1870, Alaska and its resources: Lee and Shepard, Boston, 627 p.

Eichelberger, J.C., 1975, Origin of andesite and dacite: evidence of mixing at Glass Mountain in California and at other circum-Pacific volcanoes: Geological Society of America Bulletin, v. 86, p. 1381-1391.

Fontes, J.Ch., 1980, Environmental isotopes in groundwater hydrology, *in* Fritz, P. and Fontes, J.C., eds., Handbook of Environmental Isotope Geochemistry: Elsevier Scientific Publishing Company, New York, p. 75-134.

Fournier, R.O., 1979, Geochemical and hydrological considerations and the use of enthalpy-chloride diagrams in the prediction of underground conditions in hot-spring systems: Journal of Volcanology and Geothermal Research, v.5, p. 1-16.

Fournier, R.O., 1981, Application of water chemistry to geothermal exploration and reservoir engineering, *in* Ryback, L. and Muffler, L.P.J., eds., Geothermal Systems: Principles and Case Histories: John Wiley and Sons, New York, p. 109-144.

Fournier, R. O., and Potter, R. W. II., 1982, A revised and expanded silica (quartz) geothermometer: Geothermal Resources Council Bulletin, v. 11,, p. 3-12.

Fournier, R. O., and Truesdell, A. H., 1973, An empirical Na-K-Ca geothermometer for natural waters: Geochimica et Cosmochimica Acta, v. 37, p. 1255-1275.

Fournier, R. O., and Truesdell, A. H., 1974, Geochemical indicators of subsurface temperature, II. Estimation of temperature and fraction of hot water mixed with cold water: U.S. Geological Survey Journal of Research, v. 2, p. 263-270.

Gat, J.R., 1980, The isotopes of hydrogen and oxygen in precipitation, *in* P. Fritz, P. and Fontes, J.C., eds., Handbook of Environmental Isotope Geochemistry: Elsevier Scientific Publishing Company, New York, p. 75-144.

Geist E.L., Childs, J.R., and Scholl, D.W., 1988, The origin of summit basins of the Aleutian ridge: implications for block rotation of an arc massif: Tectonics, v. 7, p. 327-341.

Giggenbach, W.F., 1988, Geothermal solute equilibria. Derivation of Na-K-Mg-Ca geoindicators: Geochimica et Cosmochimica Acta, v. 52, p. 2749-2765.

Gill, J.B., 1981, Orogenic Andesites and Plate Tectonics: Springer-Verlag, New York, 390 pp.

Goguel, R., 1983, The rare alkalies in hydrothermal alteration as Waireki and Broadlands geothermal fields, New Zealand: Geochimica et Cosmochimica Acta, v. 47, p. 429-437.

Grewingk, C., 1850, Beitrag zur Kenntniss der orographischen Besschaffenheir der Nordwest-Kuste Amerikas mit den anliegenden Inseln, *abstracted from* Verhandlungen der Russich-Kaiserlichen Mineralogishen Gesellschalt zur St. Petersburg, Jahrgan 1848 ung 1849, p. 76-342.

Grove, T.L., and Bryan, W.B., 1983, Fractionation of pyroxene phyric MORB at low pressure: an experimental study: Contributions to Mineralogy and Petrology, v. 84, p. 293-309.

Grove, T.L., Gerlach, D.C., and Sando, T.W., 1982, Origin of calc-alkaline series lavas at Medicine Lake Volcano by fractionation, assimilation and mixing: Contributions to Mineralogy and Petrology, v. 80, p. 160-182.

Henley, R.W., Truesdell, A.H., and Barton, Jr., P.B., 1984, Fluid-Mineral Equilibria in Hydrothermal Systems: Reviews in Economic Geology, v. 1, 267 p.

Jacob, K.H., Nakamura, K., and Davies, J.N., 1977, Trench-volcano gap along the Alaska-Aleutian arc: facts, and speculations on the role of terrigenous sediments, *in* Talwani, M. and Pitman W.C., eds., Island Arcs, Deep Sea Trenches, and Back-arc Basins: American Geophysical Union, Washington, D.C., p. 243-258

Kay, S.M., and Kay, R.W., 1985, Aleutian tholeiitic and calc-alkaline magma series I: the mafic phenocrysts: Contributions to Mineralogy and Petrology, v. 90, p. 276-290.

Kay, S.M., Kay, R.W., and Citron, G.P., 1982, Tectonic controls on tholeiitic and calc-alkaline magmatism in the Aleutian arc: Journal of Geophysical Research, v. 87, p. 4051-4072.

Keith, T.E.C., Thompson, J.M., and Mays, R.E., 1983, Selective concentration of cesium in analcime during hydrothermal alteration, Yellowstone National Park, Wyoming: Geochimica et Cosmochimica Acta, v. 47, p. 795-804.

Krause, K., 1986, Transmission powerline and road corridor geotechnical study for the proposed Makushin geothermal field power facility on Unalaska Island, *in* Engineering Geology Technical Feasibility Study Makushin Geothermal Power Project Unalaska, Alaska: Alaska Division of Geological and Geophysical Surveys Public Data File 86-60, p. C1-C17.

Krauskopf, K.B., 1979, Introduction to Geochemistry, Second edition: McGraw-Hill, New York, 617 p.

Mariner, R.H., Brook, C.A., Swanson, J.R., and Mabey, D.R., 1978, Selected data for hydrothermal convection systems in the United States with reservoir temperatures greater than or equal to 90°C: U.S. Geological Survey Open-file Report 78-858, 475 p.

McKenzie, W.F. and Truesdell, A.H., 1977, Geothermal reservoir temperatures estimated from the oxygen isotope compositions of dissolved sulfate and water from hot springs and shallow drillholes: Geothermics, v. 5, p. 51-61.

McLean, H., and Hein, J.R., 1984, Paleocene geology and chronology of southwestern Umnak Island, Aleutian Islands, Alaska: Canadian Journal of Earth Sciences, v.21, p. 171-180.

Miyashiro, A., 1974, Volcanic rock series in island arcs and continental margins: American Journal of Science, v. 274, p. 321-355.

Motyka, R. J., Moorman, M. A., and Liss, S. A., 1981, Assessment of thermal spring sites, Aleutian Arc, Atka Island to Becharof Lake--Preliminary results and evaluation: Alaska Division of Geological and Geophysical Surveys, Open File Report AOF-144, 173 p.

Motyka, R.J., Queen, L.D., Janik, C.J., Sheppard, D.S., Poreda, R.J., and Liss, S.A., 1988, Fluid geochemistry and fluid mineral equilibria in test

wells and thermal gradient holes at the Makushin Geothermal area, Unalaska Island, Alaska: Alaska Division of Geological and Geophysical Surveys, Report of Investigations 88-14, 90 p.

Motyka, R.J., Liss, S.A., and Nye, C.J., Geothermal resources of the Aleutian arc: in preparation.

Muffler, L.J.P., 1979, Assessment of Geothermal Resources of the United States-1978: United States Geological Survey Circular 790, 163pp.

Myers, J.D., and Marsh, B.D., 1987, Aleutian lead isotopic data: additional evidence for the evolution of lithospheric plumbing systems: Geochemica et Cosmochemica Acta 51, p. 1833-1842.

Myers, J.D., Marsh, B.D., and Sinha, A.K., 1985, Strontium isotopic and selected trace element variations between two Aleutian volcanic centers (Adak and Atka): implications for the development of arc volcanic plumbing systems. Contributions to Mineralogy and Petrology, v. 91, p. 221-234.

Nakamura, K., Jacob, K.H., and Davies, J.N., 1977, Volcanoes as possible indicators of tectonic stress orientation - Aleutians and Alaska: Pure and Applied Geophysics, v. 115, p. 87-112.

Nakamura, K., Plafker, G., Jacob, K.H., and Davies, J.N., 1980, A tectonic stress trajectory map of Alaska using information from volcanoes and faults: Bulletin of the Earthquake Research Institute, v.55, p. 89-100.

Nehring, N.L., Bowen, P.A., and Truesdell, A.H., 1977, Techniques for the conversion to carbon dioxide of oxygen from dissolved sulfate in thermal waters: Geothermics, v. 5, p. 63-66.

Nye, C.J., and Turner, D.L., 1990, Petrology, geochemistry, and age of the Spurr volcanic complex, eastern Aleutian arc: Bulletin of Volcanology, v. 52, p. 205-226.

Palmer, M.R., Spivack, A.J. and Edmond, J.M., 1985, Absorption of boron on marine sediments: EOS, v. 66, p. 916.

Panichi, C., and Gonfiantini, R., 1978, Environmental isotopes in geothermal studies: Geothermics, v. 6, p. 143-161.

Panuska B.C., and Stone, D.B., 1985, Latitudinal motion of the Wrangellia and Alexander terranes and the southern Alaska Superterrane, *in* Howell, D.G., ed., Tectonostratigraphic Terranes of the Circum-Pacific Region: Circum-Pacific Council for Energy and Mineral Resources, Houston Texas, p. 109-120.

Poreda R.J., 1983, Helium, neon, water and carbon in volcanic rocks and gases: University of California, San Diego, Ph.D. thesis, 215 p.

Poreda, R.J. and Craig, H., 1989, Helium isotope ratios in circum-Pacific volcanic arcs: Nature, v. 338, p. 473-478.

Presser, T.S. and Barnes, I., 1974, Special techniques for determining chemical properties of geothermal waters: United State Geological Survey Water Resources Investigation Report 22-74, 11 pp.

Scholl, D.W., Vallier, T.L., and Stevenson, A.J., 1987, Geologic evolution and petroleum geology of the Aleutian ridge, *in* Scholl, D.W., Grantz, A., and Vedder, J.G., eds., Geology and Resource Potential of the Continental Margin of Western North America and Adjacent Ocean Basins - Beaufort Sea to Baja California: Circum-Pacific Council for Energy and Mineral Resources Earth Science Series Volume 6, Houston Texas, p. 123-155.

Skougstad, M.W., Fishman, M.J., Friedman, M.J., Erdmann, D.E. and Duncan, S.S., 1979, Methods for determination of inorganic substances in water and fluvial sediments: United States Geological Survey Techniques of Water-Resource Investigations, Book 5, Chap. A1, 626 p.

Smith, D.R., and Leeman, W.P., 1987, Petrogenesis of Mount St. Helens dacitic magmas: Journal of Geophysical Research, v. 92, p. 10,313-10,334.

Spencer, S.G., Long, G.A., and Chapman-Riggsbee, W., 1982, An analysis of geothermal resource development on Unalaska Island, Alaska: Geothermal Resources Council Transactions, v. 6., p. 393-396.

Stauffer, R.E., and Thompson, J.M., 1984, Arsenic and antimony in geothermal waters of Yellowstone National Park, Wyoming, USA: Geochimica et Cosmochimica Acta, v. 48, p. 2547-2562.

Stone, D.B., 1988, Bering Sea - Aleutian Arc, Alaska, *in* Nairn, A.E.M., F.G. Stehli, and S. Uyeda, eds., The Ocean Basins and Margins, Vol 7b: Plenum Publishing, p. 1-84.

Thompson, J.M., Keith, T.E.C., and Consul, J.J., 1985, Water chemistry and mineralogy of Morgan and Growler Hot Springs, Lassen KGRA, California: Geothermal Resources Council Transactions, v. 9, part I, p. 357-362.

Thompson, J.M., 1985, Chemistry of thermal and nonthermal springs in the vicinity of Lassen Volcanic National Park: Journal of Volcanology and Geothermal Research, v. 25, p. 81-104.

Truesdell, A.H. and Hulston, J.R., 1980, Isotopic evidence on environments of geothermal systems, *in* Fritz, P. and Fontes J.C., eds., Handbook of Environmental Isotope Geochemistry: Elsevier Scientific Publishing Company, New York, p. 179-226.

Truesdell, A.H., Nathenson, M. and Rye, R.O., 1977, The effects of subsurface boiling and dilution on the isotopic compositions of Yellowstone thermal waters: Journal of Geophysical Research, v. 82, p. 3694-3704.

Viglino, J.A., Harmon, R.S., Borthwick, J., Nehring, N.L., Motyka, R.J., White, L.D. and Johnson D.A., 1985, Stable-isotope evidence for a magmatic component in fumarole condensates from Augustine Volcano, Cook Inlet, Alaska, USA: Chemical Geology, v. 49, p. 141-157.

Walker, D., Shibata, T., and DeLong, S.E., 1979, Abyssal tholeiites from the Oceanographer Fracture Zone II - Phase equilibria and mixing: Contributions to Mineralogy and Petrology, v. 70, p. 111-125.

Waring, G.A., 1917, Mineral springs of Alaska: United States Geological Survey Water-Supply Paper 418, 114p.

White, D.E., 1967, Some principles of geyser activity, mainly from Steamboat Springs, Nevada: American Journal of Science, v. 265, p. 641-684.

Worner, G., Harmon, R.S., Davidson, J., Moorbath, S., Turner, D.L., McMillan, N., Nye, C., Lopez-Escobar, L., and Moreno, H., 1988, The Nevados de Payachata volcanic group (18°S/69°W, N. Chile): I. Geological, geochemical and isotopic observations: Bulletin of Volcanology, v. 50, p. 287-303.

12

Plate I

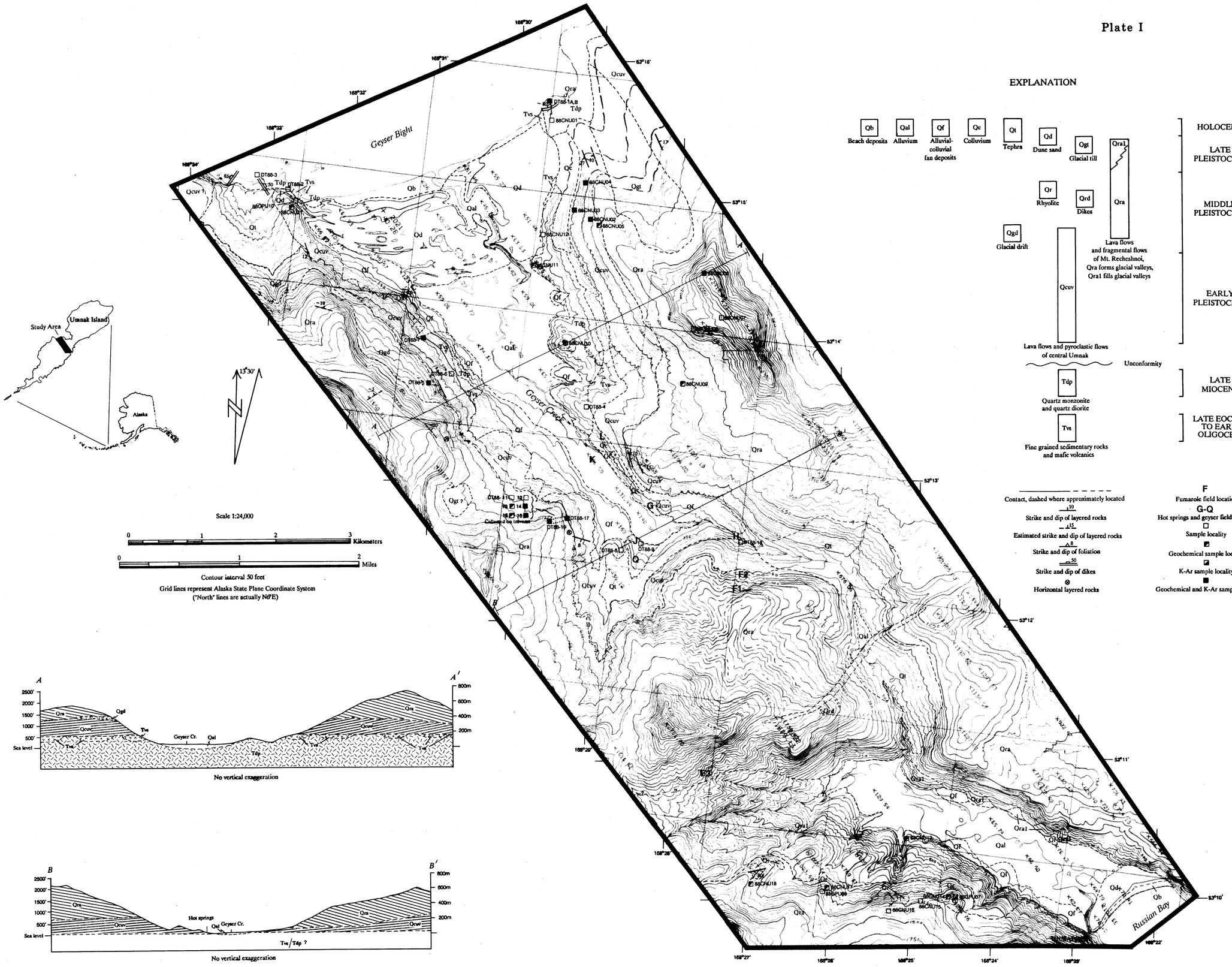

EXPLANATION

Qb Beach deposits
Qal Alluvium
Qf Alluvial-colluvial fan deposits
Qc Colluvium
Qt Tephra
Qd Dune sand
Qgt Glacial till
Qra1 Qra Lava flows and fragmental flows of Mt. Recheshnoi, Qra forms glacial valleys, Qra1 fills glacial valleys
Qr Rhyolite
Qrd Dikes
Qgd Glacial drift
Qcuv Lava flows and pyroclastic flows of central Umnak

HOLOCENE
LATE PLEISTOCENE
MIDDLE PLEISTOCENE
EARLY PLEISTOCENE

Unconformity

Tdp Quartz monzonite and quartz diorite
Tvs Fine grained sedimentary rocks and mafic volcanics

LATE MIOCENE
LATE EOCENE TO EARLY OLIGOCENE

Contact, dashed where approximately located
10 Strike and dip of layered rocks
15 Estimated strike and dip of layered rocks
8 Strike and dip of foliation
50 Strike and dip of dikes
⊗ Horizontal layered rocks

F Fumarole field location
G-Q Hot springs and geyser field location
Sample locality
Geochemical sample locality
K-Ar sample locality
Geochemical and K-Ar sample locality

GEOLOGIC MAP AND CROSS SECTIONS OF GEYSER CREEK VALLEY AND VICINITY UMNAK ISLAND, ALASKA

by

Christopher J. Nye, Donald L. Turner and Eugene A. Pavia

1990

Cartography by Robin Cottrell
Base map prepared by North Pacific Aerial Surveys

Plate 2

Explanation.

A Major spring group or fumarole field

Thermal spring sampled in 1988

Thermal spring not sampled in 1988

0 1 2 3 km

0 1 2 mi

Contour interval 250 ft.

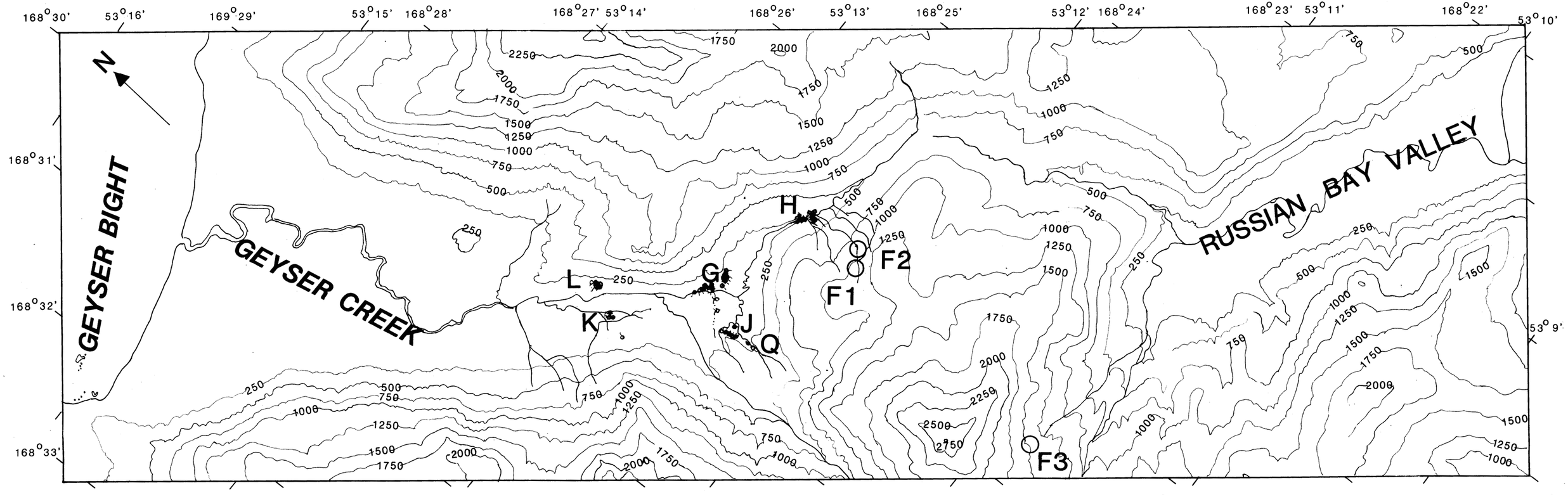

Location map for the thermal springs and fumaroles of Geyser Bight, central Umnak Island.